2021

# ACYLATED NANOFIBROUS CHITOSAN BIOMATERIALS FOR PROLONGED BIOFILM INHIBITION AND PAIN MITIGATION

Carlos Montez Wells

# ACYLATED NANOFIBROUS CHITOSAN BIOMATERIALS FOR PROLONGED BIOFILM INHIBITION AND PAIN MITIGATION

by

Carlos Montez Wells

A Dissertation

Submitted in the Partial Fulfillment of the

Requirements for the Degree of

Doctor of Philosophy

Major: Biomedical Engineering

The University of Memphis

May 2021

## Dedication

I want to dedicate this dissertation to my loving and supportive mom, Nancy Wilson-White, my son, Montez Adonis Wells, and my magnificent life partner, Barbara Denise Davis. My mom is and has been my foundation and motivation throughout my life. Her presence and sacrifices are the primary reasons for my journey and why I continue to strive for more. My son reminds me that we must take advantage of the opportunities that many of those before us did not have, fought for, and some, unfortunately, paid an unjust sacrifice. Not seeing self-representation in our global society should not limit my son's future aspirations and goals; therefore we must increase diversity in all aspects. Doing this affords him the opportunity to be limitless in his academic, career and life goals. His birth is a primary catalyst in my renewed academic career. My loving life partner has been steadfast in her support, guidance, and reassurance throughout my graduate education, no matter if the times were good or bad.

**Acknowledgements**

First and foremost, I would like to thank my committee chair, advisor, and mentor, Dr. J. Amber Jennings, whose inspiration, guidance, understanding, and fortitude were critical to completing this work. Additionally, I would like to thank my graduate committee members, Drs. Joel D. Bumgardner, Tomoko Fujiwara, Daniel Baker, and Warren O. Haggard for their insight and valuable guidance. I want to extend additional thanks to Dr. Warren O. Haggard for being my first graduate advisor, mentorship, acceptance, and willingness to assist with any aspect of life. Without the assistance of the following individuals, this dissertation could not have been brought to fruition; therefore, I would like to thank the following individuals: Dr. Vishnu Priya Murali for research collaboration and input; Zoe Harrison for her willingness to assist with anything necessary at a moment's notice; Dr. Lauren Priddy, Luke Tucker, and Mississippi State Wise Center and College of Veterinary Medicine's staff and students for their collaborative efforts on the animal model; Dr. Omar Skalli and Lauren Wilson for their assistance with SEM imaging and histological processing; Dr. Mallesh Kurakula for assisting with material characterization, Emily C. Coleman and Alexis Johnson for their willingness to perform whatever task they were able to, Regina Hairston for being a life mentor, advocate, and sponsor; Rabeta Yeasmin for her assistance, desire to learn, and conducting FTIR analysis; Dr. Kwei-Yu for helping with FTIR training; Landon Choi for providing materials, taking elution samples, and performing SEM imaging; Omar A. Mohamed, John-David Ross, Lydia Ross, Brittany Spencer, Austin Davenport, Bharat Jothilingam, and Ezzuddin Abuhussein for their assistance during various times; Melanie James and Hope Clippinger for moral and administrative support; Deborah Scott and Benita Williams for administrative support; and Tennessee Doctoral Scholars for providing me a graduate research fellowship. Finally, I would like to thank my mom, Nancy

Wilson-White, my son, Montez A. Wells, my life partner Barbara D. Davis, my family, immediate and extended, and friends, for their love, moral support, and COVID-19-tested perseverance.

## Preface

This dissertation comprises several manuscripts that have been or will be submitted for publication in peer-reviewed journals. The manuscript in Chapter 2 entitled "Synthesis and Characterization of 2-decenoic Acid Modified Chitosan for Infection Prevention and Tissue Engineering" will be submitted to Marine Drugs (April 2021). The manuscript in Chapter 3 entitled "Antimicrobial and Anti-Biofilm Efficacy of Local Anesthetics Combined with *Cis*-2-decenoic Acid against *Staphylococcus aureus*, *Pseudomonas aeruginosa*, and *Acinetobacter baumannii*" will be submitted to Frontiers in Microbiology (March 2021). The Military Burn Research Program of the Congressionally Directed Medical Research Program award #W81XWH-20-1-0430 funded the research in Chapters 2 and 3. The manuscript in Chapter 4 entitled "Efficacy of Chitosan-mannitol Paste Loaded with Bupivacaine for Treatment of a Rat *S. aureus* Infection Model" will be submitted to Engineering Cells and Materials (eCM) (April 2021). The National Institutes of Arthritis and Musculoskeletal and Skin Disease of the National Institutes of Health (NIH) under Award Number R01AR066050 and UMRF Ventures at the University of Memphis funded the research in Chapter 4.

## Abstract

Wells, Carlos Montez. PhD. The University of Memphis. May 2021. Acylated Nanofibrous Chitosan Biomaterials for Prolonged Biofilm Inhibition and Pain Mitigation. Major Professor: J. Amber Jennings

Microbial contamination and biofilm formation in complex musculoskeletal trauma is an ongoing clinical challenge. Infection and biofilm formation in these injuries cause significant pain in addition to physical, socioeconomic, mental, and familial burdens to patients while increasing strains on the healthcare system. Biofilm-based infections are prevalent and are particularly difficult to treat due to the biofilm's tolerance to antimicrobials and ability to evade natural body defenses. Primary strategies to treat biofilm are 1) inhibition, 2) dispersal, and 3) removal. A promising strategy is to use the biofilm dispersal agent 2-decenoic acid (2DA) and its analogs combined with antimicrobials to inhibit and treat biofilm-based infections. Also, high concentrations of local anesthetics (LA) that effectively block pain locally may provide advantages for preventing and treating biofilm-based infections. Local antimicrobial delivery systems offer benefits over systemic delivery of therapeutics, but release kinetics, residency time, and ability to deliver hydrophobic therapeutics, i.e., LA and 2DA, are challenging. Burst release of antimicrobials is ineffective at eradicating infection and may also contribute to the growing incidence of antimicrobial tolerance. Surface modifications of chitosan biomaterials through acylation have demonstrated an ability to improve hydrophobic therapeutics' release kinetics while supporting wound healing. In these studies, we investigated the combinatorial antimicrobial effects of 2DA and LA for common pathogenic microorganisms. We further tested the hypothesis that direct acylation of chitosan with 2DA analogs could inhibit biofilm formation. We then evaluated the efficacy of acylated chitosan biomaterials in releasing therapeutics and treating biofilm-based infections in *in vitro* and *in vivo* infection models.

Results revealed that combinations of LA ≥ 5 mg $mL^{-1}$ and 2DA ≥ 250 mg $mL^{-1}$ have additive or synergistic activity against microorganisms. We confirmed that chitosan biomaterials could:

1. Be directly acylated with 2DA to resist biofilm formation even without therapeutics loaded.
2. Extend the release of loaded therapeutics to at least one week after acylation.
3. Reduce infection occurrence in both *in vitro* and *in vivo* infection models after acylation and loading with 2DA and LA.

## Table of Contents

**Table of Contents**

## Table of Contents

## List of Tables

## List of Figures

## List of Figures

## List of Figures

## Keys to Symbols or Abbreviations (Abbr.)

| Abbr./Symbol | Meaning | Page |
|---|---|---|
| ° | Degrees | 29 |
| ℃ | Degrees Celsius | 25 |
| ∅ | Diameter | 68 |
| α | Alpha | 27 |
| 2DA | 2-decenoic Acid | 24 |
| *A. baumannii* | *Acinetobacter Baumannii* | 14 |
| AAOS | American Academy of Orthopaedic Surgeons | 9 |
| ANOVA | Analysis of Variance | 27 |
| ATCC | American Type Culture Collection | 27 |
| ATP | Adenosine Triphosphate | 57 |
| ATR | Attenuated Total Reflectance | 26 |
| BAHP | Bupivacaine Acylated Hydrophilic Paste | 67 |
| BHI | Brain Heart Infusion | 68 |
| BUP | Bupivacaine | 41 |
| C | Combination | 44 |
| C2DA | *Cis*-2-decenoic Acid | 16 |
| $CaSO_4$ | Calcium Sulfate | 65 |
| CDC | Centers for Disease Control and Prevention | 12 |
| CFU | Colony Forming Unit | 27 |
| cm | Centimeter | 25 |

## Keys to Symbols or Abbreviations (Abbr.)

| Abbr./Symbol | Meaning | Page |
|---|---|---|
| $CO_2$ | Carbon Dioxide | 27 |
| CPI | Consumer Price Index | 13 |
| CPI-U | Consumer Price Index for All Urban Consumers | 13 |
| DAIR | Debridement and Irrigation with Retention | 41 |
| DC | Decanoic Chloride | 25 |
| DCM | Dichloromethane | 25 |
| DDA | Degree of De-acetylation | 19 |
| DMEM | Dulbecco's Modified Eagle Medium | 26 |
| EDC | 1-ethyl-3-(3-dimethyl-aminopropyl)-1-carbodiimide Hydrochloride | 24 |
| EPS | Exopolymeric Substance | 31 |
| FA | Fatty Acid | 10 |
| FBS | Fetal Bovine Serum | 26 |
| FICI | Fractional Inhibitory Concentration Index | 44 |
| FTIR | Fourier Transform Infrared | 26 |
| g | Gram | 25 |
| GBR | Guided Bone Regeneration | 23 |
| GI | Gastrointestinal | 14 |
| H & E | Hematoxylin and Eosin | 70 |
| HC | Hexanoic Chloride | 25 |
| HPLC | High-performance Liquid Chromatography | 67 |
| IACUC | Institutional Animal Care and Use Committee | 68 |

## Keys to Symbols or Abbreviations (Abbr.)

| Abbr./Symbol | Meaning | Page |
|---|---|---|
| ISO | International Organization for Standardization | 32 |
| IVIS | *In Vivo* Imaging System | 69 |
| kDa | Kilodalton | 24 |
| kg | Kilogram | 68 |
| kV | Kilovolt | 25 |
| L | Liter | 11 |
| LA | Local Anesthetic | 10 |
| LID | Lidocaine | 41 |
| M | Molar | 25 |
| MBIC | Minimum Biofilm Inhibitory Concentration | 44 |
| mg | Milligram | 25 |
| MIC | Minimum Inhibitory Concentration | 16 |
| min | Minute | 25 |
| mL | Milliliter | 25 |
| mm | Millimeter | 25 |
| mmol | Millimole | 25 |
| MRSA | Methicillin-resistant *Staphylococcus Aureus* | 40 |
| MSCRAMM | Microbial Surface Components Recognizing Adhesive Matrix Molecules | 35 |
| NaOH | Sodium Hydroxide | 25 |
| nm | Nanometer | 25 |
| $O_2$ | Oxygen | 68 |

## Keys to Symbols or Abbreviations (Abbr.)

| Abbr./Symbol | Meaning | Page |
|---|---|---|
| *P. aeruginosa* | *Pseudomonas Aeruginosa* | 13 |
| PBS | Phosphate-Buffered Saline | 27 |
| PCR | Polymerase Chain Reaction | 13 |
| PEG | Polyethylene Glycol | 66 |
| PMMA | Poly(Methyl Methacrylate) | 18 |
| rhBMP-2 | Recombinant Human Bone Morphogenetic Protein-2 | 20 |
| ROP | Ropivacaine | 41 |
| rpm | Revolutions per Minute | 67 |
| S | Alone | 44 |
| *S. aureus* | *Staphylococcus Aureus* | 13 |
| *S. epi* | *Staphylococcus Epidermis* | 13 |
| SEM | Scanning Electron Microscope | 28 |
| SSI | Surgical Site Infection | 9 |
| T2DA | Trans-2-decenoic Acid | 27 |
| TFA | Trifluoroacetic Acid | 23 |
| THA | Total Hip Arthroplasty | 9 |
| TSB | Tryptic Soy Broth | 27 |
| UAMS | University of Arkansas Medical School | 27 |
| USA | United States of America | 13 |
| v/v | Volume/Volume | 24 |
| VRSA | Vancomycin Resistant Staphylococcus Aureus | 14 |

## Keys to Symbols or Abbreviations (Abbr.)

| Abbr./Symbol | Meaning | Page |
|---|---|---|
| w/v | Weight/Volume | 24 |
| WHO | World Health Organization | 12 |
| β | Beta | 22 |
| µg | Microgram | 26 |
| µL | Microliter | 44 |

# CHAPTER 1

# Introduction

## Background

### Incidence

Many musculoskeletal procedures and traumatic injuries require bone fixation devices to assist with the healing process. Estimates predict that open fracture and extremity trauma occur at least six million times per year in the United States (1). Musculoskeletal injuries requiring fixation devices have infection rates of 5% (2), which increases to over 50% for complex injuries such as compound fractures (3-5). Damaged tissue and pain are always consequences of traumatic musculoskeletal wounds that require active treatment efforts. The wounds can result from traumatic musculoskeletal injuries, medical device implantation, or surgical procedures. Medical device implantation annually accounts for ~2 million healthcare-associated infections, often requiring aggressive debridement of surrounding tissue after implant removal causing patient trauma and pain (6, 7).

### Infection Rates

The American Academy of Orthopaedic Surgeons (AAOS) estimates that more than 500,000 surgical site infections (SSIs) occur after an orthopaedic procedure (8). The infection rate that causes total hip arthroplasty (THA) revisions is 14.8% (9). The increase in bacterial antibiotic resistance in musculoskeletal infections further complicates the fight against eradicating or inhibiting infections (8). Antibiotic misuse is a significant contributor to the multi-drug resistant bacterial strains compounded by antibiotic-resistant biofilm, limiting broad-spectrum practical treatment options in the fight against infections (10, 11). Bacterial colonization and subsequent biofilm formation can occur during the first 72 hours of a traumatic injury (12, 13), making wound protection during this time frame critical. Infection-related complications increase socioeconomic costs for patients (14). Local delivery systems may have advantages in treating musculoskeletal injuries, such as complex extremity wounds requiring fixation hardware, when used as adjunctive therapy to

systemic delivery. Local delivery devices are increasing in demand due to the need to treat and prevent infection and pain management during wound healing processes. Local antimicrobial delivery, including but not limited to anti-biofilm fatty acids (FA) and local anesthetics (LA), may be efficacious in treating or preventing infection and moderating pain while reducing patient trauma and economic costs. The anti-biofilm FAs assist in inhibiting biofilm formation, which increases infectious bacteria's susceptibility to natural host defenses and antimicrobial agents. Besides their primary pain treatment function, LAs can exhibit antimicrobial properties that can enhance locally delivered antimicrobial agents' efficacy.

Additionally, when treatment solutions include LAs, pain mitigation may reduce the need for prescription and systemically delivered opioids. This project's principal goals include developing and evaluating local delivery systems for hydrophobic therapeutics such as fatty acids and local anesthetics. The local delivery systems may extend their elution profiles for infection prevention in wounds or other complex traumas.

**Normal Healing**

Physiological impairments resulting from damage to skin, muscle, bone, or other tissue define wounds. Traumatic injuries, acute wounds, surgical wounds, or accompanying co-morbidities can result in musculoskeletal wound infections, which further complicate and impair patient healing and recovery (15). Bacterial colonization occurs with a greater probability in open fractures in comparison with surgically created wounds due to contamination from the environment (16). Co-morbidities, including diabetes, malnutrition, chronic steroid use, and peripheral vascular disease, among other chronic illnesses, exacerbate tissue healing impairments (17), and increase infection risks (18). Musculoskeletal infectious complications may cause physical, emotional, and monetary stresses to those patients experiencing them (19).

Natural wound healing processes include various cell types responsible for hemostasis, inflammation, proliferation, and remodeling (20). During the first eight hours, neutrophils migrate from surrounding areas

removing foreign bodies, bacteria, non-viable tissue, and other debris from the wound site (21). Macrophages migrate to the wound site 24 - 48 h after injury, with concentrations starting to decline at 72 h or longer depending on the wound size (19). Neutrophils evacuate the wound site as macrophages and mast cells clear the area of debris (17). Within hours 48 - 72, or longer depending on wound austerity, epithelial cells construct a thin epithelial layer over the cleaned and disinfected wound, providing a barrier from the external environment (16, 22). Tissue remodeling begins, on average, within 4 - 8 weeks of the injury and persists for months to years, depending on wound severity (21).

**Musculoskeletal Injuries**

Efficacious wound management can assist innate responses in restoring the wound site. Musculoskeletal injury treatments that mitigate complications such as pain and infection result in improved patient outcomes and prognosis (23). Some of the primary principles for managing complex musculoskeletal wounds include infection prevention, irrigation, debridement, fixation, and closure (24). While there are currently few treatment standards (25), there is a consensus that early intervention in applying preventative measures results in more favorable outcomes (14). Debridement removes non-viable tissue and foreign materials from the wound (26); however, debridement has limited efficacy when surgeons cannot visualize where infecting microorganisms reside. Non-viable tissue leads to necrotic tissue, which can activate natural inflammatory processes that inhibit wound healing and promote microbe proliferation (27). In absence of methods to visualize bacteria, a common practice by surgeons is to debride skin and subcutaneous tissue debridement until capillary bleeding occurs, as this is a sign of healthy undamaged tissue (28). The magnitude of soft tissue damage and contamination may require additional debridement, typically occurring after 24 - 48 h (29).

Irrigation or lavage removes smaller foreign bodies by rinsing with an aqueous solution to reduce bacterial concentrations. Copious amounts of irrigation fluid, approximately 10 L, are discussed in practice; however, this is not without controversy (30). The risk for infectious complications increases when ballistic or

explosions occur due to the possibility of bacteria spreading along tissue planes (31). Antimicrobial administration during irrigation is a potential treatment solution that moderates the risk of patient infection (32). The presiding surgeon can adjust the antibiotic lavage treatment to counter suspected bacterial contaminants (33). Recent clinical practice guidelines issued by the World Health Organization (WHO) and the Centers for Disease Control and Prevention (CDC) recommend the inclusion of aqueous povidone-iodine solutions for the prevention of SSI (31, 33-36). Some current physician-directed or selected wound irrigation solutions include povidone-iodine (0.35%), chlorhexidine (0.05%), sodium hypochlorite (0.125%) and solutions containing two or more antimicrobials (37). Fixation and closure inhibit additional bone and soft tissue damage and provide a nidus for bacterial attachment and biofilm formation (38). Intramedullary nails, screws, and plates are a few current methods used to stabilize fractures; future improvements are possible for every modus (39). Intramedullary nail implementation to treat lower-extremity fractures may disrupt bone circulation (34, 35). Precision in fracture bone alignment usually requires the use of plates and screws (39, 40).

Additionally, transarticular or upper-extremity fracture treatments often require screws and plates (14, 41). More severe wounds involving crushed or pulverized bone and surrounding soft tissue damage may require titanium or stainless steel alloy rods, plates, wires, and screws (1, 42). Total hip and knee arthroplasties necessitate fixation and stabilization for adequate bone repair (41). Wound closure stipulations dictate if available soft tissue or local or free muscle flaps may assist in soft tissue reconstruction (41). In the most extreme cases, non-abated infection or nonrepairable damage may force the surgeon to amputate the affected extremity (43).

Currently, prevention is the most successful infection treatment; however, microorganisms at a rate of up to 65% reportedly contaminate severe, open musculoskeletal wounds (44). In the absence of instrumentation implanted during surgical procedures, infection rates are a much lower 5%, demonstrating the role these implants play in biofilm-associated infection (44, 45). Preexisting co-morbidities increase the probability of

infection onset (44). Infection symptoms may include chills, headaches, fever, and stiffness, pain, erythema, and wound drainage (46). Infection diagnostic tools include blood tests, imaging, polymerase chain reaction (PCR), and microbiological cultures (43-45). Administering systemic antibacterial therapy is typically recommended, especially if the patient cannot undergo additional surgical procedures (47). Systemically delivered concentration levels at the wound site generally are below biofilm inhibiting levels, which can be up to 1,000 times greater than inhibitory concentrations for planktonic bacteria. Biofilm-inhibiting antibiotic levels delivered to a wound site systemically would cause harmful side effects to the ear, kidneys, or other organ systems (48, 49).

**Financial Burden**

Potential long-term wound infection effects include reducing the quality of life, prolonged systemic antibiotic therapy, delayed wound healing, latent infection recurrence, loss of limb, and revision surgeries (50). These outcomes can significantly increase medical costs (44), with SSIs in the USA accounting for approximately a $1.6 billion annual healthcare cost inflation (51). SSI attributable costs can average between $10,000 – 30,000 per occurrence (52-54). SSIs have the most significant annual costs comparing to all other infection sites (51). SSIs cost between $3.2 - 8.6 billion using the consumer price index for all urban consumers (CPI-U) and $3.5 - 10 billion using the consumer price index (CPI) for hospital inpatient services, according to a CDC report (51). The U.S. Bureau of Labor Statistics constructs the CPI-U which measures the average change over time in prices paid by all urban consumers for goods and services purchased for day-to-day living (51). Several additional variables can result in the most undesired outcomes, i.e., treatment failure or patient death (2, 41)

**Infection/Biofilm Formation**

The most common microorganisms that lead to pathogenic infections are *Staphylococcus aureus* (*S. aureus*), *Staphylococcus epidermis* (*S. epi*), *Pseudomonas aeruginosa* (*P. aeruginosa*), and

*Acinetobacter baumannii* (*A. baumannii*) (55). These bacteria, often isolated from gastrointestinal (GI) tracts and skin of healthy individuals' flora, may become pathogenic when introduced to wound sites (56). *S. aureus,* which is the culprit in up to 50% of all infections, including arthritis, myositis, osteomyelitis, and implanted devices (46, 55), is a prominent contributor to prosthetic joint infections (57, 58) and a leading cause of nongonococcal bacterial arthritis (2). These problems are exacerbated as resistance by *S. aureus* to antibiotics, first discovered in the '90s, is increasing at alarming rates (55). *S. aureus'* resistance nullifies many βετα-lactam antibiotics' efficacy, including methicillin-based specific-antibiotics, which work by inhibiting peptidoglycan cell wall synthesis in Gram-positive bacteria peptidoglycan cell wall synthesis (59). As bacteria resistance propagates, vancomycin-resistant *S. aureus* (VRSA) has become an increasingly problematic issue (60, 61), becoming a major nosocomial pathogen in the USA (60).

Gram-positive and Gram-negative specific broad-spectrum are antimicrobial agents typically administered to open fracture wounds to prevent infections. Bacteria adhering to wound tissue, on surfaces of implanted biomaterials, or to both may form a biofilm, which consists of a community of attached bacteria that can secrete ions, nutrients, polysaccharides, and other survival-promoting exopolymeric secretions (62). Persister cells within biofilm have lowered metabolic activity, making them less susceptible to antibiotics that work by interfering with growth or division. The low metabolic activity of the persister cells requires higher doses and concentrations of antibiotics to eradicate biofilm.

When the injury involves open fractures, infections develop at a 50% rate (8, 41). Due to open fractures' exposure to the environment, local antimicrobial agents combined with simple debridement and irrigation procedures are ineffective at infection prevention in complex injuries involving open fractures (8, 41). Infection prevention solutions are considered advantageous for novel research because of the increasing number of orthopaedic implant procedures with an infection rate of 5% (14, 42). Biofilm, surface adhering bacteria, present costly and exceptionally difficult-to-overcome ongoing challenges to infection management (63).

Biofilm formation begins as a single planktonic bacterium attaches to a surface, e.g., an implanted device or wound bed (Figure 1.1). Bacteria within the biofilm directly communicate with each other through secretion and recognition of small molecules such as diffusible signaling factors (64). Biofilm can readily form on implanted devices due to the biomaterial's surfaces through passive adsorption, presenting additional treatment challenges (65). Implanted devices passively adsorb bacteria on their biomaterial-based surfaces after implantation procedures. Post-surgical infection risk may increase in the presence of implanted biomaterials due to the host defense weakness exploitation by established biofilm bacteria (65). Microbial colonization of surfaces, known as biofilm formation, can cause damage to adjacent tissue damage and spread to cause pathogenic biomaterial-centered sepsis (66). Microbial colonization has implications as a primary causative pathogenesis factor in implant failures (44, 45). Additional surgeries for implant removal and replacement are often the only solution to eradicate implant-associated biofilm infections due to current treatment options' effectiveness (8, 67). Gram-positive aerobes, largely *staphylococci*, are responsible for a vast majority of implant device-associated orthopaedic infections (68).

Antimicrobial vulnerability and tolerance of biofilm can contribute to challenges in preventing and treating biofilm-associated infections (69). Conventional methods demonstrate limited success in preventing and treating biofilm-associated infections partly due to the evolution of biofilm antimicrobial tolerance. Antibiotics that possess high activity levels against various planktonic bacteria have demonstrated minimal to no success when evaluated against biofilm at the same concentration level; however, high activity antibiotics can be efficacious against biofilm at increased concentrations. Antimicrobials may penetrate the exopolymeric substance formed by bacteria; however, dormant persister cells may inhibit antibiotics from penetrating the cell membrane (70). Due to persister cells' nature and presence, a principal antibiotic mechanism targeting metabolically active or dividing cells becomes less effective, often requiring 1000x concentrations than efficacious planktonic concentrations (71). Some studies indicate that combining antimicrobials may increase

efficacy against biofilm with some antibiotics allowing bacteria recurrence when used alone (72). Implant-associated biofilm infection that requires removal directly impacts patient comfort, quality of life and increases the risk for surgical complications (64, 65). Novel treatment options' development and implementation are needed to reduce implant-associated biofilm infection removal surgeries.

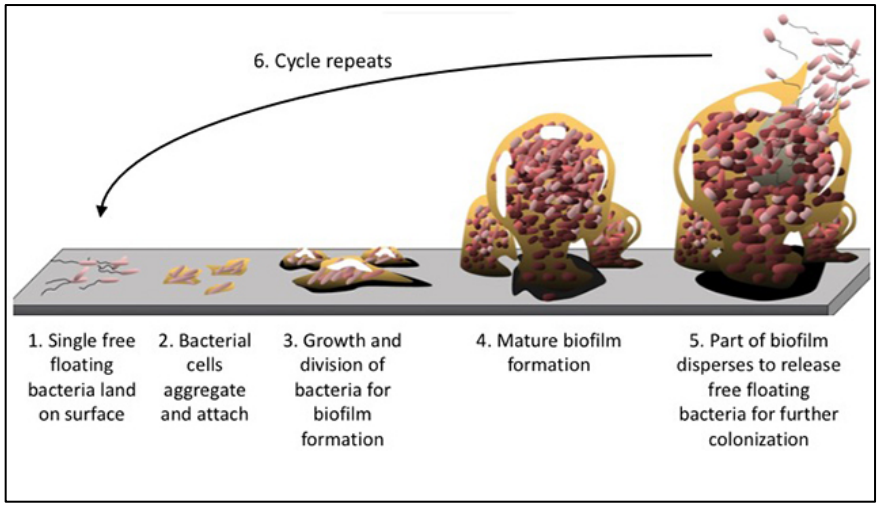


**Figure 1.1**. Biofilm formation and dispersion cycle pictorial depiction (reproduced with permission from © Springer Nature Singapore Pte Ltd. 2019)

Three aspects: visual assessment, definitive treatment goals, and treatment confirmation inform the antibiotic selection process for musculoskeletal wound infection treatment (73). These aspects include injury location, presenting symptoms, and common nosocomial pathogens, if present. Early antimicrobial administration increases infection prevention effectiveness and moderates the wound's exposure to the surrounding environment (74). A pathogen's susceptibility to antibiotics is a limiting factor when selecting antibiotics for infection treatment. Other constraints include maintaining an antibiotic concentration at the infection site above the minimal inhibitory concentration (MIC) level for a period long enough to ensure eradication of all microorganism contaminants. Antimicrobial tolerance increases the difficulty of combating musculoskeletal wound infections (63). Recent advances in wound screening allow identifying certain microbes before treatment (67, 75).

Fatty acids have shown an ability to disperse biofilms in many strains of microorganisms, with *cis*-2-decenoic acid (C2DA) showing particular activity against multiple strains of bacteria (68). Bacteria such

as *P. aeruginosa* produce C2DA, a medium-chain fatty acid chemical messenger (Figure 1.2) that signals biofilm dispersion for numerous bacterial strains (68). Davies et al. report that C2DA can disperse biofilm (76), and Jennings et al. demonstrated that it has inhibitory effects against *S. aureus* biofilm (62). The biofilm-inhibitory characteristic of C2DA makes it a potentially useful adjunct to antimicrobial therapy. Reports of several medium- and long-chain fatty acids, including C2DA, indicate bactericidal or growth inhibitory properties (77, 78). When combined with other antimicrobial therapeutics that are less successful against biofilm, C2DA could improve overall antimicrobial efficacy (62).

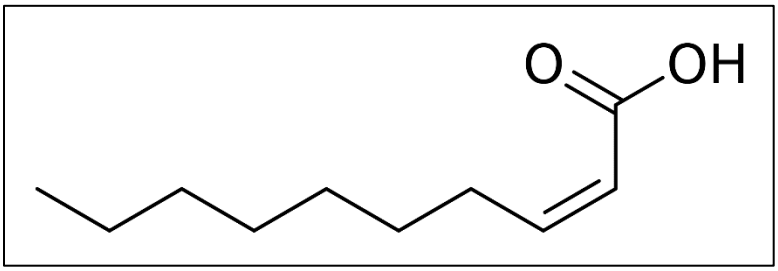


**Figure 1.2.** Skeletal structure of *cis*-2-decenoic acid showing ten-carbon chain backbone.

**Current Therapies**

Pain management strategies remain at the forefront of clinical needs, especially for musculoskeletal injuries. Cocaine's 1884 inception began the use of local anesthetics as pain management therapeutics (79). Not only are local anesthetics used to mitigate pain, but during recent decades several studies have illustrated their potential role as antimicrobials (79). Some anesthetics have exhibited fungistatic, fungicidal, bactericidal, and bacteriostatic properties against a broad spectrum of microorganisms (80). During the same period, multiple *in vitro* and *in vivo* studies have confirmed the auxiliary role of local anesthetics in SSI prevention and treatment (79). Most of the studies over the past 30 years validating the antimicrobial effect of local anesthetics have been *in vitro* (79). Reports of reductions in SSI rates are due to surgeon-directed therapies that include the practice of applying local anesthetics on incision sites before incision, during incision, or at closure (81). The LA antimicrobial *in vitro* properties combined with results indicating their efficacy in clinical practice warrants

further investigation of their applications in preventing infection, particularly when combined with other antimicrobials in local delivery systems.

Oral or intravenous drug delivery is well established; however, there are undesired effects, e.g., off-target consequences, reduced efficacy, and organ toxicity (82). Oral or intravenous antimicrobial therapy must maintain inhibitory concentrations in infected tissue to be effective but should not exceed systemic levels that are toxic to tissue (81). Local delivery devices loaded with antimicrobials are often implemented as an adjunct to systemic antimicrobial therapy for open wound and fracture treatments. The overall goal of local delivery is to achieve high local levels of bioactive antimicrobials with negligible serum levels and delivery over extended periods until healing is complete (82). The elution or release of antimicrobials from the local delivery system into the surrounding tissue depends on the delivery system matrix, surface area, volume, and concentration of loaded antimicrobial (83). Systemically administered antimicrobials have low penetration into bone; conversely, locally-delivered antimicrobials can achieve greater diffusion to bone and avascular wound areas (81). Local antimicrobial delivery increases potency while simultaneously minimizing systemic toxicity providing the basis for an improved delivery system (82).

Biodegradable delivery devices may improve local antimicrobial delivery efficacy with the added advantage of being implanted at the wound site reducing delays between delivery and action. Biodegradable devices are broken down naturally through hydrolytic mechanisms in the presence or absence of supplemental enzymes. A principal advantage of locally delivered biodegradable devices is their ability to alleviate the need for additional surgeries to remove the foreign antimicrobial delivery device. The current “gold standard” local delivery systems include poly(methyl methacrylate) (PMMA) beads and spacers that do not biodegrade (83, 84). Alternatives to PMMA have been considered, including bioresorbable calcium sulfate, which could mix with antibiotics before casting; however, these materials release high concentrations of antimicrobials that may be toxic and lead to seroma formation (83).

Chitosan is a linear polysaccharide composed of N-acetyl glucosamine and glucosamine repeat units (85). Chitin, widely distributed in nature, is used to derive chitosan (86). Chitin, white, rigid, and inelastic, is a natural polysaccharide composed of N-acetyl-glucosamine units isolated from the exoskeletons of arthropods, e.g., crustaceans and insects, fungi cell walls, mollusks radulae, fish scales, cephalopod beaks, and lissamphibian skin. One major procedure utilized to obtain chitosan involves subjecting the chitin polymer to a strong alkaline solution that slowly removes acetyl groups from N-acetyl-glucosamine repeat units in a process referred to as de-acetylation (87). Chitosan is distinguished from chitin by the number of remaining acetyl units. Chitin has a degree of acetylation ranging from 0 - 50% compared to a degree of de-acetylation (DDA) for chitosan of > 50%. Once DDA is > 50% the copolymer becomes chitosan. The DDA impacts how chitosan performs (88, 89). Chitosan possesses a weak cationic base, is insoluble in water and organic solvents; however, the polymer is soluble in dilute acidic conditions (86, 90). Chitosan has biodegradable (90-93) and antibacterial (94) characteristics making it advantageous in drug delivery applications (91-93, 95).

Chitosan's DDA affects degradability; when DDA is close to 50%, chitosan demonstrates high degradability *in vivo*; however, when DDA is > 95%, chitosan may reside *in vivo* for months (90). Lysozyme, N-acetyloglucosaminidase, and lipases degrade chitosan within the body (96). Lysozyme degrades chitosan through cleavage of glycosidic bonds between repeating units, producing saccharides and glucosamines byproducts, which are incorporated into glycoproteins or excreted as carbon dioxide (97). Chitosan's biodegradability allows implementation into local delivery systems for antimicrobials averting the need for removal surgeries, reducing total cost and patient trauma, in direct contrast to comparable devices, e.g., PMMA beads.

Currently, there are more than 200 applications or practical applications involving chitin, chitosan, or a derivative (98-102). Applications include cosmetics, food, agriculture, biomedical, and textiles, to name only a few. Medical applications for chitosan include utilization as wound dressings (103, 104), orthopaedic and

craniofacial implant bioactive coatings (105, 106), and local drug delivery systems, amongst others (98, 99, 107-111). Chitosan local delivery systems have included vancomycin (107), amikacin (110), gentamicin (99), prednisolone (109), daptomycin (110), recombinant human bone morphogenetic protein-2 (rhBMP-2) (98), rifampin (112), and ciprofloxacin (112) among many others. Chitosan leads to rapid clot formation when partially hydrated, providing potential usage as a bandage or hemostatic agent (99). When fully hydrated, chitosan has properties allowing rapid rehydration and drug absorption (103).

Recent work involving nanofibrous chitosan-based biomaterials fabricated with an electrospinning process offers advantages in drug delivery that may provide for extended-release of antimicrobials, mainly when stabilized with hydrophobic modifications by acylation (113, 114). Chitosan-based biomaterials require stabilization methods to be functional as a sustained local delivery device due to their pH levels. Sodium hydroxide or acetate buffer stabilized previous chitosan-based biomaterials to increase pH to near neutral (112, 115, 116). Previous chitosan-based biomaterials, i.e., chitosan sponges and chitosan paste, were stabilized and possessed functionality; however, they had limitations in their ability to load or release hydrophobic compounds (112, 115, 117, 118). The electrospun nanofibers' acylation techniques (113, 114) can extend to the broad range of other chitosan-based biomaterials, such as particles or paste. Acylated nanofibrous biomaterials not only can load hydrophobic compounds; once loaded, their elution kinetics extend (114), which would be advantageous over the typical first-order release kinetics observed for other chitosan-based biomaterials (112, 115, 117). Sustained-release promotes increased infection and biofilm inhibition.

Infected musculoskeletal wounds are challenging; specifically, those associated with biofilm, and they present challenges to the healthcare system with ongoing research efforts to combat them. Current clinical practices, including wound debridement, lavage, and fixation, may not be adequate to manage biofilm-associated infections without systemic delivery, local antibiotic delivery, or the combination. Crucial objectives for immediate management of traumatic musculoskeletal wounds or surgical site injuries include

wound healing promotion, pain management, and infection prevention (38). Increasing numbers of SSIs and growing antibiotic resistance are growing concerns in the fight against infections (45, 56). C2DA, along with other biofilm inhibitors and dispersal agents, may increase antibiotic efficacy against biofilm and minimize antimicrobial tolerance. Local anesthetics can provide localized and targeted pain relief along with antimicrobial benefits, which may reduce the need for prescription or intravenous opioids. Local delivery of antimicrobials using a biodegradable chitosan-based system offers a potential solution for delivering antimicrobial and anesthetic molecules over extended periods as an adjunctive musculoskeletal wound treatment.

**Hypothesis**

Chitosan-based biomaterials, modified by acylation, will form a cytocompatible and biocompatible local delivery system capable of loading multiple hydrophobic therapeutics and deliver them for at least 72 hours. It was also hypothesized that various local anesthetics and *cis*-2-decenoic acid would have antimicrobial efficacy against numerous bacterial strains. Combined bupivacaine and C2DA delivery from modified chitosan paste was expected to reduce infection when evaluated in an *in vivo* model effectively. Answers to these research questions will characterize these biomaterials' potential as adjunctive therapies for infection and biofilm inhibition and the potential to provide localized targeted pain relief.

# CHAPTER 2

## Synthesis and Characterization of 2-decenoic Acid Modified Chitosan for Infection Prevention and Tissue Engineering

### Introduction

Chitosan is considered a promising therapeutic delivery agent due to its biodegradability, biocompatibility, non-toxicity, and inherent antimicrobial activity (1, 2). Chitosan is a sugar-based biopolymer derived from exoskeletons of arthropods. Structurally, chitosan is a heteropolymer composed of N-acetyl-D-glucosamine and D-glucosamine unit connected through β (1-4) glycosidic bond. Chitosan has three reactive functional groups: an amine group at the C-2 position and primary and secondary hydroxyl groups at C-6 and C-3 positions, respectively. Chitosan is polycationic at a pH below six and interacts with negatively charged molecules, such as proteins, anionic polysaccharides, fatty acids, bile acids, and phospholipids (3). Chitosan is a versatile biopolymer due to its flexibility that allows manufacturing into various forms such as gels, nanofibers, pastes, films, etc. Electrospun chitosan membranes are of particular interest for biomedical applications due to their porous nanofibrous structure and high surface area that mimics the extracellular matrix. Multiple biomedical applications, including wound dressings, drug delivery, and tissue engineering, involve nanofibrous chitosan membranes (4, 5).

Chemical modification of electrospun chitosan membranes can enhance their physicochemical properties, further functionalizing the material to allow for a broader range of applications. For example, the incorporation of hydrophobic substituents such as fatty acids generates a domain for absorbing and carrying poorly soluble drugs. Literature supports fatty acid (FA)-treated electrospun chitosan membranes' ability to control the hydrophobic drug simvastatin release (6). Linoleic and α-linolenic acid-modified chitosan has demonstrated

potential as a multifunctional catheter coating by improving the lubricity and antimicrobial properties (7). A study also found that fatty acid incorporated chitosan can improve the self-nano-emulsifying drug delivery system's mucoadhesive property (8). Studies investigated decanoic acid grafted chitosan as a potential carrier of insulin by combining the mucoadhesive and permeative properties of chitosan and decanoic acid, respectively (9). Decanoic, oleic, and linoleic acid-modified chitosan have enhanced wound healing rates (10, 11). The length of the fatty acyl chain incorporated through O-acylation improves its stability in the moist environment while maintaining its non-toxic property and has shown promise for regenerating bone in guided bone regeneration (GBR) applications in rodent models (12-14). A study using buriti oil containing volatile compounds and fatty acids indicated that chitosan and buriti oil could be combined into a gel to improve chemical properties and activity against Gram-negative pathogens (15). Besides the antimicrobial activity, chitosan gel with buriti showed antioxidant and anti-inflammatory properties, good healing activity, and an adequate wound retraction rate (15).

Trifluoroacetic acid (TFA) is one of the most commonly used solvents for electrospinning chitosan membranes because it provides adequate viscosity for the polymer solution to be pulled into nanofibers (6, 16). Despite this benefit, TFA forms a salt with chitosan's amino groups, requiring removal without compromising the nanofibrous structure or deteriorating the membrane's mechanical properties. One technique to achieve this balance involves grafting FA groups to the hydroxyl groups outside of the chitosan fibers to create a hydrophobic covering to prevent fiber swelling during subsequent washing steps to remove TFA ions (13). FA chains can be attached to any of the three reactive groups; acid chlorides and methanol crosslink FAs in the amine position (17, 18). Acylation reactions may also use a

coupling agent such as 1-ethyl-3-(3-dimethyl-aminopropyl)-1-carbodiimide hydrochloride (EDC) to improve the reactivity (7). The TFA salt in the electrospun chitosan membrane occupies the amine group (16). Wu et al. developed an O-acylation method in which the chitosan membrane is acylated by acid anhydride in the presence of a pyridine catalyst to improve its stability in an aqueous solution (12, 14). Attempts to incorporate fatty acyl chains before electrospinning the membrane resulted in non-uniform size and distribution of the fibers; due to steric hindrance of the long FA chain in uniform and fine formation fibers (19-21).

The fatty acid 2-decenoic acid (2DA) and its analogs are medium-chain FA chemical messengers naturally produced by bacteria. Studies have shown that the *cis*- form of 2DA (C2DA) disperses existing biofilm and inhibits biofilm formation (22). Studies suggest that 2DA could increase microbes' metabolic activity and the bactericidal ability of commonly used antimicrobials (23). These properties could make 2DA a potential complementary therapy for infection. Additionally, 2DA could lessen antibiotic tolerance by improving the efficacy of these drugs against biofilm infection. Acylating chitosan membranes with 2DA or analogs may provide the advantages of bacterial biofilm resistive materials and the ability to load with hydrophobic therapeutics for extended-release. However, chlorides or anhydrides of 2DA are not commercially available. This study investigates a custom-synthesis route for acyl chlorides and their ability to stabilize and functionalize chitosan nanofibers. Additionally, it determined physicochemical properties, antimicrobial properties, and cytocompatibility (24).

## Materials and Methods

### Fabrication of Electrospun Membranes

Nanofibrous chitosan membranes were electrospun using Primex (Iceland) chitosan (71% DDA, 311.5 kDa). Chitosan was dissolved overnight at 5.5% (w/v), of 70:30% (v/v) TFA

and dichloromethane (DCM) purchased from Sigma Fisher (USA). The 10 mL solution was centrifuged to remove any insoluble chitosan, transferred to a syringe with a 20gauge blunt needle, and electrospun at a rate of 15 mL $min^{-1}$ and a voltage of 27 kV using a syringe pump onto an aluminum foil covered collector plate rotating at ~8.4 revolutions per minute, with constant monitoring of the Taylor Cone to ensure high-quality membranes. The electrospinning apparatus was housed inside a ventilated box which was vented to the fume hood. The apparatus was operated at room temperature and 40 to 60% humidity, using humidity monitors and humidifiers. Membranes were spun from three 10 mL volumes to obtain a diameter of 15 cm and a thickness of approximately 700 nm. After membranes were fabricated, 10 mm diameter discs were punched out for use in experiments.

**Synthesis of 2-decenoyl Chloride**

A reflux reaction was used to synthesize 2-decenoyl chloride by first placing 1 M (40 g $L^{-1}$) of sodium hydroxide (NaOH) in a covered beaker on ice. The NaOH beaker was then connected to a condenser unit in a water bath set at 35 °C. First, 150 mmol thionyl chloride was added to a three-neck round bottom flask. Second, while slightly shaking the flask, 100 mmol of 2-decenoic acid was added. Once both compounds were in the flask, the flask was connected to the condenser system, sealed, and reacted for five hours. After reaction completion, the synthesized 2-decenoyl chloride was removed from the flask and stored until later use. Decanoyl chloride (DC) and hexanoyl chloride (HC) were purchased from Sigma Fisher (USA).

**Acylation Reactions**

The direct acylation of chitosan materials by acyl chlorides was achieved by first making a 5 mg $mL^{-1}$ solution of chitosan material in pyridine. With a ratio of 3:1 (v/v) pyridine to acyl chloride, the acyl chloride was slowly added while stirring. The solution reacted for 1.5 hours.

Once the reaction was complete, the chitosan materials were removed and 1) placed in 10% acetone solution (1 L), 2) removed and placed in 70% ethanol solution, and 3 - 5) removed and placed in deionized water (DI) each step lasted for at least one hour. After the final washing step, the chitosan materials were removed from the solution, placed flat onto a glass surface, and frozen at -80 °C. The frozen materials were lyophilized. After lyophilization, the materials were stored in a desiccator until further analysis.

**FTIR**

Attenuated Total Reflectance (ATR) Fourier Transform Infrared (FTIR) spectra were collected using an FTIR spectrometer, Frontier (Perkin-Elmer, USA). ATR spectra were collected to confirm the attachment of FA groups to the chitosan polymer chain and TFA salt removal by the treatments.

**Contact angle**

Water contact angles of modified membranes were determined using a VCA optima measurement machine (AST products, INC, USA). Water droplets (5 μL) were placed carefully onto the membrane surfaces. A digital camera recorded the photographs of the droplets after approximately one minute. The goniometry software of VCA OptimaXE calculated the contact angles. For each modification, four different membranes were tested at three regions.

**Cytocompatibility**

NIH 3T3 (American Type Culture Collection) fibroblasts were seeded at a concentration of $10^4$ cells $cm^{-2}$ in a 24-well plate in Dulbecco's Modified Eagle's Medium (DMEM) high glucose supplemented with 10% fetal bovine serum (FBS, Gibco) and 2% (100 μg $mL^{-1}$) Normocin (InvivoGen, San Diego, CA). Chitosan membranes were placed into well inserts and then immersed into the wells containing cells and media. Plates were incubated at 37 °C with 5%

carbon dioxide ($CO_2$). Every 24 hours, the inserts were removed, the wells were bright field imaged, and the media was refreshed. Controls with no membranes were used to normalize the cells' viability percentage. After 48 hours, viability was determined using CellTiter-Glo® (Promega) and expressed as a percentage of tissue culture plastic controls.

**Antimicrobial Activity**

*Pseudomonas aeruginosa* (*P. aeruginosa,* ATCC #27317) and *Staphylococcus aureus* (*S aureus*, UAMS-1, a clinical osteomyelitis strain) grown overnight were diluted to 1:50 and 1:10 respectively. Diluted bacteria (500 μL) were added to the well containing HC, DC, trans-2-decenoic acid (T2DA) chloride modified membranes, sponge, or gauze, and incubated for 24h. The membranes, sponges, and gauzes were taken out of the solution after the incubation period and washed three times with 500 μL of 1X phosphate-buffered saline (PBS). They were then immersed in 500 μL of sterilized tryptic soy broth (TSB) and sonicated for 5 min to detach the bacteria. After sonication, the detached bacteria solution was used for colony forming unit (CFU) counting by plating dilutions.

**Statistical Analysis**

SigmaPlot and GraphPad Prism 7.2 software (GraphPad Software Incorporation, La Jolla, CA, USA) was used to perform the statistical analysis. Data was assessed first by performing Shapiro-Wilk normality test, followed by Brown-Forsythe equal variance test. If both passed, a one-way analysis of variance (ANOVA) further analyzed the data, followed by Holm-Sidak's post-hoc analysis to detect significance between experimental groups ($\alpha = 0.05$). Kruskal-Wallis ANOVA on ranks, followed by Tukey post-hoc test, completed additional analysis if necessary normality and equal variance requirements did not occur.

## Results

### Fabrication

Scanning Electron Microscope (SEM) images showed that fibers formed and stabilized with each acylation method without significant swelling when compared to the fibers of an unmodified nanofibrous chitosan membrane (Figure 2.1).

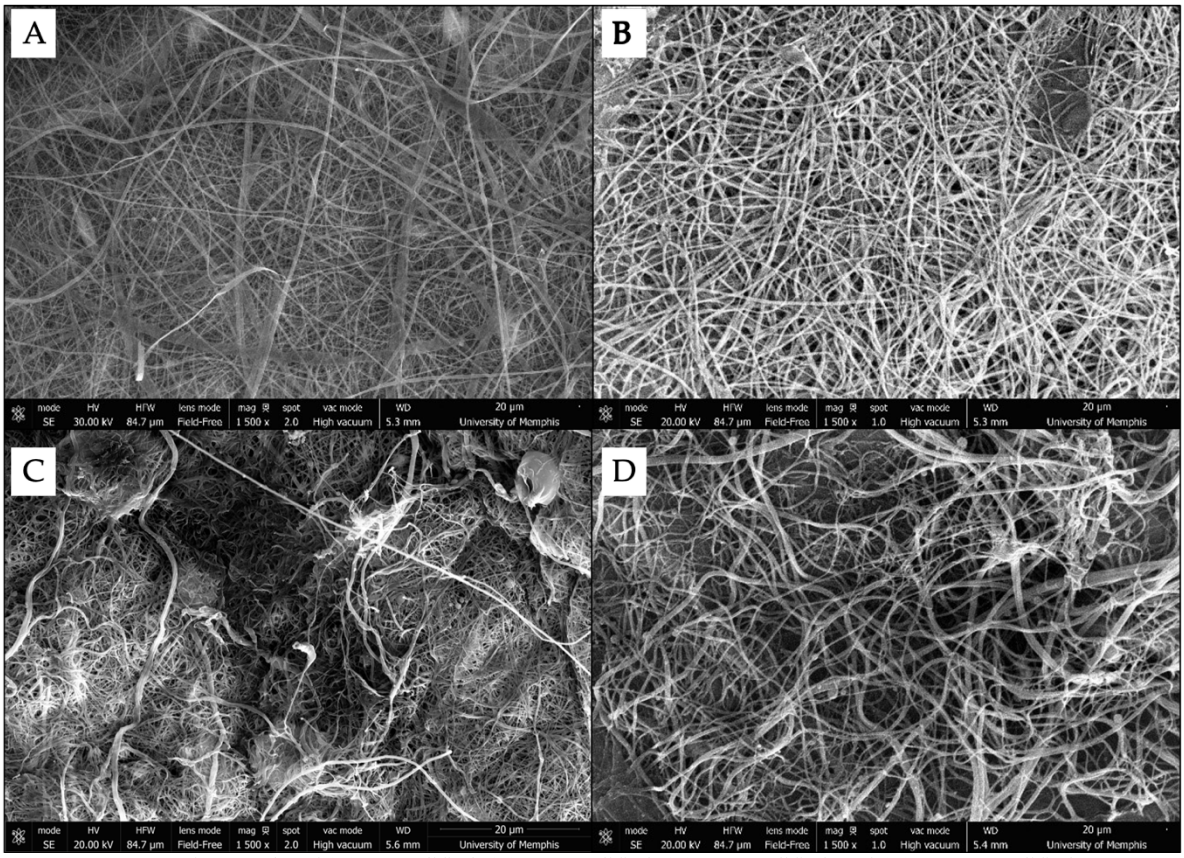


**Figure 2.1**. SEM micrographs of (A) unmodified, (B) HC modified, (C) HC modified, and (D) T2DA modified membranes.

### FTIR

FTIR analysis comparing chitosan membranes with various acylation treatments confirms a presence of an ester carbonyl group on the treated membranes (peak at 1750 $cm^{-1}$), indicating successful acylation for all three modifications (Figure 2.2). Peaks around 2900 $cm^{-1}$ also confirm alkyl chains at the surface of the treated membranes, with increased intensity with increasing FA chain lengths. The two peaks around 3300 and 3500 $cm^{-1}$ for DC modified and

HC modified membranes represent NH2. The lack of peaks < 1000 $cm^{-1}$ in treated membranes confirms the removal of TFA salts.

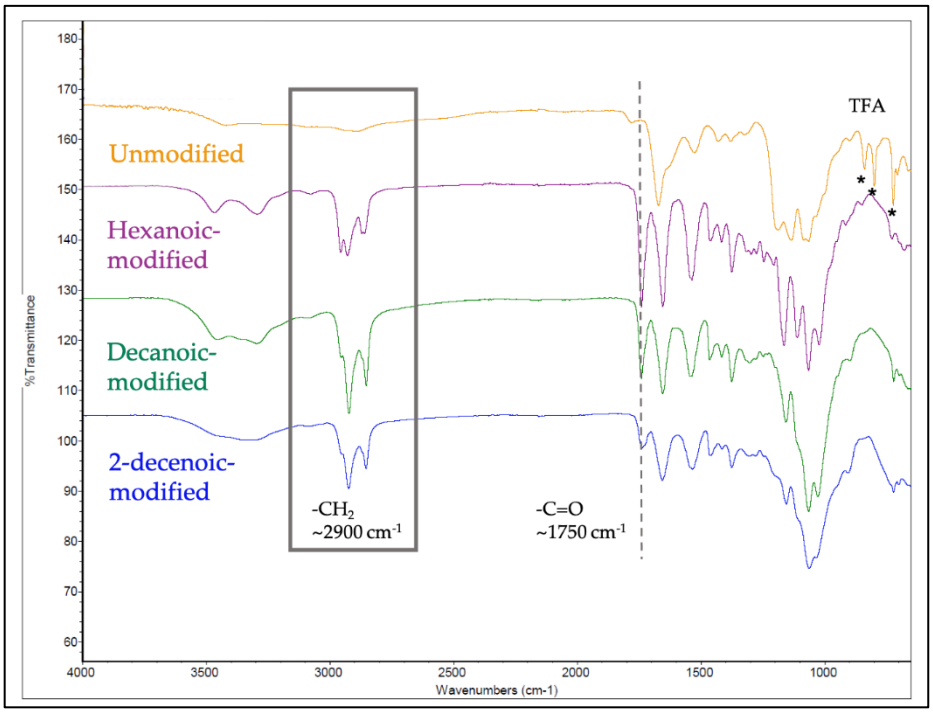


**Figure 2.2.** FTIR spectra of chloride modified and unmodified nanofibrous chitosan membranes.

## Contact angle

Water droplets remained stable on hexanoic-acylated membranes for 3 - 5 minutes, whereas for decanoic-acylated and 2-decenoic-acylated, the drop remained stable even after 15 min. Among all the treatments, 2-decenoic-acylated membranes were the most hydrophobic (121.50° ± 6.2°) as seen in Table 2.1.

**Table 2.1**. Water contact angle measurement (mean ± standard deviation) of modified membranes (n = 3).

| Membrane Modification | Water contact angle (°) |
|---|---|
| HC | 74.10°± 3.5* |
| DC | 93.20°± 5.6* |
| 2-decenoic | 121.50° ± 6.2* |

* indicates statistically different groups, $p < 0.05$

**Antimicrobial activity**

The sponge control had significantly more *P aeruginosa* CFUs counted than all other groups (Figure 2.4). The CFU count for hexanoic modified membranes was similar to the CFU count for the gauze control; however, the CFU counts for decanoic modified and 2-decenoic modified membranes was noticeably less than the gauze and sponge controls for *S aureus* (Figure 2.4) and *P. aeruginosa* (Figure 2.5).

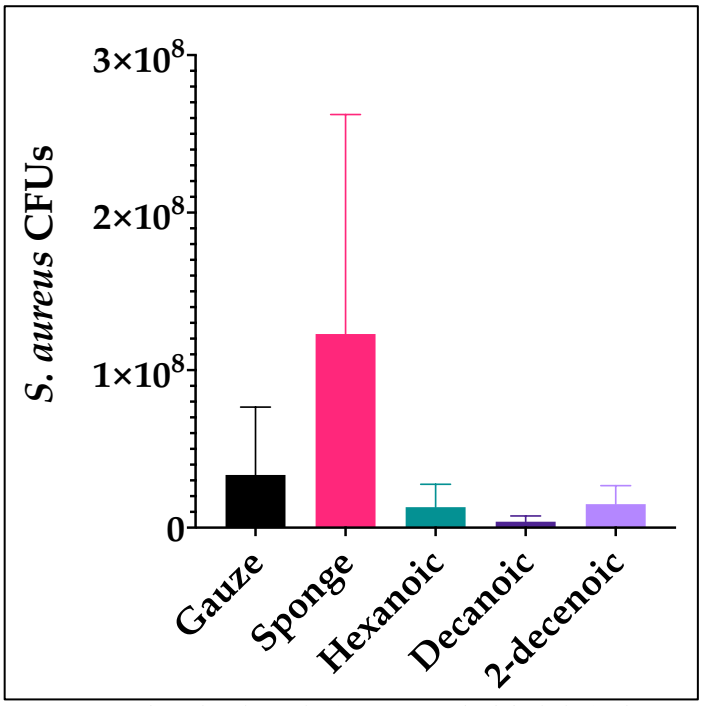


**Figure 2.3**. Colony forming units (mean ± standard deviation) of *S. aureus* on the modified chitosan membranes (n = 3). No statistically significant differences were detected.

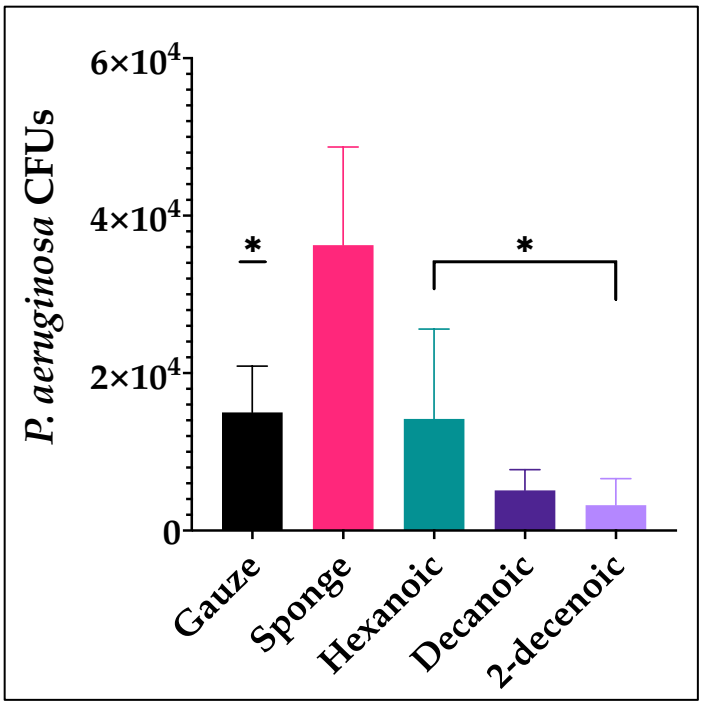


**Figure 2.4**. Colony forming units (mean ± standard deviation) of *P. aeruginosa* on the modified chitosan membranes (n = 3). * indicates significant difference ($p < 0.05$) between sponge and denoted groups.

SEM images of biofilm attached to membranes confirmed that some sparse colonies of *S. aureus* exist on hexanoic- and decanoic-acylated membranes, with very few observed on 2-decenoic membranes. *P. aeruginosa* formed abundant exopolymeric substance (EPS) on gauze fibers (Figure 2.6). In contrast, while *P. aeruginosa* subsisted on acylated membranes, EPS formation was minimal.

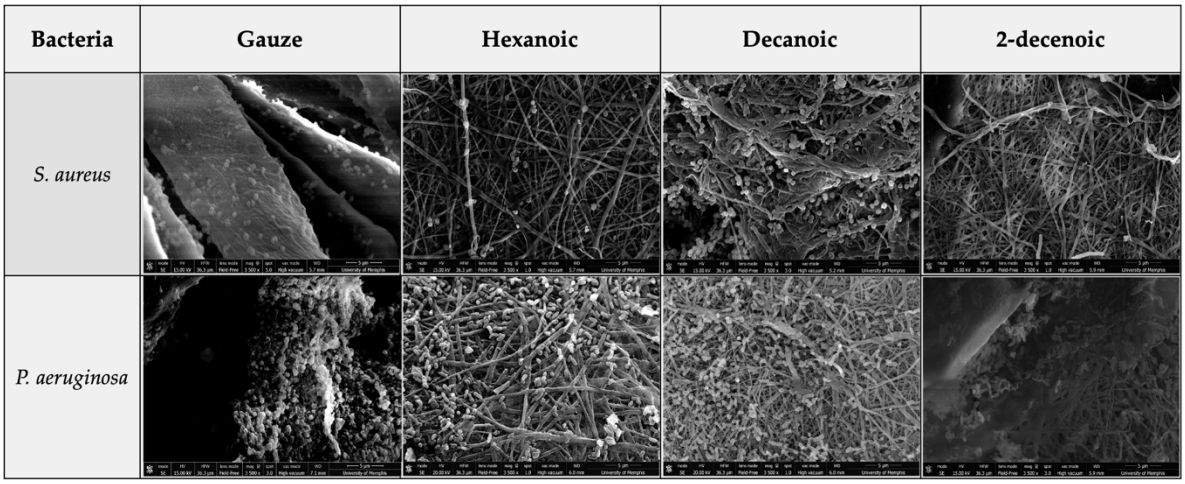


**Figure 2.5**. SEM micrographs of biofilms attached to gauze and modified chitosan membranes. The chitosan sponge is not shown due to issues relating to the critical point drying procedure.

## Cytocompatibility

When exposed to membranes modified by acyl chlorides, the percent viability of cells showed no significant differences, and all were above the ISO standard 70% cytocompatibility threshold (25), denoted by the black line (Figure 2.7).

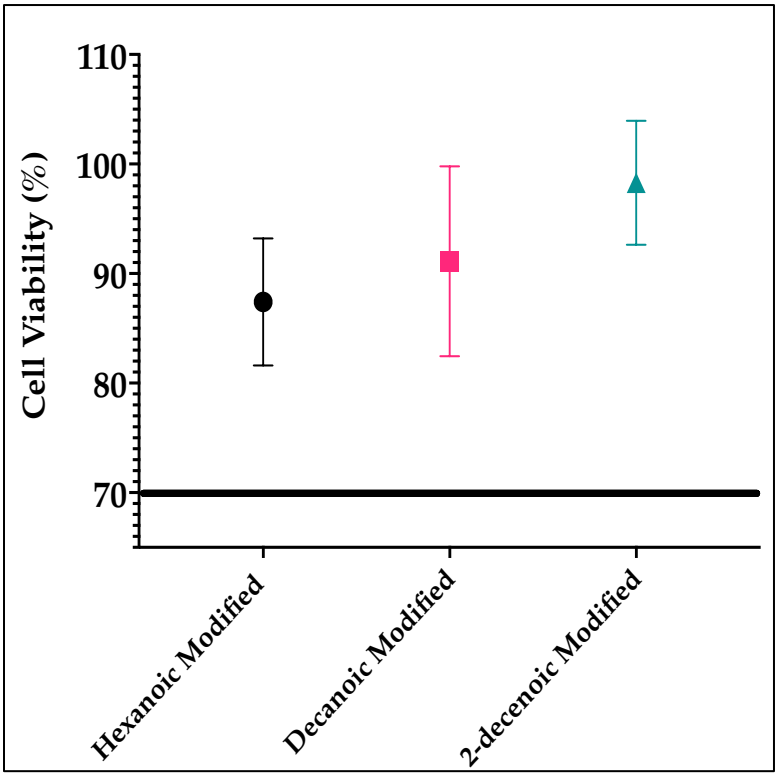


**Figure 2.6**. Graph shows cytocompatibility testing of acyl-chloride modified membranes (n = 3) in transwell in contact with NIH 3T3 cells.

## Discussion

The study results show the initial success of the acyl chloride synthesis and chitosan modification process. Synthesized chlorides are customizable, making previously commercially unavailable compounds accessible for acylation processes. Synthesized chlorides can modify various chitosan-based biomaterials' properties in a nondetrimental way, particularly in that the functionalization imparts hydrophobic properties that limit bacterial attachment and may also allow loading and release of therapeutics (6, 7). Acidic hydrochloride salt formulations are not necessary for loading local anesthetics in acylated chitosan biomaterials. The ability to

synthesize chlorides that are not commercially available could expand the possible applications to other fatty acid analogs, including *cis*-2-decenoic acid and 2-heptylcyclopropane-1-carboxylic acid, to expand possible antimicrobial solutions in the continuing fight against antibiotic resistance and complex biofilm-associated infections.

FTIR results indicate immobilization of FAs on the fibers. The absorption peak around 1750 $cm^{-1}$ representing the acyl group (C = O) and ester bond formation confirms acylation. Ester bonds may be particularly advantageous for these materials in infection prevention. In the presence of acidic environments such as those found locally at tissue injury sites or in the presence of bacterial enzymes, such as lipase, they may hydrolyze (22, 23). Environment-influenced hydrolysis may cause acylated chitosan biomaterials to be less reactive until interaction with bacteria or damaged tissue. This study did not measure the hydrolysis rate of fatty acids; future studies will investigate whether conjugated 2DA release is lipase- or pH-sensitive. FTIR spectra broad peaks at 3100 - 3500 $cm^{-1}$ represent inter- and intra-molecular hydrogen bonding of the —NH2 and —OH vibration stretching of chitosan molecules (13). Of note, TFA salt representative transmittance peaks at 720, 802, and 837 $cm^{-1}$ are not present in any of the modified chitosan biomaterials that confirm the salts are no longer present.

Water contact angle provides a preliminary validation of the introduced hydrophobic properties to the hydrophilic chitosan biomaterial. The contact angle results for this study using acyl chlorides are consistent with prior studies that used acyl anhydrides (6) in that the contact angle increases with the chain length. Decanoic and 2-decenoic acids have the same chain length, with 2DA having one unsaturated bond. However, the unsaturated fatty acid should have less hydrophobicity than the saturated decanoic acid. The differences in contact angle observed in this evaluation may be due to varying degrees of substitution. Introducing hydrophobic

properties to biomaterials may affect protein adsorption properties, improve hydrophobic compounds' elution kinetics, and stabilize structures. Previous investigations produced numerous chitosan-based biomaterials that can load and deliver hydrophilic therapeutics, e.g., paste and sponges (26-30). The acylation modification strategy may enable improved hydrophobic molecule usage with the same chitosan-based biomaterials, which past hydrophobic molecule inclusion proved to be a challenge (31).

Fibers did not significantly swell after the acylation process, as evident by SEM analysis. Being able to maintain nanofibrous structure is critical to the development and function of this chitosan biomaterial. Future studies will need to address these limitations to improve the chances for modified chitosan biomaterials' use in specific clinical applications. Future studies will use more materials characteristic methods, i.e., NMR, to determine structure and base catalysis methods to conclude the degree of substitution.

Acylated chitosan membranes demonstrated the ability to inhibit bacterial growth and attachment (CFUs). In all antimicrobial testing conditions, the acylating nanofibers showed evidence of reduced biofilm attachment. The modified materials' degree of substitution is one potential characteristic that reinforces the demonstrated inhibition. Surface attachment is one of the biofilm mechanisms to develop and persist. Modified chitosan nanofibrous membranes have more surface area for bacteria to attach than chitosan sponge or gauze and still produced better bacteria inhibition results. These findings support the hypothesis that acyl-modification contributes to improved material antimicrobial properties. Acyl-modified materials seem to inhibit *P. aeruginosa* EPS production. Reducing EPS secretion from *P. aeruginosa* blocks a primary mechanism *P. aeruginosa* uses to form a biofilm, and modified materials may interfere with type IV pili (32-34). *S. aureus* biofilm inhibitory effects may be due to interference with

microbial surface components recognizing adhesive matrix molecules (MSCRAMM). MSCRAMMs are instrumental in *S. aureus* attachment and subsequent biofilm formation (35). When unattached bacteria remain in the planktonic state longer, they are more susceptible to antimicrobials and the innate immune system. This study chose *S. aureus* and *P. aeruginosa* as representative Gram-positive and Gram-negative strains that are common pathogenic strains in bone and wound injuries. The modified membranes' efficacy against other bacterial and fungal strains is necessary to understand their broad antimicrobial efficacy.

Bacterial inhibition without maintaining cyto- and bio-compatibility invalidates any potential antimicrobial therapy. All acyl-modified materials demonstrated cytocompatibility with no statistical significance between any of the evaluated groups. All modified membranes met or exceeded the minimum 70% cellular compatibility threshold. Future studies will evaluate the effects of these materials on other cell types, such as immune cells, and assess biocompatibility *in vivo* . While this study did not assess unmodified material as controls, the acyl-modified materials performed similarly to previously investigated chitosan-based materials (6, 27, 36). There are no signs of acyl-modified materials adversely affecting cells or any signals that healing would be negatively affected (10). The modified nanofibers' bacterial inhibitory effects would be advantageous in clinical applications involving wound dressings or wraps, bone scaffolds, or guided tissue regeneration membranes, among others.

In summary, modified chitosan biomaterials possess characteristics that support their use in infection prevention treatment strategies. We can functionalize chitosan with a specific fatty acid which may have applicability to other fatty acid conjugation with our synthesis route. Future studies will evaluate conjugated fatty acid hydrolysis rate in physiological relevant solutions, including acidic and in the presence of enzymes, e.g., lipase. Additional future and ongoing

studies will characterize the modified materials' drug delivery capabilities, including therapeutic loading and release, including but not limited to local anesthetics, statins, chemotherapeutics, and antimicrobials.

**References**


1. Goy RC, Britto Dd, Assis OB. A review of the antimicrobial activity of chitosan. Polímeros. 2009;19(3):241-7.
2. Mohebbi S, Nezhad MN, Zarrintaj P, Jafari SH, Gholizadeh SS, Saeb MR, et al. Chitosan in biomedical engineering: a critical review. Current stem cell research & therapy. 2019;14(2):93-116.
3. Ahmed S, Ikram S. Chitosan based scaffolds and their applications in wound healing. Achievements in the life sciences. 2016;10(1):27-37.
4. Azad AK, Sermsintham N, Chandrkrachang S, Stevens WF. Chitosan membrane as a wound-healing dressing: characterization and clinical application. J Biomed Mater Res B Appl Biomater. 2004;69(2):216-22.
5. Lee EJ, Shin DS, Kim HE, Kim HW, Koh YH, Jang JH. Membrane of hybrid chitosan-silica xerogel for guided bone regeneration. Biomaterials. 2009;30(5):743-50.
6. Murali VP, Fujiwara T, Gallop C, Wang Y, Wilson JA, Atwill MT, et al. Modified electrospun chitosan membranes for controlled release of simvastatin. International Journal of Pharmaceutics. 2020:119438.
7. Niemczyk A, Kmieciak A, El Fray M, Piegat A. The influence of C18-fatty acids on chemical structure of chitosan derivatives and their thermal properties. Progress on Chemistry and Application of Chitin and its Derivatives. 2016;21:165-75.
8. Efiana NA, Mahmood A, Lam HT, Zupančič O, Leonaviciute G, Bernkop-Schnürch A. Improved mucoadhesive properties of self-nanoemulsifying drug delivery systems (SNEDDS) by introducing acyl chitosan. International journal of pharmaceutics. 2017;519(1-2):206-12.
9. Costa Fo, Sousa DM, Parreira P, Lamghari M, Gomes P, Martins MCL. N-acetylcysteine-functionalized coating avoids bacterial adhesion and biofilm formation. Scientific reports. 2017;7(1):1-13.
10. Dang Q, Zhang Q, Liu C, Yan J, Chang G, Xin Y, et al. Decanoic acid functionalized chitosan: Synthesis, characterization, and evaluation as potential wound dressing material. International journal of biological macromolecules. 2019;139:1046-53.
11. Bonferoni M, Sandri G, Dellera E, Rossi S, Ferrari F, Mori M, et al. Ionic polymeric micelles based on chitosan and fatty acids and intended for wound healing. Comparison of linoleic and oleic acid. European Journal of Pharmaceutics and Biopharmaceutics. 2014;87(1):101-6.
12. Zhang Z, Jin F, Wu Z, Jin J, Li F, Wang Y, et al. O-acylation of chitosan nanofibers by short-chain and long-chain fatty acids. Carbohydrate polymers. 2017;177:203-9.
13. Wu C, Su H, Karydis A, Anderson KM, Ghadri N, Tang S, et al. Mechanically stable surface-hydrophobilized chitosan nanofibrous barrier membranes for guided bone regeneration. Biomedical Materials. 2017;13(1):015004.
14. Wu C, Su H, Tang S, Bumgardner JD. The stabilization of electrospun chitosan nanofibers by reversible acylation. Cellulose. 2014;21(4):2549-56.
15. Ferreira MOG, Lima IS, Ribeiro AB, Lobo AO, Rizzo MS, Osajima JA, et al. Biocompatible Gels of Chitosan–Buriti Oil for Potential Wound Healing Applications. Materials. 2020;13(8):1977.
16. Hasegawa M, Isogai A, Onabe F, Usuda M. Dissolving states of cellulose and chitosan in trifluoroacetic acid. Journal of applied polymer science. 1992;45(10):1857-63.

17. Xu J, McCarthy SP, Gross RA, Kaplan DL. Chitosan film acylation and effects on biodegradability. Macromolecules. 1996;29(10):3436-40.
18. Le Tien C, Lacroix M, Ispas-Szabo P, Mateescu M-A. N-acylated chitosan: hydrophobic matrices for controlled drug release. Journal of Controlled Release. 2003;93(1):1-13.
19. Davies DG, Marques CN. A fatty acid messenger is responsible for inducing dispersion in microbial biofilms. Journal of bacteriology. 2009;191(5):1393-403.
20. Namazi H, Dadkhah A. Convenient method for preparation of hydrophobically modified starch nanocrystals with using fatty acids. Carbohydrate Polymers. 2010;79(3):731-7.
21. Dinescu S, Ionita M, Pandele AM, Galateanu B, Iovu H, Ardelean A, et al. In vitro cytocompatibility evaluation of chitosan/graphene oxide 3D scaffold composites designed for bone tissue engineering. Bio-medical materials and engineering. 2014;24(6):2249-56.
22. Jaeger K-E, Steinbüchel A, Jendrossek D. Substrate specificities of bacterial polyhydroxyalkanoate depolymerases and lipases: bacterial lipases hydrolyze poly (omega-hydroxyalkanoates). Applied and Environmental Microbiology. 1995;61(8):3113-8.
23. Jendrossek D. Microbial degradation of polyesters: a review on extracellular poly (hydroxyalkanoic acid) depolymerases. Polymer degradation and stability. 1998;59(1-3):317-25.
24. Tay FR, Pashley DH, Williams MC, Raina R, Loushine RJ, Weller RN, et al. Susceptibility of a polycaprolactone-based root canal filling material to degradation. I. Alkaline hydrolysis. Journal of endodontics. 2005;31(8):593-8.
25. Trampuz A, Widmer AF. Infections associated with orthopedic implants. Current opinion in infectious diseases. 2006;19(4):349-56.
26. Noel SP, Courtney HS, Bumgardner JD, Haggard WO. Chitosan sponges to locally deliver amikacin and vancomycin: a pilot in vitro evaluation. Clinical Orthopaedics and Related Research®. 2010;468(8):2074-80.
27. Smith JK, Moshref AR, Jennings JA, Courtney HS, Haggard WO. Chitosan sponges for local synergistic infection therapy: a pilot study. Clinical Orthopaedics and Related Research®. 2013;471(10):3158-64.
28. Parker AC. Fungal and Bacterial Infection Mitigation with Antibiotic and Antifungal Loaded Biopolymer Sponges: The University of Memphis; 2014.
29. Rhodes CS, Alexander CM, Berretta JM, Courtney HS, Beenken KE, Smeltzer MS, et al. Evaluation of a chitosan-polyethylene glycol paste as a local antibiotic delivery device. World journal of orthopedics. 2017;8(2):130.
30. Berretta JM, Jennings JA, Courtney HS, Beenken KE, Smeltzer MS, Haggard WO. Blended chitosan paste for infection prevention: preliminary and preclinical evaluations. Clinical Orthopaedics and Related Research®. 2017;475(7):1857-70.
31. Wells CM, Beenken KE, Smeltzer MS, Courtney HS, Jennings JA, Haggard WO. Ciprofloxacin and rifampin dual antibiotic-loaded biopolymer chitosan sponge for bacterial inhibition. Military medicine. 2018;183(suppl_1):433-44.
32. O'Toole GA, Kolter R. Flagellar and twitching motility are necessary for Pseudomonas aeruginosa biofilm development. Molecular microbiology. 1998;30(2):295-304.
33. Klausen M, Heydorn A, Ragas P, Lambertsen L, Aaes-Jørgensen A, Molin S, et al. Biofilm formation by Pseudomonas aeruginosa wild type, flagella and type IV pili mutants. Molecular microbiology. 2003;48(6):1511-24.
34. Qi L, Christopher GF. Role of flagella, type IV Pili, biosurfactants, and extracellular polymeric substance polysaccharides on the formation of pellicles by Pseudomonas aeruginosa. Langmuir. 2019;35(15):5294-304.

35. Moormeier DE, Bayles KW. Staphylococcus aureus biofilm: a complex developmental organism. Molecular microbiology. 2017;104(3):365-76.
36. Parker AC, Jennings JA, Bumgardner JD, Courtney HS, Lindner E, Haggard WO. Preliminary investigation of crosslinked chitosan sponges for tailorable drug delivery and infection control. Journal of Biomedical Materials Research Part B: Applied Biomaterials. 2013;101(1):110-23.

# CHAPTER 3

## Antimicrobial and Anti-biofilm Efficacy of Local Anesthetics Combined with *Cis*-2-decenoic Acid against *Staphylococcus Aureus*, *Pseudomonas Aeruginosa*, and *Acinetobacter Baumannii*

### Introduction

Infections related to traumatic musculoskeletal wounds often are challenging to treat and painful, requiring multiple surgeries while increasing patient morbidity, costs, and treatment time. Traumatic injuries often involve numerous tissues susceptible to environmental contamination, and wounds such as open bone fractures and burns are particularly at risk for infection (1, 2). Microorganisms can enter injured tissue through the patient's microflora or contact with the environment or healthcare workers (3, 4), i.e., patient to patient, hospital environment, and fomites, or unwashed hands (5). Osteomyelitis infections can be particularly devastating to the healthcare system and deemed incurable due to deep bacterial persistence (6). Complex wound infections resulting from burns account for approximately 51% of burn-related deaths (2). Traumatic complex extremity injuries have increased susceptibility to multiple pathogenic and multi-drug resistant bacterial strains, including methicillin-resistant *Staphylococcus aureus* (MRSA), *Pseudomonas aeruginosa*, and *Acinetobacter baumannii* (7, 8). Gram-positive *Staphylococcus aureus* (*S. aureus*) is the predominant pathogen in orthopaedic infection (9) and contributes to approximately 50% of burn wound infections (10). In addition to Gram-positive microorganisms, Gram-negative microorganisms, such as *P. aeruginosa* and *A. baumannii*, often contaminate soft tissue injuries and burns (11).

Systemic antibiotics, the current prophylaxis, and treatment for infections require high doses due to traumatic wound sites' avascular areas. Upon injury, the skin's protective

mechanisms (i.e., defensins from keratinocytes and acidic secretions from sebaceous glands) are severely impaired or lost entirely, allowing microorganisms to colonize and form a biofilm rapidly (12). With complex traumatic injury and the accompanying reduced blood supply along with the limited systemic antibiotic diffusion, bacteria, especially biofilm-forming bacteria, can be highly tolerant to low levels of antimicrobials due to a combination of semi-dormant persister cells, exopolymeric substance (EPS) secretion, and metabolic adaptations (3, 13). Studies have shown that *P aeruginosa* isolates from a burn wound developed EPS within 5 hours and has the characteristics of a mature biofilm within 10 hours, demonstrating the necessity of taking immediate preventative measures after injury (14). Furthermore, clinical studies showed that while debridement of burn wounds could remove biofilm from wound beds, biofilms recolonized two days after this initial debridement (15). Similarly, orthopaedic implant-associated infections managed with debridement and irrigation with retention (DAIR) of the implant have high infection recurrence rates, in part due to biofilm formation (16, 17). Each of these studies indicates the need for prompt and sustained non-antibiotic methods to treat and prevent biofilm in wounds.

Musculoskeletal trauma also causes significant pain for patients. Due to the recent opioid misuse and addiction epidemic, non-opioid pain management strategies are of great clinical interest (18). Local anesthetics (LA) block voltage-gated sodium channels, temporarily blocking nerve conduction through nociceptive afferent nerves and subsequently numbing local pain (19). Their chemical structure typically consists of a hydrophobic aromatic group linked via an intermediate ester or amide chain to a hydrophilic amine group (20). In addition to their pain-relieving ability, some LA, including bupivacaine (BUP), ropivacaine (ROP), and lidocaine (LID), also have reported antimicrobial capabilities (21). A previous *in vivo* study on a topical

local anesthetic spray against mixed microflora of the oral cavity showed a time-dependent effect of 10% LID on certain bacterial strains, mostly Gram-negative (22). The study reduced the number of oral biofilms on the buccal mucosa by 60–95% compared to a group without LA (22).

Additionally, an infection mice model study showed an almost 10-fold reduction in CFUs of *S. aureus* compared to a saline control after 48 hours of continuous 2% LID infusion (23). Few studies have investigated the effects of LA against biofilm. However, Gil et al. recently reported that polyethylene loaded with BUP-hydrochloride had a dose-dependent inhibitory effect on *S. aureus* biofilm formation (24). Many studies investigating LA's antimicrobial characteristics use commercial preparations of hydrochloride salts, which can be acidic and confound results.

Biofilm-associated bacteria use quorum sensing to communicate with each other, reduce metabolic activity, and produce polysaccharide EPS, which allow the bacteria to evade innate immune activity and most antimicrobials. Treating established implant biofilms has proven to be virtually impossible without surgical intervention, which places additional burdens on patients, insurance companies, and the healthcare system. *Cis*-2-decenoic acid (C2DA) is a medium-chain fatty acid that disperses and inhibits biofilm (8, 25). C2DA induces the biofilm dispersion response native to many Gram-negative and Gram-positive bacteria and yeast, reverses biofilms' persistence, increases the metabolic activity of microbials, and significantly enhances the -cidal effects of conventional antimicrobial agents (26, 27). In a previous analysis, C2DA concentrations $\geq$ 500 μg $mL^{-1}$ inhibited planktonic growth, while 125 μg $mL^{-1}$ C2DA inhibited biofilm (25). There were no adverse cytocompatibility effects on fibroblasts at these concentrations (25). Studies by Rahmani-Badi et al. demonstrated that combining the biofilm-active C2DA with antibiotics or antimicrobials enhances the activity against biofilm (28,

29). Additive and synergistic effects of C2DA combined with common antimicrobials were reported by Masters et al., particularly for antibiotics with mechanisms of action internal to the cell membrane (30). This study's objective was to evaluate different LA molecules on pathogenic microorganisms that commonly contribute to an infection and determine whether combining LA with C2DA has additive, synergistic, or antagonistic effects against planktonic and biofilm-associated *S. aureus, P. aeruginosa,* and *A. baumannii*.

## Materials and Methods

### Checkerboard assays

*S. aureus* (UAMS-1, a clinical osteomyelitis strain) overnight growth was diluted 1:10 in tryptic soy broth (TSB). *P. aeruginosa* (ATCC #27317) and *A. baumannii* (ATCC #BAA-1710™) overnight growths were diluted 1:50 in TSB. Antimicrobials tested included bupivacaine (Alfa Aesar™), lidocaine (TCI America™), ropivacaine (Alfa Aesar™), and C2DA, with the final LA concentrations ranging from 0 - 10 mg $mL^{-1}$ and C2DA from 0 - 500 mg $mL^{-1}$. Due to the hydrophobic characteristics of LAs and C2DA, they were solubilized in 200 proof ethanol and added to bacterial culture in amounts that diluted concentrations to 2.5% ethanol in TSB. ROP still required the addition of 6.25 mM HCl due to solubility issues in 100% ethanol. Bacteria and antimicrobial solutions were added to 96-well plates and incubated for 24 hours.

### Planktonic growth

General antimicrobial activity of LA, C2DA, and combinations against planktonic bacteria was determined by concurrently inoculating 96-well plates with bacteria. Wells were inoculated with $10^6$ CFUs of *S. aureus*, *P. aeruginosa*, or *A. baumannii*, then combined with LAs (0, 0.3125, 0.625, 1.25, 2.5, 5, or 10 mg $mL^{-1}$), C2DA (500 mg $mL^{-1}$), or combinations. After 24

hours of incubation, 100 µL of planktonic growth was removed, and BacTiter-Glo™ viability reagent was used to determine bacterial survival. Luminescence was determined using a Biotek Synergy™ H1 microplate reader, with increased luminescence indicating a higher number of viable cells. Percent viability was determined using the control with PBS only.

**Biofilm growth**

After removing TSB with planktonic growth, biofilm attached to plates was gently rinsed three times with sterile PBS. BacTiter-Glo™ viability reagent was used to compare biofilm viability on polystyrene plates after exposure to the therapeutics. A Biotek Synergy™ H1 microplate reader determined luminescence, with increased fluorescence indicating a higher number of viable cells. Percent viability was determined using the control with PBS only.

**Fractional Inhibitory Concentration**

The fractional inhibitory concentration index (FICI) was calculated using the concentrations alone (S) and in combination (C) that reduced viability to under 10% of non-treated controls. FICI is determined using the ratio of minimum biofilm inhibitory concentration (MBIC) for the antimicrobial alone to the MBIC for the antimicrobial in combination with C2DA was added to the ratio of MBIC for C2DA alone to MBIC of C2DA when combined with antimicrobial (Equation 3.1) (31). The lowest antimicrobial concentration that inhibits biofilm growth determines the MBIC. Minimum inhibitory concentration (MIC) is determined using the same calculation except for planktonic growth. Synergism occurs when the antimicrobials' effect is greater than the sum of their effect individually or when the FICI is less than one. Antagonism occurs when the antimicrobials' effect reduces when combined or when the FICI is greater than two. A FICI value of two represents neither improvement nor reduction in effectiveness with the combination of antimicrobials. Following similar studies (32, 33), we

considered FICI values < 0.5 synergistic, ≥ 0.5 - < 1 additive, ≥ 1 - < 2 indifferent, and ≥ 2 antagonistic. The FICI was calculated separately for each bacterial strain.

$$FICI = \frac{MBIC/MIC_{LA(C)}}{MBIC/MIC_{LA(S)}} + \frac{MBIC/MIC_{C2DA(C)}}{MBIC/MIC_{C2DA(S)}}$$

**Equation 3.1**. Fractional Inhibitory Concentration Index (FICI) calculation using the concentrations alone (S) and in combination (C).

**Statistical analysis**

GraphPad Prism 9.0.0 software (GraphPad Software Incorporation, La Jolla, CA, USA) performed the statistical analysis. Data was assessed first by completing the Shapiro-Wilk normality test, followed by the Brown-Forsythe equal variance test. If both passed, data were further analyzed with a two-way analysis of variance (ANOVA) followed by Holm-Sidak post-hoc analysis to detect significance between experimental groups ($\alpha = 0.05$).

**Results**

**Planktonic growth**

For *S. aureus*, there was a decrease in viability for all groups as LA concentration increased; however, BUP reduced the planktonic viability more than LID and ROP and at lower concentrations than the other LAs (Figure 3.1). Combining LAs with C2DA significantly decreased planktonic *S. aureus* viability for wells treated with LID and ROP and slightly reduced viability for wells treated with BUP (Figure 3.2).

ROP did not reduce *A. baumannii* planktonic growth even at increasing therapeutic concentrations. BUP appeared more efficacious against *A. baumannii* at lower concentrations than the other LA, but BUP and LID were equally effective at 10 mg $mL^{-1}$ (Figure 3.3). Overall, LAs were more efficacious in planktonic viability reduction than C2DA alone or in combination with C2DA for all groups (Figure 3.4).

Finally, all LA demonstrated activity against *P. aeruginosa* and had similar viability percentages at all concentrations (Figure 3.5). C2DA alone was the least active against *P. aeruginosa* than the other strains, but all LAs effectively prevented planktonic bacterial growth (Figure 3.6). The combination of C2DA and LA reduced planktonic viability compared to C2DA alone, but planktonic growth was still higher with the combination than with LA alone.

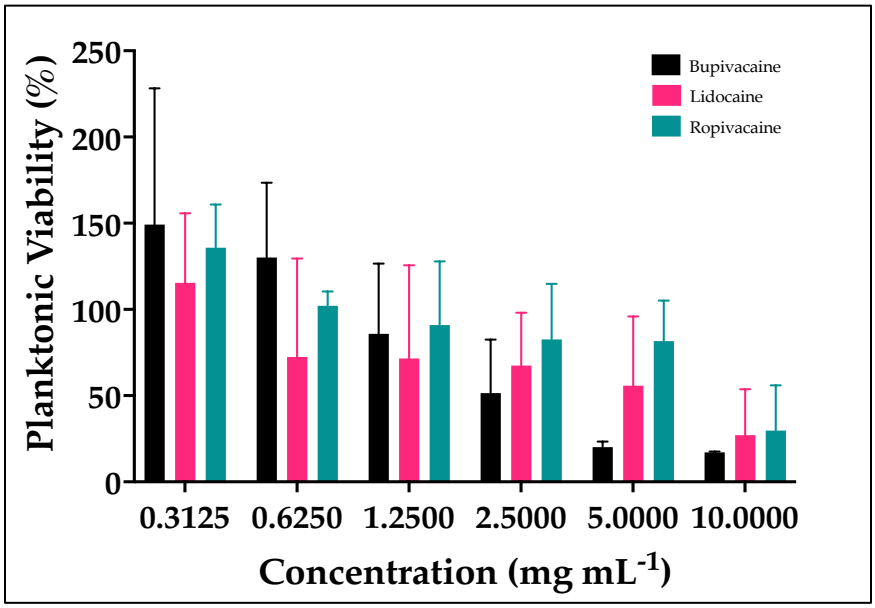


**Figure 3.1**. Mean standard ± deviation of *S. aureus* planktonic viability of local anesthetics alone (n = 3).

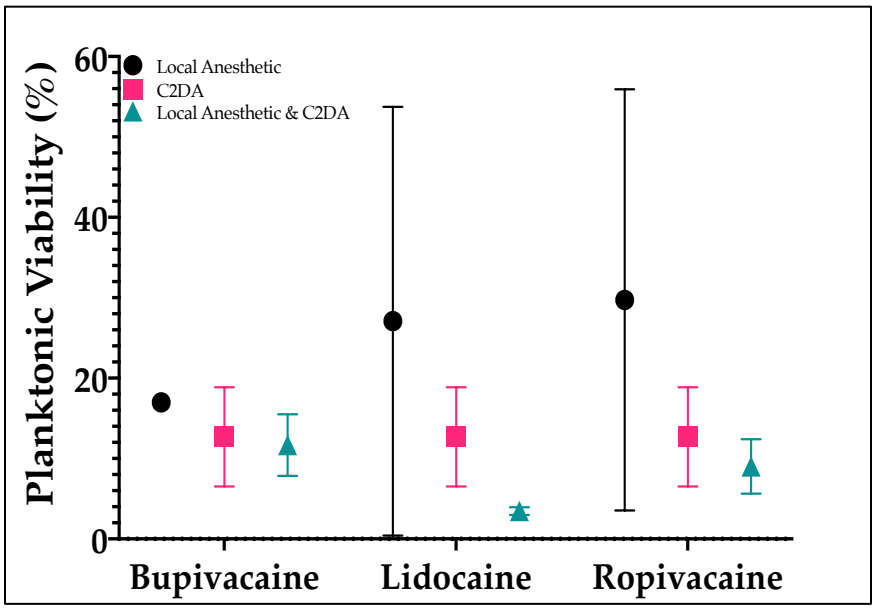


**Figure 3.2**. Mean standard ± deviation of *S. aureus* planktonic viability of local anesthetics alone (5 mg $mL^{-1}$), C2DA alone (500 mg $mL^{-1}$), and in combination (5 mg $mL^{-1}$ and 500 mg $mL^{-1}$), respectively (n = 3).

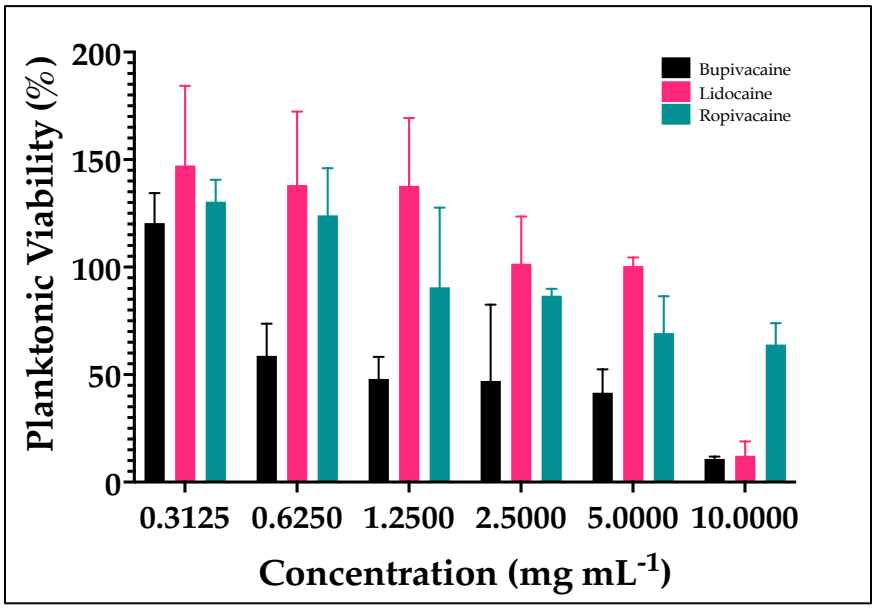


**Figure 3.3.** Mean standard ± deviation of *A. baumannii* planktonic viability of local anesthetics alone (n = 3).

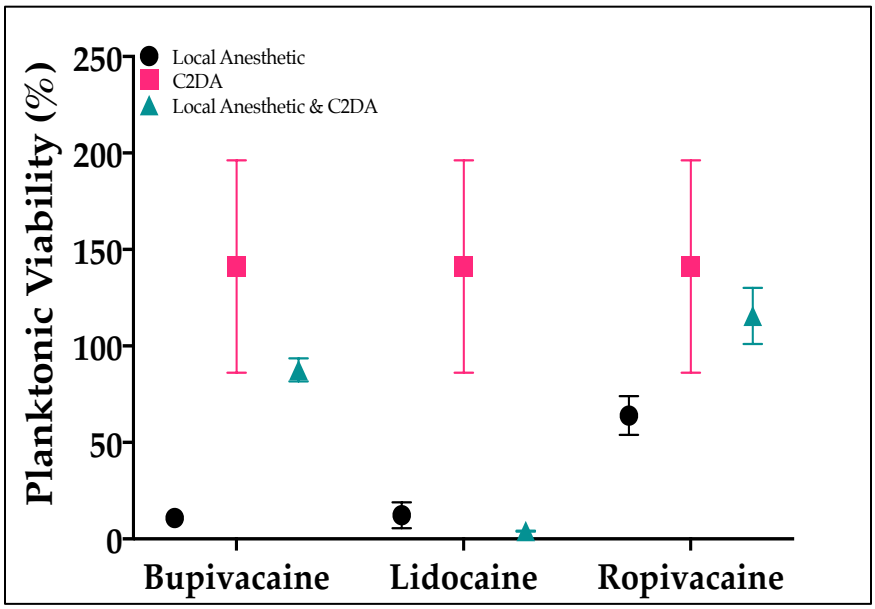


**Figure 3.4**. Mean standard ± deviation of *A. baumannii* planktonic viability of local anesthetics alone (5 mg $mL^{-1}$), C2DA alone (500 mg $mL^{-1}$), and in combination (5 mg $mL^{-1}$ and 500 mg $mL^{-1}$), respectively (n = 3).

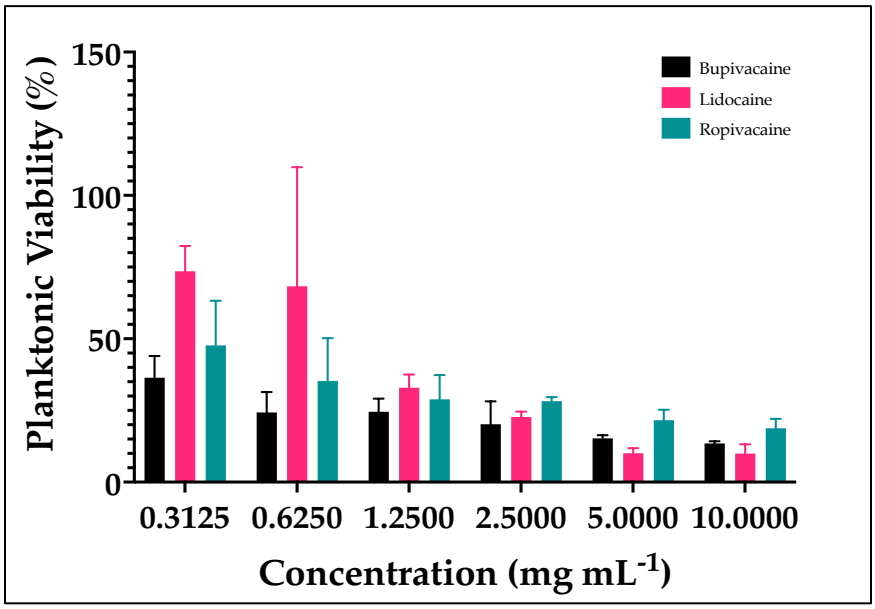


**Figure 3.5.** Mean standard ± deviation of *P. aeruginosa* planktonic viability of local anesthetics alone (n = 3).

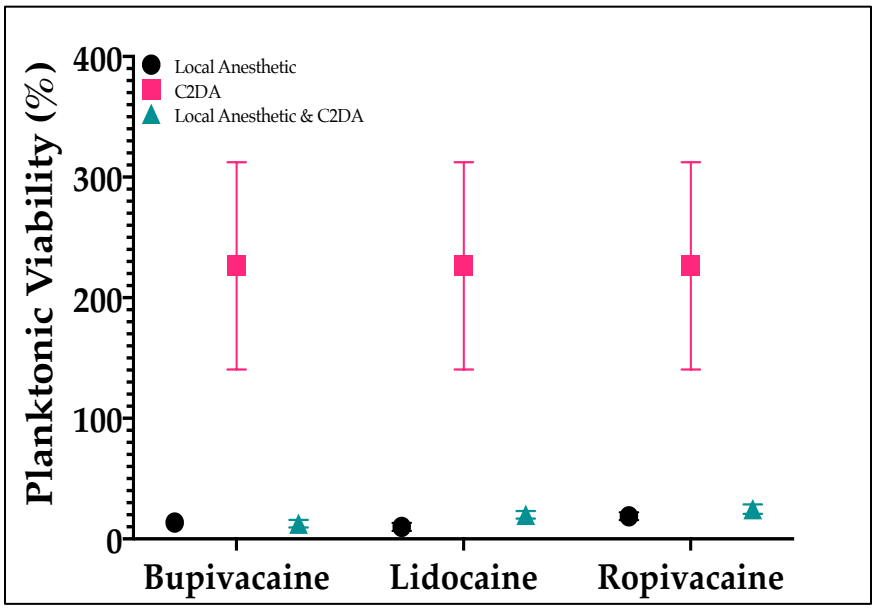


**Figure 3.6**. Mean standard ± deviation of *P. aeruginosa* planktonic viability of local anesthetics alone (5 mg $mL^{-1}$), C2DA alone (500 mg $mL^{-1}$), and in combination (5 mg $mL^{-1}$ and 500 mg $mL^{-1}$), respectively (n = 3).

**Biofilm growth**

The biofilm viability of *S. aureus* was similar for BUP and LID and slightly higher for ROP compared to other LAs (Figure 3.7). The combination of C2DA and LA significantly reduced *S. aureus* biofilm viability with BUP and ROP but had no reducing effect with LID (Figure 3.8).

LID reduced *A. baumannii* biofilm growth the most effective, compared to BUP and ROP, which had similar reduction trends (Figure 3.9). While C2DA alone was ineffective at biofilm viability reduction, LA alone and in combination with C2DA showed a significant decrease in viability, especially for BUP and LID (Figure 3.10).

All LAs alone were mostly ineffective at *P. aeruginosa* biofilm reduction, with little change in biofilm viability with LA concentration changes (Figure 3.11). Additionally, LAs combined with C2DA did not significantly reduce *P. aeruginosa* biofilm viability (Figure 3.12).

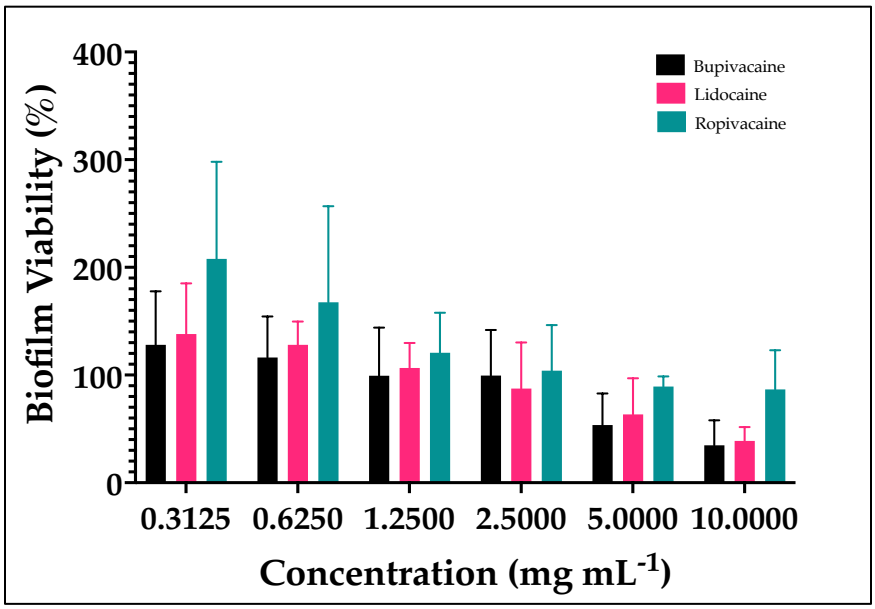


**Figure 3.7**. Mean standard ± deviation of *S. aureus* biofilm viability of local anesthetics alone (n = 3).

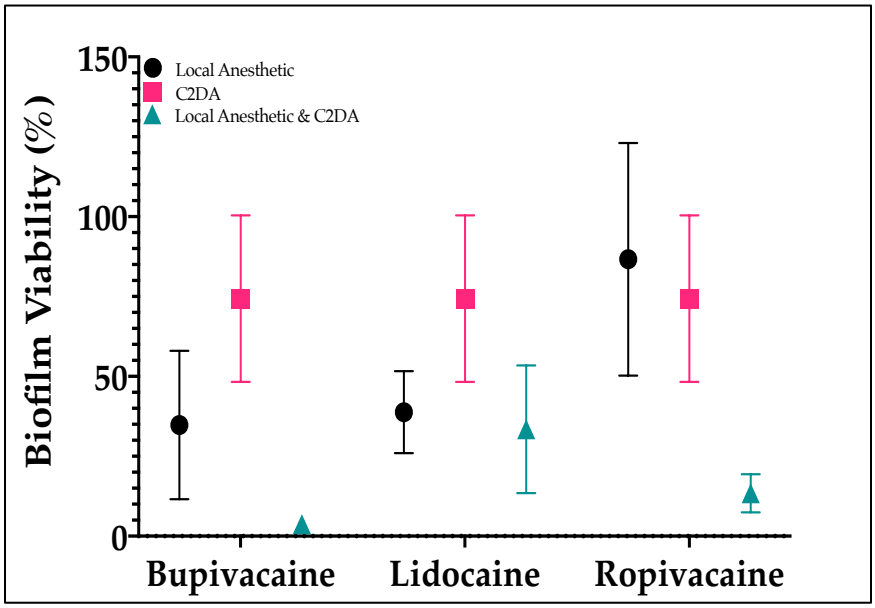


**Figure 3.8**. Mean standard ± deviation of *S. aureus* biofilm viability of local anesthetics alone (5 mg $mL^{-1}$), C2DA alone (500 mg $mL^{-1}$), and in combination (5 mg $mL^{-1}$ and 500 mg $mL^{-1}$), respectively (n = 3).

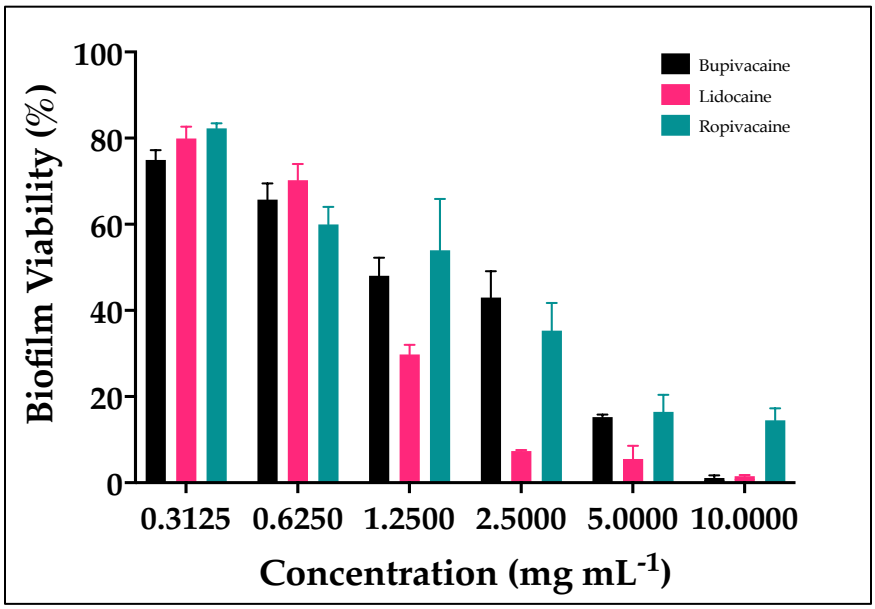


**Figure 3.9.** Mean standard ± deviation of *A. baumannii* biofilm viability of local anesthetics alone (n = 3).

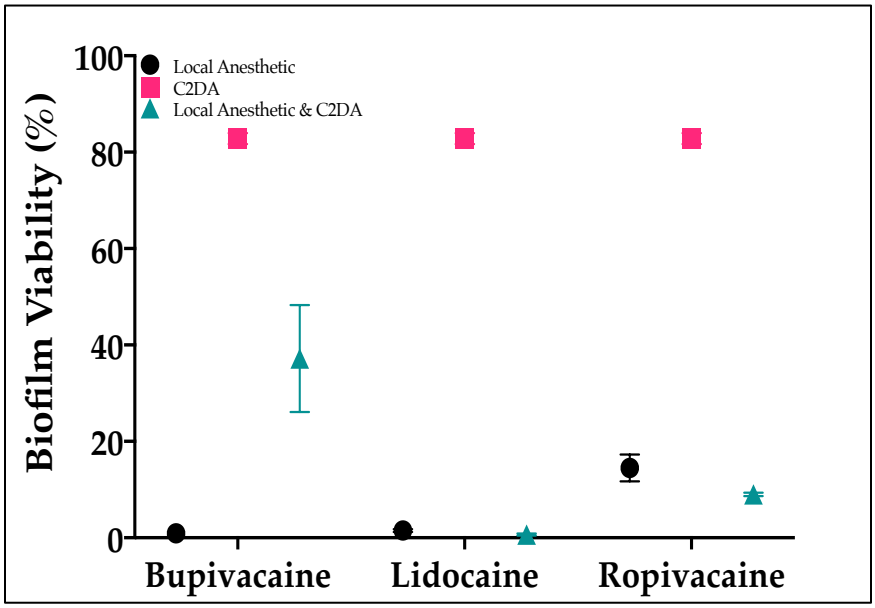


**Figure 3.10**. Mean standard ± deviation of *A. baumannii* biofilm viability of local anesthetics alone (5 mg $mL^{-1}$), C2DA alone (500 mg $mL^{-1}$), and in combination (5 mg $mL^{-1}$ and 500 mg $mL^{-1}$), respectively (n = 3).

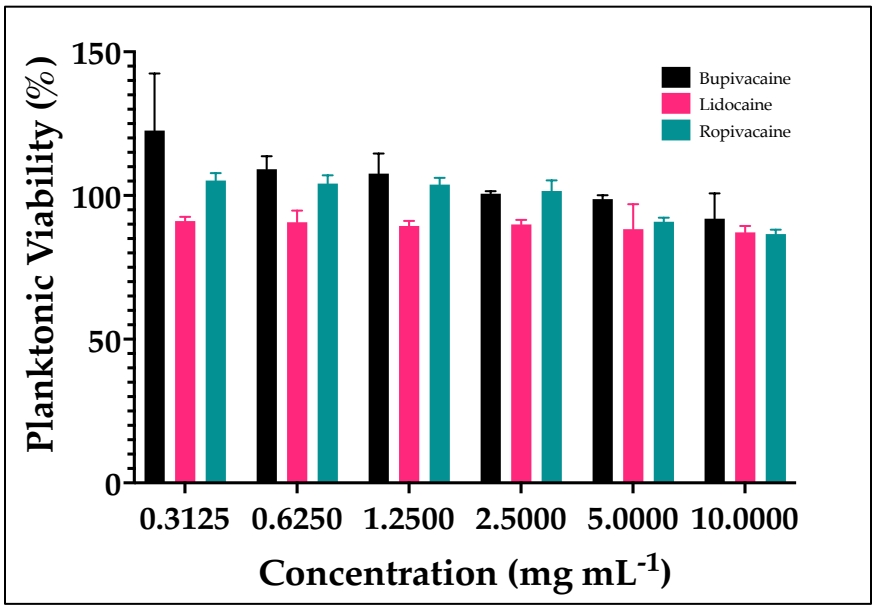


**Figure 3.11**. Mean standard ± deviation of *P. aeruginosa* biofilm viability of local anesthetics alone (n = 3).

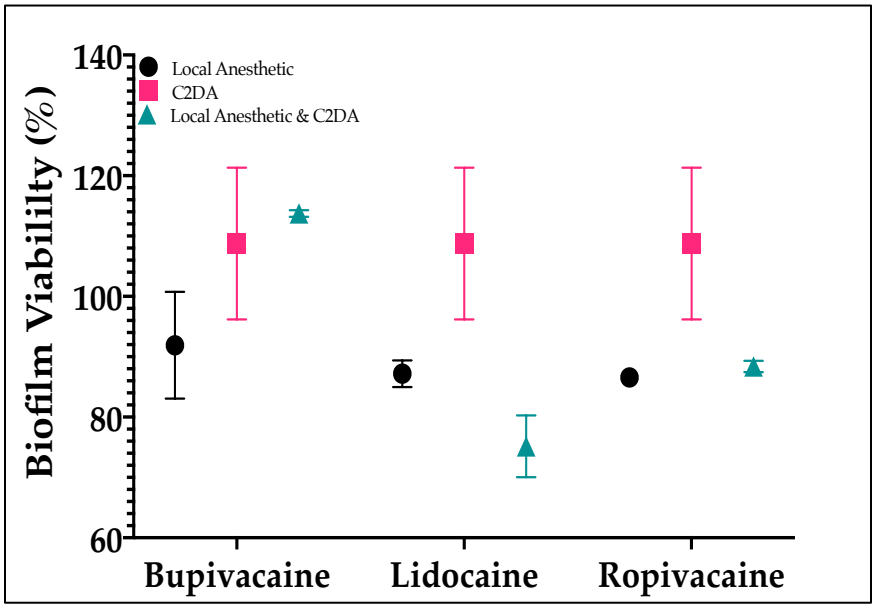


**Figure 3.12**. Mean standard ± deviation of *P. aeruginosa* biofilm viability of local anesthetics alone (5 mg $mL^{-1}$), C2DA alone (500 mg $mL^{-1}$), and in combination (5 mg $mL^{-1}$ and 500 mg $mL^{-1}$), respectively (n = 3).

## FICI

LAs did not reduce *S. aureus* planktonic or biofilm viability below the 10% threshold when tested alone. Figures 3.1 and 3.2 demonstrate the effect of using the LA in combination with C2DA, graphically represented concentrations are LA (10 mg $mL^{-1}$) and C2DA (500 mg $mL^{-1}$). In most instances, the combination's reduction was more significant than either

LA or C2DA tested singularly. BUP and ROP are synergistic, with additive effects for LID combined with C2DA against planktonic *S. aureus.* Tables 3.1, 3.2, and 3.3 show MIC and MBIC values used in the calculations. BUP demonstrated an additive effect with C2DA against *S. aureus* biofilm, with other LAs being indifferent. Since no LA nor C2DA reduced viability below 10% at their highest concentrations alone, 2x those concentrations were used in FICI calculations when necessary. This study did not directly evaluate values that exceeded LA solubility limits or C2DA's critical micelle concentration. No statistically significant differences were present for LAs when tested against Gram-positive *S. aureus*. BUP accounted for more than 50% of statistically significant differences for the Gram-negative bacterial strains (Tables 3.4 and 3.5).

## Tables

**Table 3.1.** MIC and MBIC values (mg $mL^{-1}$) used in FICI calculations for tested local anesthetics and C2DA, evaluated alone (S) or in combination (C) against *S aureus*.

| | **Biofilm** | | | | | | **Planktonic** | | | | | |
|---|---|---|---|---|---|---|---|---|---|---|---|---|
| | **MBIC** | | | | FICI | Interpretation | **MIC** | | | | FICI | Interpretation |
| | C2DA (S) | C2DA (C) | LA (S) | LA (C) | | | C2DA (S) | C2DA (C) | LA (S) | LA (C) | | |
| **BUP** | 1 | 0.25 | 10 | 5 | 0.75 | Additive | 1 | 0.25 | 20 | 2.5 | 0.375 | Synergistic |
| **ROP** | 1 | 1 | 20 | 20 | 2 | Indifferent | 1 | 0.031 | 10 | 0.625 | 0.094 | Synergistic |
| **LID** | 1 | 1 | 20 | 20 | 2 | Indifferent | 1 | 0.25 | 20 | 5 | 0.5 | Additive |

**Table 3.2.** MIC and MBIC values (mg $mL^{-1}$) used in FICI calculations for tested local anesthetics and C2DA, evaluated alone (S) or in combination (C) against *A baumannii*.

| | **Biofilm** | | | | | | **Planktonic** | | | | | |
|---|---|---|---|---|---|---|---|---|---|---|---|---|
| | **MBIC** | | | | FICI | Interpretation | **MIC** | | | | FICI | Interpretation |
| | C2DA (S) | C2DA (C) | LA (S) | LA (C) | | | C2DA (S) | C2DA (C) | LA (S) | LA (C) | | |
| **BUP** | 1 | 0.25 | 10 | 2.5 | 0.5 | Synergistic | 1 | 0.5 | 10 | 5 | 1 | Additive |
| **ROP** | 1 | 1 | 10 | 10 | 2 | Indifferent | 1 | 0.25 | 10 | 1.25 | 0.375 | Synergistic |
| **LID** | 1 | 1 | 10 | 10 | 2 | Indifferent | 1 | 1 | 10 | 10 | 2 | Indifferent |

**Table 3.3.** MIC and MBIC values (mg $mL^{-1}$) used in FICI calculations for tested local anesthetics and C2DA, evaluated alone (S) or in combination (C) against *P aeruginosa*.

| | Biofilm | | | | | | Planktonic | | | | | |
|---|---|---|---|---|---|---|---|---|---|---|---|---|
| | MBIC | | | | FICI | Interpretation | MIC | | | | FICI | Interpretation |
| | C2DA (S) | C2DA (C) | LA (S) | LA (C) | | | C2DA (S) | C2DA (C) | LA (S) | LA (C) | | |
| **BUP** | 1 | 0.25 | 10 | 2.5 | 0.5 | Synergistic | 1 | 0.5 | 10 | 5 | 1 | Additive |
| **ROP** | 1 | 1 | 10 | 10 | 2 | Indifferent | 1 | 0.25 | 10 | 1.25 | 0.375 | Synergistic |
| **LID** | 1 | 1 | 10 | 10 | 2 | Indifferent | 1 | 1 | 10 | 10 | 2 | Indifferent |

**Table 3.4.** Local anesthetics' statistically significant results of *A. Baumannii* planktonic and biofilm growth.

| Bacteria State | Comparison | Concentration (mg $mL^{-1}$) | Mean Difference | P Value |
|---|---|---|---|---|
| **Planktonic** | BUP v. LID | 0.625 | 79.45 | 0.0002 |
| | BUP v. ROP | 0.625 | 65.33 | 0.0014 |
| | BUP v. LID | 1.25 | 89.73 | <0.0001 |
| | BUP v. ROP | 1.25 | 42.61 | 0.0219 |
| | LID v. ROP | 1.25 | 47.12 | 0.0219 |
| | BUP v. LID | 2.5 | 54.53 | 0.0111 |
| | BUP v. LID | 5 | 58.91 | 0.0057 |
| | BUP v. ROP | 10 | 53.16 | 0.0137 |
| | LID v. ROP | 10 | 51.70 | 0.0137 |
| **Biofilm** | LID v. ROP | 0.625 | 10.27 | 0.0183 |
| | BUP v. LID | 1.25 | 18.30 | 0.0002 |
| | LID v. ROP | 1.25 | 24.22 | <0.0001 |
| | BUP v. LID | 2.5 | 35.63 | <0.0001 |
| | LID v. ROP | 2.5 | 27.94 | <0.0001 |
| | BUP v. LID | 5 | 9.708 | 0.0410 |
| | LID v. ROP | 5 | 10.93 | 0.0303 |
| | BUP v. ROP | 10 | 13.56 | 0.0061 |
| | LID v. ROP | 10 | 13.01 | 0.0061 |

**Table 3.5.** Local anesthetics' statistically significant results of *P. aeruginosa* planktonic and biofilm growth.

| Bacteria State | Comparison | Concentration (mg $mL^{-1}$) | Mean Difference | P Value |
|---|---|---|---|---|
| **Planktonic** | BUP v. LID | 0.3125 | 37.16 | 0.0017 |
| | LID v. ROP | 0.3125 | 25.86 | 0.0245 |
| | BUP v. LID | 0.625 | 43.97 | 0.0002 |
| | LID v. ROP | 0.625 | 32.99 | 0.0037 |
| **Biofilm** | BUP v. LID | 0.3125 | 31.50 | <0.0001 |
| | BUP v. ROP | 0.3125 | 17.38 | 0.0029 |
| | LID v. ROP | 0.3125 | 14.11 | 0.0082 |
| | BUP v. LID | 0.625 | 18.40 | 0.0025 |
| | LID v. ROP | 0.625 | 13.43 | 0.0230 |
| | BUP v. LID | 1.25 | 18.17 | 0.0028 |
| | LID v. ROP | 1.25 | 14.35 | 0.0146 |

**Discussion**

The results of this study confirm our hypothesis that certain combinations of LA and C2DA can reduce both planktonic and biofilm-associated bacterial growth for *S. aureus*, *P. aeruginosa*, and *A. baumannii*. Overall, C2DA exhibited antimicrobial properties consistent with previous publications (25). Slight differences in LA structure may explain their varying efficacies in each study. BUP is an amide with slow onset and prolonged action (20). Razavi et al. further validated that BUP is typically more effective against Gram-positive strains, including *S. aureus*. Previous studies have shown BUP to be the least effective against *P. aeruginosa* (20, 34). LID is also an amide but with a rapid onset and intermediate duration of action compared to BUP (20, 35). ROP is very similar in structure to BUP, with differences in length of the alkyl tail (20, 36). Based on these similarities to BUP, one could hypothesize that similar antimicrobial activity may be present for ROP. However, in most tested metrics, ROP's antimicrobial activity was less robust than BUP (37, 38). This study confirms that the alkyl chain length may play a role in the mechanism of action, with longer chain lengths interacting with lipophilic parts of the cell membrane. Studies of phenolipids have indicated that increasing alkyl lengths support more significant interaction and penetration into lipid bilayers (39, 40). Solubility differences between LAs may further explain their varying efficacies, as we observed poor solubility of ROP at neutral pH.

Because LAs mechanism of action against bacteria remains unclear, it is not easy to pinpoint the reasons for our observed differences in susceptibility between Gram-negative *P. aeruginosa* and *A. baumannii*, which have similar antimicrobial susceptibility (41). LID had limited efficacy against *S. aureus* at concentrations below 10 mg $mL^{-1}$, as seen in previous studies (42) but was markedly more effective when combined with C2DA. ROP and *S. aureus*

demonstrated similar results based on previous studies (37, 42) and was more potent when combined with C2DA. BUP was more inhibitory in planktonic studies than other LAs and particularly active against *S. aureus*; this result confirms previous accounts that BUP possesses the lowest MIC of these three tested LAs (24, 43). Results reveal that all LAs inhibit planktonic growth of all bacterial strains at 10 mg $mL^{-1}$, except for ROP against *A. baumannii*. The apparent inactivity of ROP against *A. baumannii* may have been due to the solubility issues mentioned earlier, which was one limitation of this study. We chose pure formulations over hydrochloride salts to avoid confounding effects of varying pH and other excipients included in commercial anesthetic solutions. Further, non-salt forms may facilitate loading into biomaterial drug delivery systems more readily, including wound dressings (44, 45), calcium sulfate (46), and polyethylene (24).

Many antimicrobials have decreased efficacy in inhibiting biofilm formation than planktonic growth (47), with lower concentrations sometimes driving increased biofilm formation as an adaptive response (48). This tolerance of biofilm to antimicrobials fits with the observation that *S. aureus* biofilm reduction followed a similar dose-response pattern for both planktonic and biofilm but with higher concentrations required to inhibit biofilm formation by more than 50%. LAs may interact with surface-attached proteins instrumental in *S. aureus* biofilm formation, termed microbial surface components recognizing adhesive matrix molecules (MSCRAMM), to prevent attachment and thus inhibit biofilm formation (49). The *P. aeruginosa* results also reflect biofilm's tolerance and may indicate that the stress of exposure to antimicrobial LA molecules promotes biofilm formation. Another explanation of *P. aeruginosa* biofilm tolerance may be type IV pili and EPS to attach to surfaces, which LAs and C2DA may not target (50-52).

In contrast, our results for *A. baumannii* show that although planktonic growth was not inhibited and may increase in response to LAs, biofilm inhibition occurred in a dose-dependent fashion. This high efficacy against biofilm formation may be due to LAs interfering with chaperone-usher pili used by *A. baumannii* to attach to abiotic surfaces (53, 54). Biofilm dispersal may explain the increased planktonic viability and biofilm decrease (55). A study limitation is that we investigated initial biofilm formation only; future studies may explore the application of LAs and C2DA to existing biofilms. A further limitation is that only one measure of bacterial viability was used, which may vary based on metabolic state (ATP production). Future studies may use additional criteria such as CFU counting, although ATP-based assays help initial screening studies.

Combining antimicrobials, particularly antibiofilm and antimicrobial molecules, may work in multiple or divergent ways to increase the efficacy of both (56). C2DA may increase membrane permeability, which may allow for more antimicrobial molecules to enter the cell (30). Our additive and synergy findings for planktonic *S. aureus* but indifference against biofilm may be due to the limited ability of C2DA to access cell membranes when *S. aureus* is in a biofilm instead of a planktonic state. *P. aeruginosa* produces C2DA, a natural dispersal molecule that is effective against multiple bacteria and fungi strains (8). The additive responses observed for *P. aeruginosa* and *A. baumannii* may be due to C2DA stimulating dispersal events. C2DA has an alkyl tail ten carbons long, facilitating interaction with and penetration into lipid bilayers (39, 57, 58). Both C2DA and BUP may act as penetration enhancers due to their alkyl chain lengths (59), meaning that their combination could allow for more entry of both inside the membrane and increased membrane damaging effects. The acidic nature of C2DA may protonate

the amine groups in LA molecules and increase their solubility (60). However, *in vivo* studies must be performed to confirm additive and synergistic activities of C2DA and LAs.

This study indicates the potential success of combining LAs and C2DA as a therapeutic combination to prevent or treat infection following musculoskeletal trauma. Clinical applications involving deep tissue damage such as joint replacement surgery, dressings for burn wounds, compound fracture fixation, or other traumatic injuries may benefit from local delivery of these therapeutics, alone or in combination. The development of biomaterial delivery systems can achieve this clinical need for infection prevention and possible treatment. Further studies will investigate sustained delivery strategies and *in vivo* efficacy to validate the potential of LAs and C2DA combination in infection treatment and prevention. In addition to preventing infection, local delivery of anesthetics may provide additional pain relief for orthopaedic trauma or total joint procedures, lessen systemic delivery shortcomings, and reduce the need for prescription opioids, which in turn may mitigate opioid misuse and addiction.

**References**


1. Owens BD, Kragh Jr JF, Macaitis J, Svoboda SJ, Wenke JC. Characterization of extremity wounds in operation Iraqi freedom and operation enduring freedom. Journal of orthopaedic trauma. 2007;21(4):254-7.
2. Norbury W, Herndon DN, Tanksley J, Jeschke MG, Finnerty CC, Society SSCotSI. Infection in burns. Surgical infections. 2016;17(2):250-5.
3. Hammond AA, Miller KG, Kruczek CJ, Dertien J, Colmer-Hamood JA, Griswold JA, et al. An in vitro biofilm model to examine the effect of antibiotic ointments on biofilms produced by burn wound bacterial isolates. Burns. 2011;37(2):312-21.
4. Uçkay I, Hoffmeyer P, Lew D, Pittet D. Prevention of surgical site infections in orthopaedic surgery and bone trauma: state-of-the-art update. Journal of Hospital Infection. 2013;84(1):5-12.
5. Hospenthal DR, Green AD, Crouch HK, English JF, Pool J, Yun HC, et al. Infection prevention and control in deployed military medical treatment facilities. Journal of Trauma and Acute Care Surgery. 2011;71(2):S290-S8.
6. Masters EA, Trombetta RP, de Mesy Bentley KL, Boyce BF, Gill AL, Gill SR, et al. Evolving concepts in bone infection: Redefining "biofilm","acute vs. chronic osteomyelitis","the immune proteome" and "local antibiotic therapy". Bone Res. 2019;7(1):1-18.
7. Brady RA, Leid JG, Calhoun JH, Costerton JW, Shirtliff ME. Osteomyelitis and the role of biofilms in chronic infection. Fems Immunology and Medical Microbiology. 2008;52(1):13-22.
8. Davies DG, Marques CN. A fatty acid messenger is responsible for inducing dispersion in microbial biofilms. Journal of bacteriology. 2009;191(5):1393-403.
9. Urish KL, Cassat JE. Staphylococcus aureus Osteomyelitis: Bone, Bugs, and Surgery. Infect Immun. 2020;88(7).
10. Moghadam SO, Pourmand MR, Aminharati F. Biofilm formation and antimicrobial resistance in methicillin-resistant Staphylococcus aureus isolated from burn patients, Iran. The Journal of Infection in Developing Countries. 2014;8(12):1511-7.
11. Tarashi S, Goudarzi H, Erfanimanesh S, Pormohammad A, Hashemi A. Phenotypic and molecular detection of metallo-beta-lactamase genes among imipenem resistant Pseudomonas aeruginosa and Acinetobacter baumannii strains isolated from patients with burn injuries. Archives of Clinical Infectious Diseases. 2016;11(4).
12. Kennedy P, Brammah S, Wills E. Burns, biofilm and a new appraisal of burn wound sepsis. Burns. 2010;36(1):49-56.
13. Crabbé A, Jensen PØ, Bjarnsholt T, Coenye T. Antimicrobial tolerance and metabolic adaptations in microbial biofilms. Trends in microbiology. 2019;27(10):850-63.
14. Harrison-Balestra C, Cazzaniga AL, Davis SC, Mertz PM. A wound-isolated Pseudomonas aeruginosa grows a biofilm in vitro within 10 hours and is visualized by light microscopy. Dermatologic surgery. 2003;29(6):631-5.
15. Wolcott RD, Rumbaugh KP, James G, Schultz G, Phillips P, Yang Q, et al. Biofilm maturity studies indicate sharp debridement opens a time-dependent therapeutic window. Journal of wound care. 2010;19(8):320-8.
16. Choi H-R, Von Knoch F, Zurakowski D, Nelson SB, Malchau H. Can implant retention be recommended for treatment of infected TKA? Clinical Orthopaedics and Related Research®. 2011;469(4):961-9.

17. Izakovicova P, Borens O, Trampuz A. Periprosthetic joint infection: current concepts and outlook. EFORT open reviews. 2019;4(7):482-94.
18. Rothstein MA. The opioid crisis and the need for compassion in pain management. American Public Health Association; 2017.
19. Catterall WA, Mackie K. Local anesthetics. Goodman & Gilman's the pharmacological basis of therapeutics: McGraw-Hill, New York (NY); 2011. p. 565-82.
20. Razavi BM, Bazzaz BSF. A review and new insights to antimicrobial action of local anesthetics. European Journal of Clinical Microbiology & Infectious Diseases. 2019:1-12.
21. Johnson SM, Saint John BE, Dine AP. Local anesthetics as antimicrobial agents: a review. Surgical infections. 2008;9(2):205-13.
22. Srisatjaluk RL, Klongnoi B, Wongsirichat N. Antimicrobial effect of topical local anesthetic spray on oral microflora. J Dent Anesth Pain Med. 2016;16(1):17.
23. Lin T, Chiu K, Chu S. Antimicrobial effect of continuous lidocaine infusion in a staphylococcus aureus induced wound infection mice model: 8AP7-4. European Journal of Anaesthesiology| EJA. 2011;28:127.
24. Gil D, Grindy S, Muratoglu O, Bedair H, Oral E. Antimicrobial effect of anesthetic-eluting ultra-high molecular weight polyethylene for post-arthroplasty antibacterial prophylaxis. Journal of Orthopaedic Research®. 2019;37(4):981-90.
25. Jennings JA, Courtney HS, Haggard WO. Cis-2-decenoic acid inhibits S. aureus growth and biofilm in vitro: a pilot study. Clinical orthopaedics and related research. 2012;470(10):2663-70.
26. Marques CNH, Davies DG, Sauer K. Control of Biofilms with the Fatty Acid Signaling Molecule cis-2-Decenoic Acid. Pharmaceuticals. 2015;8(4):816-35.
27. Harrison Z, Pace L, Awais R, Jennings JA. Local Delivery of Anti-biofilm Therapeutics. Racing for the Surface: Springer; 2020. p. 477-510.
28. Rahmani-Badi A, Sepehr S, Mohammadi P, Soudi MR, Babaie-Naiej H, Fallahi H. A combination of cis-2-decenoic acid and antibiotics eradicates pre-established catheter-associated biofilms. Journal of medical microbiology. 2014;63(11):1509-16.
29. Rahmani-Badi A, Sepehr S, Babaie-Naiej H. A combination of cis-2-decenoic acid and chlorhexidine removes dental plaque. Archives of oral biology. 2015;60(11):1655-61.
30. Masters E, Harris M, Jennings J. Cis-2-decenoic acid interacts with bacterial cell membranes to potentiate additive and synergistic responses against biofilm. J Bacteriol Mycol. 2016;3(3):1-8.
31. Hall M, Middleton R, Westmacott D. The fractional inhibitory concentration (FIC) index as a measure of synergy. Journal of Antimicrobial Chemotherapy. 1983;11(5):427-33.
32. Bouanchaud D. In-vitro and in-vivo synergic activity and fractional inhibitory concentration (FIC of the components of a semisynthetic streptogramin, RP 59500. Journal of Antimicrobial Chemotherapy. 1992;30(suppl_A):95-9.
33. Orhan G, Bayram A, Zer Y, Balci I. Synergy tests by E test and checkerboard methods of antimicrobial combinations against Brucella melitensis. Journal of clinical microbiology. 2005;43(1):140-3.
34. Rota S, Akcabay M, Emektas G. Antibacterial activity of bupivacaine. Gazi Tip Dergisi. 1993;4:69-71.
35. Parr A, Zoutman D, Davidson J. Antimicrobial activity of lidocaine against bacteria associated with nosocomial wound infection. Annals of plastic surgery. 1999;43(3):239-45.

36. Pirbudak L, Karsligil T, Zer Y, Öner Ü, Balci I. Antibacterial effect of bupivacaine and ropivacaine; effect of adjuvant drugs. The Pain Clinic. 2005;17(1):73-80.
37. Hodson M, Gajraj R, Scott N. A comparison of the antibacterial activity of levobupivacaine vs. bupivacaine: an in vitro study with bacteria implicated in epidural infection. Anaesthesia. 1999;54(7):699-702.
38. Pere P, Lindgren L, Vaara M. Poor antibacterial effect of ropivacaine: comparison with bupivacaine. The Journal of the American Society of Anesthesiologists. 1999;91(3):884-.
39. Durand E, Jacob RF, Sherratt S, Lecomte J, Baréa B, Villeneuve P, et al. The nonlinear effect of alkyl chain length in the membrane interactions of phenolipids: Evidence by X-ray diffraction analysis. European Journal of Lipid Science and Technology. 2017;119(8):1600397.
40. Laguerre M, Lopez Giraldo LJ, Lecomte J, Figueroa-Espinoza M-C, Baréa B, Weiss J, et al. Relationship between hydrophobicity and antioxidant ability of "phenolipids" in emulsion: a parabolic effect of the chain length of rosmarinate esters. Journal of agricultural and food chemistry. 2010;58(5):2869-76.
41. Zavascki AP, Carvalhaes CG, Picao RC, Gales AC. Multidrug-resistant Pseudomonas aeruginosa and Acinetobacter baumannii: resistance mechanisms and implications for therapy. Expert Rev Anti-Infect Ther. 2010;8(1):71-93.
42. Kaewjiaranai T, Srisatjaluk RL, Sakdajeyont W, Pairuchvej V, Wongsirichat N. The efficiency of topical anesthetics as antimicrobial agents: A review of use in dentistry. J Dent Anesth Pain Med. 2018;18(4):223.
43. Imani F, Mubarak SM, Mostafavi SKS, Khoda-Bakhshi M, Bojary MR, Ghasemian A. Antibacterial effects of local analgesics and anesthetics. Reviews in Medical Microbiology. 2020;31(1):47-50.
44. Vinklárková L, Masteikova R, Foltýnová G, Muselik J, Pavloková S, Bernatonienė J, et al. Film wound dressing with local anesthetic based on insoluble carboxymethycellulose matrix. Journal of Applied Biomedicine. 2017;15(4):313-20.
45. Maver T, Smrke D, Kurečič M, Gradišnik L, Maver U, Kleinschek KS. Combining 3D printing and electrospinning for preparation of pain-relieving wound-dressing materials. Journal of Sol-Gel Science and Technology. 2018;88(1):33-48.
46. Harris M, Ahmed H, Pace L, Minter J, Neel M, Jennings J. Evaluation of Antibiotic-Releasing Triphasic Bone Void Filler In-Vitro. Journal of functional biomaterials. 2018;9(4):55.
47. Olsen I. Biofilm-specific antibiotic tolerance and resistance. European Journal of Clinical Microbiology & Infectious Diseases. 2015;34(5):877-86.
48. Stewart PS, White B, Boegli L, Hamerly T, Williamson KS, Franklin MJ, et al. Conceptual model of biofilm antibiotic tolerance that integrates phenomena of diffusion, metabolism, gene expression, and physiology. Journal of bacteriology. 2019;201(22).
49. Moormeier DE, Bayles KW. Staphylococcus aureus biofilm: a complex developmental organism. Molecular microbiology. 2017;104(3):365-76.
50. O'Toole GA, Kolter R. Flagellar and twitching motility are necessary for Pseudomonas aeruginosa biofilm development. Molecular microbiology. 1998;30(2):295-304.
51. Klausen M, Heydorn A, Ragas P, Lambertsen L, Aaes-Jørgensen A, Molin S, et al. Biofilm formation by Pseudomonas aeruginosa wild type, flagella and type IV pili mutants. Molecular microbiology. 2003;48(6):1511-24.
52. Qi L, Christopher GF. Role of flagella, type IV Pili, biosurfactants, and extracellular polymeric substance polysaccharides on the formation of pellicles by Pseudomonas aeruginosa. Langmuir. 2019;35(15):5294-304.

53. Tomaras AP, Dorsey CW, Edelmann RE, Actis LA. Attachment to and biofilm formation on abiotic surfaces by Acinetobacter baumannii: involvement of a novel chaperone-usher pili assembly system. Microbiology. 2003;149(12):3473-84.
54. Pakharukova N, Tuittila M, Paavilainen S, Malmi H, Parilova O, Teneberg S, et al. Structural basis for Acinetobacter baumannii biofilm formation. Proceedings of the National Academy of Sciences. 2018;115(21):5558-63.
55. Fleming D, Rumbaugh KP. Approaches to dispersing medical biofilms. Microorganisms. 2017;5(2):15.
56. Estrela AB, Abraham W-R. Combining biofilm-controlling compounds and antibiotics as a promising new way to control biofilm infections. Pharmaceuticals. 2010;3(5):1374-93.
57. Aungst BJ. Structure/effect studies of fatty acid isomers as skin penetration enhancers and skin irritants. Pharmaceutical research. 1989;6(3):244-7.
58. Kalyanram P, Ma H, Marshall S, Goudreau C, Cartaya A, Zimmermann T, et al. Interaction of amphiphilic coumarin with DPPC/DPPS lipid bilayer: effects of concentration and alkyl tail length. Physical Chemistry Chemical Physics. 2020;22(27):15197-207.
59. Williams AC, Barry BW. Penetration enhancers. Advanced drug delivery reviews. 2012;64:128-37.
60. Becker DE, Reed KL. Essentials of local anesthetic pharmacology. Anesthesia progress. 2006;53(3):98-109.

# CHAPTER 4

## Efficacy of Chitosan-Mannitol Paste Loaded with Bupivacaine for Treatment of a Rat *S. Aureus* Infection Model

### Introduction

Implant and bone tissue contamination with bacteria poses a dire orthopaedic surgery complication, leading to bone infections. Biomaterials can, unfortunately, facilitate biofilm formation by providing a substrate for attachment but are tailorable to treat or inhibit these infections (1). Osteomyelitis commonly occurs in the long bones of the legs; however, it may happen in any bone in the body (2). Long bone metaphysis, i.e., tibia and femur, are frequently involved in long bone osteomyelitis, attributed to the metaphyseal region's anatomy (2). During an active osteomyelitis infection, blood flow becomes sluggish and disordered, allowing bacteria to settle, initiate colonization, and trigger an inflammatory response (2). Multidisciplinary treatment protocols, including surgical debridement and long-term antimicrobial therapy, are current strategies for bone infection treatment and lead to additional trauma and costs for patients (3-5). In adults, the most common organism isolated from osteomyelitis infections is *Staphylococcus aureus (S. aureus)* (6) and forms complex infections even without associated implant material (1).

*S. aureus* and *Staphylococcus epidermidis* are two of the most causative bacteria in osteomyelitis and are known for their ability to form biofilms (2). A biofilm contains a microbially derived sessile community, with cells attached to a substratum, interface, or each other. Biofilms can secrete and become embedded within an exopolymeric substance (EPS), which provides an initial barrier to immune cells and treatment. Additionally, typical biofilm characterization includes an altered phenotype that alters growth, protein production, and gene

expression, which all contribute to the ability of bacterial cells to evade clearance (7). These mechanisms lead to low metabolic levels and reduced cell division that contribute to the capacity of biofilm-associated bacteria to withstand up to 1000x the minimum inhibitory concentration of antibiotics (8).

Since 1884, local anesthetics (LAs) have been an instrumental pain management strategy; more recently, LA use has expanded due to their antimicrobial activities (9). Bacteriostatic, bactericidal, fungistatic, and fungicidal properties have been exhibited against a broad spectrum of microorganisms by many LAs with bupivacaine (BUP) and lidocaine (LID) showing inhibitory effects at clinically relevant concentrations (9). High clinical concentrations of BUP inhibit the growth of *Escherichia coli*, *S. aureus*, *S. epidermis*, *Streptococcus pneumoniae*, *S. pyogenes*, *Enterococcus faecalis*, *Bacillus cereus*, and *Candida albicans* (10).

Incorporating LAs into antimicrobial systems could be advantageous in decreasing the prevalence of infection and reducing the need for prescription pain medications. Local anesthetic delivery provides the highest possible concentration and focuses the treatment at the site where pain relief is most needed, reducing known systemic delivery issues. Numerous local delivery systems have been proposed that deliver local anesthetics (11-16). Locally delivering anesthetics minimizes the risk of adverse side effects by limiting contact or reaction with undesired targets. LAs, particularly LID, are often added to operative anesthesia solutions to reduce pain on intravenous injection (9). One study shows that while propofol alone promotes bacterial growth, combining LID with propofol inhibits growth significantly (17). These studies suggest that the inclusion of LAs within local delivery systems may effectively prevent or treat an infection. Local antimicrobial delivery systems are suitable routes for acute and chronic wound infection treatment, particularly as an adjunct to systemic antimicrobial delivery. Two commonly used

local delivery systems that administer antibiotics in clinical practice are poly (methyl methacrylate) (PMMA) and calcium sulfate ($CaSO_4$). PMMA beads loaded with antibiotics provide a predictable release for several weeks while reducing infection rates in severe open fractures (18). However, PMMA beads do not biodegrade and require additional surgeries for removal; they may also potentially deliver sub-inhibitory antibiotic concentrations, which may encourage incidences of bacteria tolerance or biofilm formation on their surface (18-24). $CaSO_4$ is biodegradable, but has several disadvantages, such as elevated wound drainage, limited antimicrobial choices and dosing, and a high initial, not sustained, burst release of loaded antimicrobial at the wound site (25-28).

Chitosan is a biocompatible, biodegradable, natural polymer that may serve as a promising alternative to existing drug delivery systems. Chitosan has been developed and studied in various formulations, including sponges, membranes, films, and pastes (29). Utilizing chitosan in paste form may be particularly useful for drug delivery to complex musculoskeletal injuries, as pastes can penetrate and conform to irregular tissue geometries. Previous studies have confirmed the efficacy of chitosan pastes in delivering antibiotics to wound beds; more recently, as an additional measure to increase the susceptibility of dormant bacterial cells to antibiotics, the sugar alcohol, mannitol, has been added to the chitosan paste (30-32). However, a limitation of previous paste formulations is that they do not allow for the loading of hydrophobic molecules readily. Previous work with acylated chitosan membranes has shown that they can load hydrophobic molecules through an ethanol evaporation process that also provides extended-release (33). In this study, we sought to determine if the addition of BUP to previously studied chitosan-mannitol pastes with an acylated component would increase the efficacy. Additionally, we sought to evaluate the antimicrobial activity of this local drug delivery system

through *in vitro* elution studies and a preliminary *in vivo* contaminated composite tissue defect model.

## Materials and Methods

### Fabrication

Chitopharm S chitosan powder (Chitinor AS, Tromsø, Norway; 82.46 ± 1.679 DDA; 250.6 kDa average molecular weight) was dissolved at 1% (w/v) with 1% (w/v) polyethylene glycol (PEG) (Sigma Aldrich, St. Louis, MO, USA; 8,000 g $mol^{-1}$ average MW) in 0.85% (v/v) acetic acid in deionized water solution; mannitol (Bulksupplements.com) was dissolved at 2% (w/v) in the previously described solution to form the chitosan-mannitol paste blend. The solutions were cast in 25 mL aluminum dishes and frozen overnight at -80 °C, then lyophilized in a benchtop freeze dryer (LabConco, Kansas City, MO, USA) to create acidic dehydrated sponges. Some sponges without mannitol were saved for use as controls during elution studies. Acidic control sponges were neutralized using 1 M sodium hydroxide (NaOH). The remaining chitosan-mannitol sponges were ground into fine powders (paste) and stored in a desiccator until sterilization with ethylene oxide gas with appropriate degassing occurring at the sterilization facility (34, 35). Hexanoic anhydride acylated the paste with a method similar to Wu et al. In brief, pyridine then hexanoic anhydride were added to the chitosan paste (10 mg $mL^{-1}$) at a 1:1 ratio and reacted under constant stirring for 1.5 hours. Once the reaction time was complete, the paste was vacuum filtered and washed five times: 1) 10% acetone (30 min), 2) 70% absolute ethanol (30 min), 3 - 5) deionized (DI) water (30 min each), and finally rinsed with acetone. The paste was removed from the filtration system and stored until further use.

To incorporate BUP into the acylated paste and achieve sterilization, BUP was solubilized in absolute ethanol (14 mg $mL^{-1}$), then 6 mL was added to 500 mg of acylated paste

in a plugged syringe. The ethanol was evaporated overnight (37 °C), leaving the BUP combined with the acylated paste in a dry state. Neutralized control sponges were diametrically sectioned (6 mm), placed into syringes (~500 mg), and loaded with BUP in the same manner as the acylated paste.

The BUP-loaded acylated paste was mixed with unmodified paste. First, 500 mg of unmodified paste was hydrated with 6 mL PBS using two 10 mL syringes and a Luer lock connector (Qosina, Ronkonkoma, NY). The PBS and unmodified paste were mixed several times until a uniform mixture formed with minimal resistance observed when transferring mixture between syringes. The bupivacaine-loaded acylated paste (500 mg) was then mixed with the unmodified hydrated paste through another coupled syringe. Like the hydration process, the mixing process was continued until a visible uniform mixture (BAHP) was obtained.

**Elution**

Sectioned sponges (n = 4) or 150 mL BAHP paste (n = 4) were placed in 8 mm pore size Costar® inserts. Inserts were placed in Costar Transwell ® plates and immersed in 1 mL PBS. Plates were covered with parafilm to minimize potential eluent evaporation. Next, plates were placed in a MidSci™ LabDoctor™ Mini Incubator Shaker at 37 °C and 30 rpm. Daily sampling occurred over seven days with complete PBS refreshing at the time of sampling. Eluates were frozen until further analysis. At the time of analysis, frozen eluates were thawed, vortexed, and centrifuged before being transferred (200 mL) to a 96-well plate for BUP concentration determination using a ThermoScientific Dionex Ultimate 3000 Series high-performance liquid chromatography (HPLC) system. BUP was detected using UV with 1.9 μg $mL^{-1}$ limit of detection using a 5 μL injection volume at λ= 200 with a 2 mL $min^{-1}$ flow rate, 5.3 min retention time using a BDS Hypersil GOLD reversed-phase C18 column (250 x 4.6 mm, 5 μm particle

size, 175 Å pore size) and an isocratic mobile phase. Mobile phase was 50% buffer (0.68% potassium dihydrogen phosphate, 0.05% triethylamine to 6.5 pH using orthophosphoric acid) and 50 % acetonitrile.

**Rat Traumatic Wound Model**

The Institutional Animal Care and Use Committee (IACUC) of Mississippi State University approved the animal research performed within this work under the protocol 20-153. Charles River Sprague Dawley 13-week old female rats were anesthetized with isoflurane at an initial concentration of 5% at 3 L $min^{-1}$ $O_2$ and sustained at 1 - 2% at 1 L $min^{-1}$ $O_2$. Following sterile left hindlimb preparation with alcohol, chlorhexidine scrubs, and fur removal, the skin was incised using an anterior approach. An incision was made from mid-diaphysis to the patella along the lower half of the femur. Muscle tissue was separated at the muscle bundle division by blunt dissection along the along the anterolateral side of the femur. Rat post-operative pain relief occurred by administering buprenorphine (1.0 - 1.2 mg $kg^{-1}$ BW, ZooPharm). A pneumatic drill (Conmed Hall) and a #65 drill bit (McMaster-Carr) were used to create a 1.2 mm (∅) bicortical defect in the mid-diaphysis. Sterile orthopaedic screws (Antrin Miniature Specialties, #00-90) were placed in 200 mL of bacterial suspension (~$1x10^8$ CFU) of ATCC 6538-GFP for an average of 5.25 min, range 4 - 6 min, to mimic orthopaedic screw *S. aureus* contamination in a traumatic wound or to develop osteomyelitis *in vivo*. The screw was subsequently dried in a 96-well plate for a 2 min average to a maximum of 5 min. Determining the contaminated screws' bacterial load was achieved by placing screws in PBS (1 mL), vigorously vortexing the screws to detach bacteria from screws, and then serially diluting the eluents for bacterial counting on BHI agar plates. Bacterial load was confirmed by vortexing and dilution plating of representative

samples inoculated at the same time to determine CFU. The superficial fascia lata and skin were closed with sutures to complete the *in vivo* procedure.

After a 7-day infection period, the area was accessed along the original incision line. The infected screw was removed and placed in 1 mL PBS for bacterial counting. The infection site was debrided, and all accessible pus was removed. The remaining defect area was either resealed without treatment, treated with unloaded chitosan paste (150 μL), or BUP-loaded chitosan paste (150 μL). Injections of treatments were done using a sterile 18-gauge needle placed onto a 1 mL syringe loaded with one of the two treatments.

**IVIS Imaging**

Two animals were chosen from each group based on temperament and reactions to isoflurane for longitudinal x-ray and fluorescence imaging 1, 7, 14, 21, and 28 days after treatment using the IVIS Lumina XRMS II system. Fluorescent and photographs were selected for one overlay image then the x-ray was captured immediately after. Fluorescent was set to auto exposure time, small binning, F $stop^{-1}$ of 1, excitation filter of 480 nm, and an emission filter of 520 nm. The photograph was set to auto exposure time, small binning, and F $stop^{-1}$ of 8. X-ray was sent to auto exposure time, high resolution binning, and F $stop^{-1}$ of 2. The animals were induced and maintained on isoflurane at 2% with 1 L $min^{-1}$ $O_2$. The lower threshold for fluorescence was increased 1/2 an order of magnitude of radiant efficiency to reduce the overlap effect of excitation and emission wavelengths.

**Retrieval**

On day 28 post-treatment, animals were euthanized via $CO_2$ inhalation. The animals had their dermis removed caudal of the scapula to their mid-tibia, and sterile instruments disarticulated the femur and adjacent soft tissues for further evaluation. For bacterial counting,

bone samples (n = 20) were initially minced with sterile bone rongeurs and further processed using a homogenizer (Cole-Parmer, LabGEN7, 30 s at setting 2 - 3, 30 s at setting 9 - 10). Soft tissue samples (n = 20) were minced using sterile scissors, then homogenized (30 s at setting 2 - 3, 30 s at setting 7 - 8). After initial processing, homogenates were vortexed (2000 RPM, 1 min), diluted as required, spread onto BHI agar plates, and incubated for 24 hours at 37 °C for enumeration, with a 25 - 250 colonies detection limit.

**Histology**

Following the sacrifice of animals, one animal in each group was selected for histological analysis. Bone and surrounding tissue were harvested and preserved in a 10% neutral formalin solution. Tissue samples were decalcified with formic acid, embedded in paraffin, sectioned into 5 μm slices, and stained with hematoxylin and eosin (H & E).

**Statistical analysis**

Statistical analysis was performed using SigmaPlot and GraphPad Prism 7.2 software (GraphPad Software Incorporation, La Jolla, CA, USA). Data was assessed first by performing a Shapiro-Wilk normality test, followed by a Brown-Forsythe equal variance test. If both passed, data were further analyzed with a one-way analysis of variance (ANOVA) followed by Holm-Sidak's post-hoc analysis to detect significance between experimental groups ($\alpha = 0.05$). If normality and equal variance were not passed, data were analyzed using Kruskal-Wallis ANOVA on ranks, followed by Tukey post-hoc test.

**Results**

**Elution**

BUP eluted from chitosan paste and control sponge groups with a pseudo-zero-order release profile, with the paste groups showing a slightly higher release on day one. Cumulative

release of BUP saw paste release at a marginally lower level compared to the sponge control. BUP continued to release at detectable levels for the duration of the 7-day study (Figure 4.1). The cumulative BUP release shows the chitosan sponge releasing at a higher rate with greater cumulative volume (Figure 4.2).

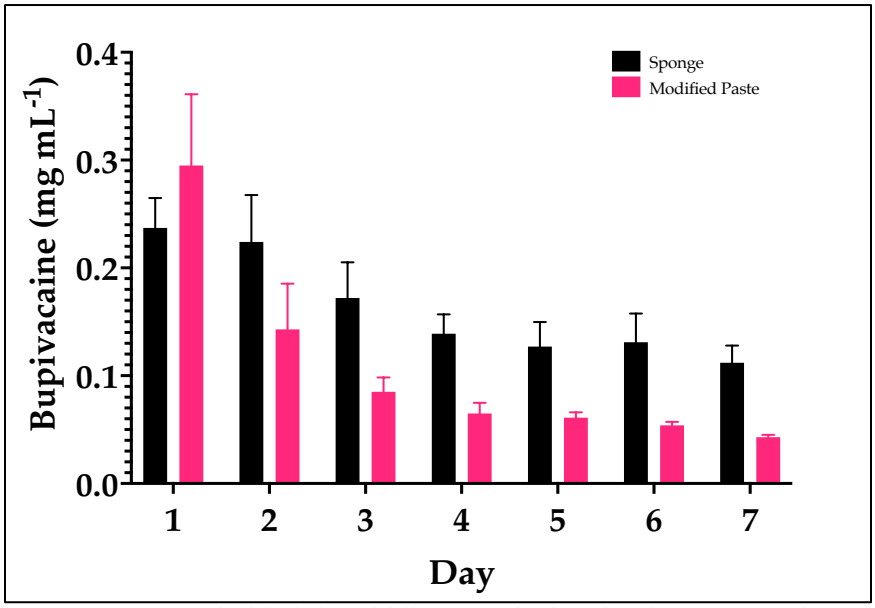


**Figure** . Mean ± standard deviation of daily average bupivacaine eluate concentration when eluted from chitosan sponge and modified paste (n = 4).

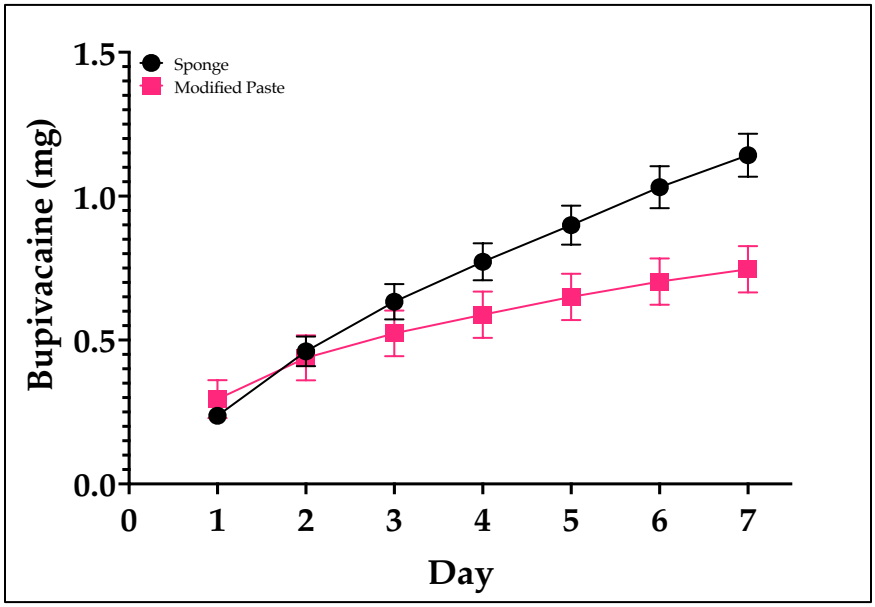


**Figure 4.1**. Mean ± standard deviation of cumulative bupivacaine eluate release when eluted from chitosan sponge and modified paste (n = 4).

## IVIS

Longitudinal IVIS images show reduced *S. aureus* growth in animals treated with BUP-loaded paste at all time points, though bacterial growth was not eliminated. Animals treated with unloaded paste showed sufficient bacterial growth at day one and week one posttreatment but subsequent reduction by week 3 (Figure 4.3).

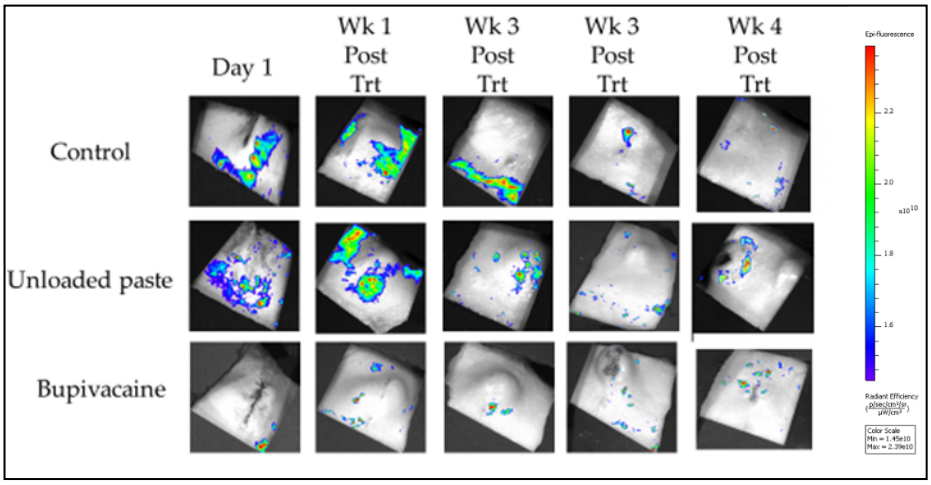


**Figure 4.2**. IVIS images of *S. aureus* over the duration of the study.

## CFU Counts

CFU counts for retrieved soft tissue were markedly lower than those for bone (Figures 4.4 & 4.5). Soft tissue bacterial counts showed similar results for untreated animals and animals treated with unloaded paste, with decreased CFUs for BUP-loaded paste and less variability. Overall, there were higher CFU counts from retrieved bone were higher. The highest bacterial burden is seen with untreated animals, followed by those treated with unloaded paste and the lowest bacterial growth for animals treated with BUP-loaded paste; again, the BUP treated animals had minor CFU count variability.

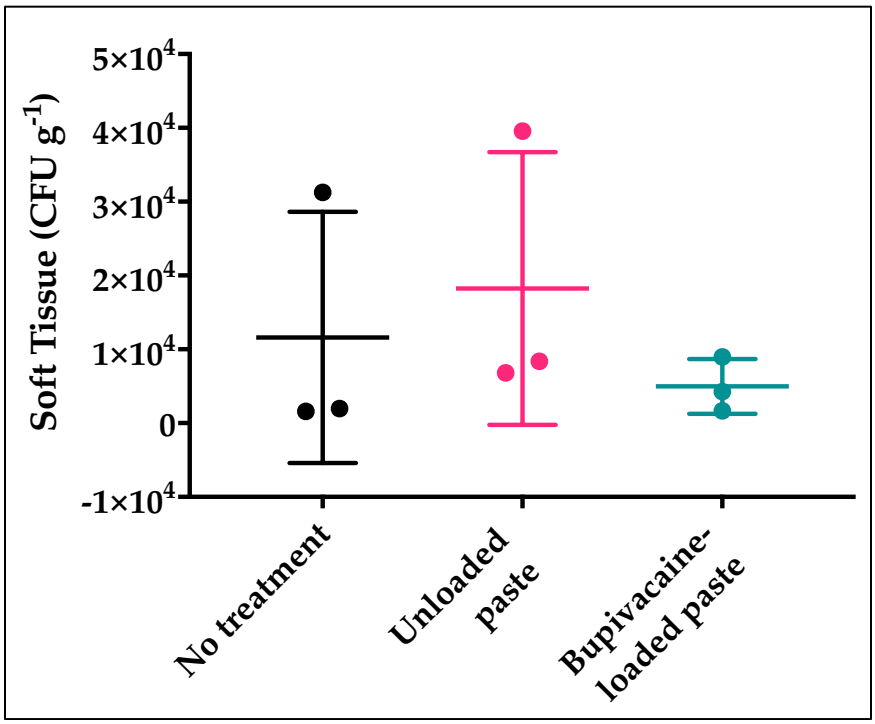


**Figure 4.3**. *S. aureus'* CFU gram$^{-1}$ of soft tissue harvested from rats following treatment with pastes (n = 3).

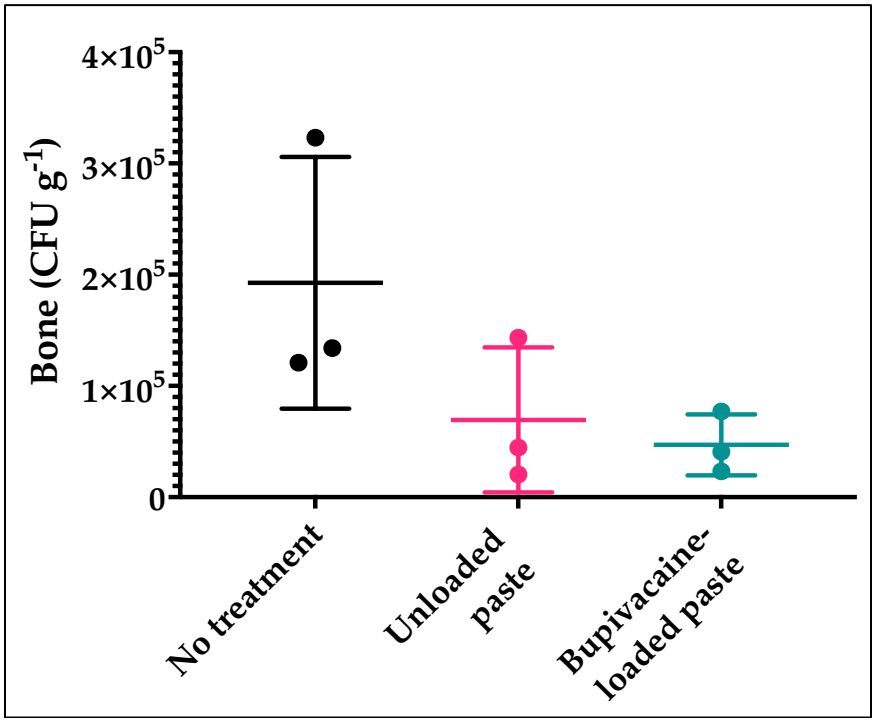


**Figure 4.4**. *S. aureus'* CFU gram$^{-1}$ of bone harvested from rats following treatment with pastes (n = 3).

## Histology

Representative histological images of treated and control animals four weeks after material implantation show mild inflammation for animals treated with unloaded paste and moderate inflammation for animals treated with BUP-loaded paste (Figure 4.5). There was no visible chitosan paste remaining in wounds.

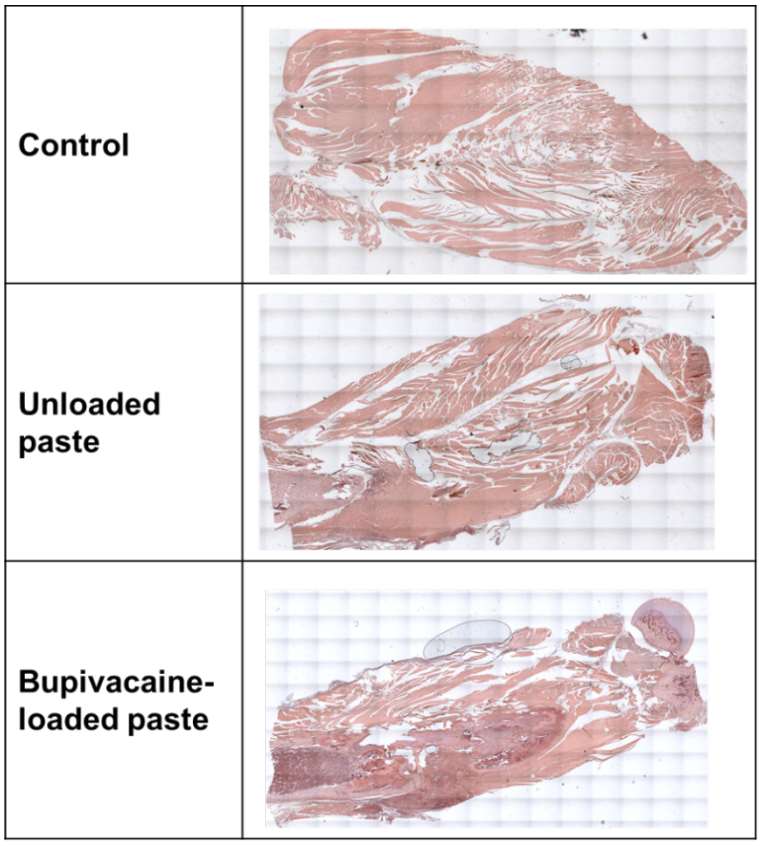


**Figure 4.5**. Photomicrographs (4x magnification) showing sections of soft tissue and bone from retrievals.

## Discussion

This model evaluated the efficacy of chitosan-mannitol paste loaded with BUP and 2-decenoic acid to prevent internal *S. aureus* osteomyelitis and contiguous soft tissue infection in a rat model. The formulation of acylated particles within an injectable paste offers advantages over other delivery vehicles in that it can be more readily applied to complex geometries of tissue injuries. Overall, the results demonstrated an effect of the proposed treatments in reducing

viable *S. aureus* CFUs in the bone and the surrounding soft tissue. However, rebounding infection indicates that doses of antimicrobial were insufficient for biofilm eradication. BUP-loaded paste produced the most significant reduction of *S. aureus* viable units in the bone, consistent with previous studies (36, 37). Modification of paste components by acylation, reported for the first time in this study, may serve as a basis for subsequent refinement of material fabrication and loading strategies for future studies.

The non-acylated paste is capable of being loaded with hydrophilic therapeutics, which results in first-order release kinetics. Multiple previous studies involving non-acylated paste could be passively loaded and subsequently release hydrophilic therapeutics at levels above investigated bacteria MICs (38-41). Previously studied paste systems have exhibited first-order release kinetics and release most if not all loaded therapeutics within 72 hours. During Beretta et al. studies, hydrophilic therapeutics were released almost entirely from pastes within 24 hours (39). Alexander et al. developed a thermogelling chitosan paste that released vancomycin for detectable levels through five days, but at deficient levels after day two. When including mannitol into the chitosan paste, Pace et al. determined elution of hydrophilic therapeutics extended through seven days and had a lower initial burst release than non-mannitol paste (30). The acylated paste, in contrast, provides opportunities to load hydrophobic therapeutics, which has previously been challenging to achieve. BUP-loaded pastes can realize pseudo-zero-order release of high concentrations of antimicrobials locally, although released levels may not totally eradicate biofilm. Elution from the acylated paste shows an ability to be sustained at a constant level for up to seven days, resulting from the hydrophobic nature of the modified paste's surface. Theoretical bupivacaine loading calculations indicate that approximately 6% of loaded bupivacaine was released from BAHP during the 7-day study, providing support for evaluating

bupivacaine release from BAHP over a longer time frame. Future studies will perform techniques to determine the exact amount of bupivacaine loaded into the BAHP. Zero-order extended-release of simvastatin, a hydrophobic therapeutic, has been reported from acylated nanofibrous membranes (33). The acyl modification of the material may enable the loading of other hydrophobic antimicrobials, such as the biofilm-active rifampin and ciprofloxacin. Previous studies of rifampin and ciprofloxacin loaded within sponges demonstrated challenges in solubilizing and releasing these for an extended time (42). When attempting to inhibit bacteria-derived infections, a sustained release is often one of the primary objectives and may provide an adjunct therapy to systemic delivery. An advantage of using bupivacaine as the antimicrobial component is that pain reduction may occur over an extended period of delivery (43). However, we did not directly measure pain outcomes in this study.

Biofilm-associated infections depend on their ability to remain in a state that is counter to their planktonic state. CFU bone analyses show that the proposed therapeutics do not eliminate the presence of bacteria. However, the longitudinal IVIS images indicate that initial bioburden may be reduced in groups loaded with antimicrobials. Failure to eliminate bacteria could be a result of insufficient loading. Maximizing therapeutic loading is critical to having a therapeutic system that can inhibit or eradicate a bacteria-derived infection, especially when treating biofilms, which can withstand high antimicrobial concentrations (44). In addition to improper loading, lack of adhesion may contribute to the pastes' limited residency time in the defects and surrounding areas and explain persisting infection. Although we did not directly measure degradation in this study, previous studies demonstrate that unmodified mannitol-based pastes degrade approximately 72% of their mass *in vitro* over 14 days (30). The majority of the paste is injected directly into the bone defect in this model. Still, it may have enhanced diffusion through

soft tissue, explaining the markedly lower CFU counts in the soft tissue than in the bone. *S. aureus* is known to invade the osteocanalicular network of bone, which also poses challenges to adequate delivery (45). The defect size required specific syringe gauge sizes for therapeutic application, which may have resulted in inconsistent delivery. The available space, which influenced the sight field and availability of components that can load therapeutics, impaired the treatment placement. Therapeutic paste composition, which affects injectability, may be refined in future experiments to ease mixing and increase the acylated component for increased loading. These issues would be less impactful in larger animal models, improving all stated limitations regarding the proper therapeutic application, placement, and residency time. Increasing the ratio of the less degradable acylated component may alco increase residency time to further extend release and efficacy.

Treatment of existing biofilm infection is particularly challenging, although the results of this study may indicate a role for this biomaterial paste in infection prevention. Future studies may evaluate these systems delivered at the time of initial contamination. Closely related to residence time is the placement of the treatment into the defect area. The chance for complete clearance significantly reduces if the therapy is inaccurately loaded. When the treatment is applied, the paste must be in the defect area, providing the best chance for effective antimicrobial activity. Not having the paste appropriately in the area requiring treatment affects residency time and antimicrobial activity since both require contact with the bacteria.

**Conclusions**

Acylated chitosan-based biomaterials provided a foundation to load and deliver hydrophobic compounds otherwise not possible without additional considerations. The therapeutic system achieved the study objective of reducing an *S. aureus*-based infection;

however, there remains room for improvement. While engineered for hydrophobic compounds, the system could benefit from slight modifications allowing for incorporation of hydrophilic antibiotics. Future studies should evaluate the antimicrobial efficacy of chitosan-based biomaterials directly acylated with known antimicrobial therapeutics. While the results are promising, future studies should assess bupivacaine combined with other proven antimicrobials, e.g., other local anesthetics, 2-decenoic analogs, antibiotics, and their combinations. Additional upcoming studies should test acylated biomaterial in a polymicrobial infection model.

## References


1. Geurts JAP, van Vugt TAG, Arts JJC. Use of contemporary biomaterials in chronic osteomyelitis treatment: Clinical lessons learned and literature review. Journal of Orthopaedic Research. 2020.
2. Brady RA, Leid JG, Calhoun JH, Costerton JW, Shirtliff ME. Osteomyelitis and the role of biofilms in chronic infection. Fems Immunology and Medical Microbiology. 2008;52(1):13-22.
3. Ferguson J, Diefenbeck M, McNally M. Ceramic biocomposites as biodegradable antibiotic carriers in the treatment of bone infections. Journal of bone and joint infection. 2017;2(1):38.
4. Garcia-Gareta E, Davidson C, Levin A, Coathup MJ, Blunn GW. Biofilm formation in total hip arthroplasty: prevention and treatment. Rsc Advances. 2016;6(83):80244-61.
5. Zimmerli W, Moser C. Pathogenesis and treatment concepts of orthopaedic biofilm infections. FEMS Immunology & Medical Microbiology. 2012;65(2):158-68.
6. Shirtliff M, Cripps M, Mader J, editors. Retrospective review of 728 patients with long bone osteomyelitis. The General Meeting of The American Society for Microbiology; 1999.
7. Donlan RM, Costerton JW. Biofilms: survival mechanisms of clinically relevant microorganisms. Clinical microbiology reviews. 2002;15(2):167-93.
8. Bjarnsholt T. The role of bacterial biofilms in chronic infections. Apmis. 2013;121:1-58.
9. Johnson SM, Saint John BE, Dine AP. Local anesthetics as antimicrobial agents: a review. Surgical infections. 2008;9(2):205-13.
10. Rosenberg PH, Renkonen OV. Antimicrobial activity of bupivacaine and morphine. Anesthesiology. 1985;62(2):178-9.
11. Gil D, Grindy S, Muratoglu O, Bedair H, Oral E. Antimicrobial effect of anesthetic-eluting ultra-high molecular weight polyethylene for post-arthroplasty antibacterial prophylaxis. Journal of Orthopaedic Research®. 2019;37(4):981-90.
12. Grindy SC, Gil D, Suhardi JV, Muratoglu OK, Bedair H, Oral E. Delivery of bupivacaine from UHMWPE and its implications for managing pain after joint arthroplasty. Acta Biomaterialia. 2019;93:63-73.
13. Khanal M, Gohil SV, Kuyinu E, Kan H-M, Knight BE, Baumbauer KM, et al. Injectable nanocomposite analgesic delivery system for musculoskeletal pain management. Acta biomaterialia. 2018;74:280-90.
14. Bagshaw KR, Hanenbaum CL, Carbone EJ, Lo KW, Laurencin CT, Walker J, et al. Pain management via local anesthetics and responsive hydrogels. Therapeutic delivery. 2015;6(2):165-76.
15. Ulery BD, Kan HM, Williams BA, Narasimhan B, Lo KWH, Nair LS, et al. Facile fabrication of polyanhydride/anesthetic nanoparticles with tunable release kinetics. Advanced healthcare materials. 2014;3(6):843-7.
16. Foley PL, Ulery BD, Kan HM, Burks MV, Cui Z, Wu Q, et al. A chitosan thermogel for delivery of ropivacaine in regional musculoskeletal anesthesia. Biomaterials. 2013;34(10):2539-46.
17. Gajraj R, Hodson M, Gillespie J, Kenny G, Scott N. Antibacterial activity of lidocaine in mixtures with Diprivan. British journal of anaesthesia. 1998;81(3):444-8.

18. Schwarz EM, McLaren AC, Sculco TP, Brause B, Bostrom M, Kates SL, et al. Adjuvant antibiotic-loaded bone cement: concerns with current use and research to make it work. Journal of Orthopaedic Research®. 2020.
19. Bint A, Burtt I. Adverse antibiotic drug interactions. Drugs. 1980;20(1):57-68.
20. Chihara S, Segreti J. Osteomyelitis. Disease-a-month: DM. 2010;56(1):5-31.
21. Dombrowski JC, Winston LG. Clinical failures of appropriately-treated methicillin-resistant Staphylococcus aureus infections. Journal of Infection. 2008;57(2):110-5.
22. Murray CK, Hsu JR, Solomkin JS, Keeling JJ, Andersen RC, Ficke JR, et al. Prevention and management of infections associated with combat-related extremity injuries. Journal of Trauma and Acute Care Surgery. 2008;64(3):S239-S51.
23. Tice AD, Hoaglund PA, Shoultz DA. Risk factors and treatment outcomes in osteomyelitis. Journal of antimicrobial chemotherapy. 2003;51(5):1261-8.
24. Westphal J, Vetter D, Brogard J. Hepatic side-effects of antibiotics. Journal of Antimicrobial Chemotherapy. 1994;33(3):387-401.
25. Diefenbeck M, Mückley T, Hofmann GO. Prophylaxis and treatment of implant-related infections by local application of antibiotics. Injury. 2006;37(2):S95-S104.
26. Kendall RW, Duncan CP, Smith JA, Ngui-Yen JH. Persistence of bacteria on antibiotic loaded acrylic depots: a reason for caution. Clinical Orthopaedics and Related Research®. 1996;329:273-80.
27. Tunney MM, Ramage G, Patrick S, Nixon JR, Murphy PG, Gorman SP. Antimicrobial susceptibility of bacteria isolated from orthopedic implants following revision hip surgery. Antimicrobial agents and chemotherapy. 1998;42(11):3002-5.
28. Yorgason JG, Fayad JN, Kalinec F. Understanding drug ototoxicity: molecular insights for prevention and clinical management. Expert opinion on drug safety. 2006;5(3):383-99.
29. Jennings JA, Bumgardner JD. Chitosan Based Biomaterials Volume 1: Fundamentals: Woodhead Publishing; 2016.
30. Pace LR, Harrison ZL, Brown MN, Haggard WO, Jennings JA. Characterization and Antibiofilm Activity of Mannitol–Chitosan-Blended Paste for Local Antibiotic Delivery System. Marine drugs. 2019;17(9):517.
31. Harrison ZL, Pace LR, Brown MN, Beenken KE, Smeltzer MS, Bumgardner JD, et al. Staphylococcal infection prevention using antibiotic-loaded mannitol–chitosan paste in a rabbit model of implant-associated osteomyelitis. Journal of Orthopaedic Research®. 2021.
32. Allison KR, Brynildsen MP, Collins JJ. Metabolite-enabled eradication of bacterial persisters by aminoglycosides. Nature. 2011;473(7346):216-20.
33. Murali VP, Fujiwara T, Gallop C, Wang Y, Wilson JA, Atwill MT, et al. Modified electrospun chitosan membranes for controlled release of simvastatin. International Journal of Pharmaceutics. 2020:119438.
34. Mendes GC, Brandao TR, Silva CL. Ethylene oxide sterilization of medical devices: a review. American journal of infection control. 2007;35(9):574-81.
35. Shintani H. Ethylene oxide gas sterilization of medical devices. Biocontrol science. 2017;22(1):1-16.
36. Imani F, Mubarak SM, Mostafavi SKS, Khoda-Bakhshi M, Bojary MR, Ghasemian A. Antibacterial effects of local analgesics and anesthetics. Reviews in Medical Microbiology. 2020;31(1):47-50.

37. Sakuragi T, Ishino H, Dan K. Bactericidal activity of clinically used local anesthetics on Staphylococcus aureus. Regional Anesthesia: The Journal of Neural Blockade in Obstetrics, Surgery, & Pain Control. 1996;21(3):239-42.
38. Rhodes CS, Alexander CM, Berretta JM, Courtney HS, Beenken KE, Smeltzer MS, et al. Evaluation of a chitosan-polyethylene glycol paste as a local antibiotic delivery device. World journal of orthopedics. 2017;8(2):130.
39. Berretta JM, Jennings JA, Courtney HS, Beenken KE, Smeltzer MS, Haggard WO. Blended chitosan paste for infection prevention: preliminary and preclinical evaluations. Clinical Orthopaedics and Related Research®. 2017;475(7):1857-70.
40. Boles L, Alexander C, Pace L, Haggard W, Bumgardner J, Jennings J. Development and evaluation of an injectable chitosan/β-Glycerophosphate paste as a local antibiotic delivery system for trauma care. Journal of functional biomaterials. 2018;9(4):56.
41. Boles LR, Bumgardner JD, Fujiwara T, Haggard WO, Guerra FD, Jennings JA. Characterization of trimethyl chitosan/polyethylene glycol derivatized chitosan blend as an injectable and degradable antimicrobial delivery system. International journal of biological macromolecules. 2019;133:372-81.
42. Wells CM, Beenken KE, Smeltzer MS, Courtney HS, Jennings JA, Haggard WO. Ciprofloxacin and Rifampin Dual Antibiotic-Loaded Biopolymer Chitosan Sponge for Bacterial Inhibition. Mil Med. 2018;183(suppl_1):433-44.
43. Dissanaike S, McCauley J, Alphonso C. Liposomal bupivacaine for the management of postsurgical donor site pain in patients with burn injuries: a case series from two institutions. Clinical case reports. 2018;6(1):129.
44. Crabbé A, Jensen PØ, Bjarnsholt T, Coenye T. Antimicrobial tolerance and metabolic adaptations in microbial biofilms. Trends in microbiology. 2019;27(10):850-63.
45. Masters EA, Trombetta RP, de Mesy Bentley KL, Boyce BF, Gill AL, Gill SR, et al. Evolving concepts in bone infection: Redefining “biofilm”,“acute vs. chronic osteomyelitis”,“the immune proteome” and “local antibiotic therapy”. Bone Res. 2019;7(1):1-18.

# CHAPTER 5

## Conclusions

The results presented in this dissertation indicate that chitosan-based biomaterials are modifiable with fatty acid chlorides. The custom chloride synthesis route increases previously inaccessible compounds to modify chitosan-based biomaterials with the acylation process. Acylated chitosan-based biomaterials are cytocompatible with properties that inhibit infection and biofilm. Based on previous studies, the pain mitigation effects of LAs are assumed to be consistent with the *in vivo* and *in vitro* functionality observed with the modified chitosan-based biomaterials.

Chapter 2 demonstrated the ability to synthesize fatty acid chlorides from compounds that are themselves synthesized or not available commercially. Unmodified chitosan-based biomaterial material characteristics, i.e., fiber structure and size, do not significantly change after modification with fatty acid chlorides. Cytocompatibility is not adversely affected and may increase after the chitosan-based biomaterials surfaces are modified. Chitosan-based biomaterials' surface modification increases the baseline antimicrobial properties compared to their unmodified counterparts. Additionally, modifying chitosan-based biomaterials with fatty acid chlorides allows elution profiles to be customized.

The antimicrobial studies conducted in Chapter 3 confirm previous studies concerning the antimicrobial ability of local anesthetics. It is critical to note that the work in Chapter 3 determined the local anesthetics' true baseline antimicrobial capabilities since the investigated compounds were not acid-formulated, as seen in many previous works. Nonacid formulated local anesthetics are more challenging to work with and may not be feasible for point-of-care loading; however, they provide an excellent basis for prefabricated treatment options.

The results in Chapter 4 support the use of modified chitosan-based biomaterials in local delivery infection prevention systems. Modified chitosan-based biomaterials can be loaded with multiple antimicrobial therapeutics and elute those loaded therapeutics at levels that assist in controlling an infection. Moreover, the results obtained during this *in vivo* infection model were for an established infection. Positive results from this chapter are more promising since the engineering of the chitosan-based biomaterials used during this investigation was for an infection inhibition role. Engineered technological enhancements are possible to make the modified chitosan-based biomaterials better suited to fight established infections. Furthermore, this study produced the results without potentially maximizing clinically relevant therapeutic loading. These factors, among others, offer promise for the future of the investigated therapeutic combination used with the modified chitosan-based biomaterial or another comparable modified chitosan-based biomaterial.

Local delivery systems that include fatty acid chloride modified chitosan-based biomaterials possess the ability to load and deliver hydrophobic therapeutics. Many local delivery systems are extremely limited in this manner. Local delivery systems with fatty acid acyl-modified biomaterials demonstrate a reduced initial burst release and subsequently perform with a pseudo-zero-order release profile over more than seven days. This study's elution release profile is an improvement over other local delivery systems that, on average, release loaded therapeutics with a first-order release profile and within the first week. Local delivery systems that include modified biomaterials do not degrade as fast as other local delivery systems. This improvement gives the local delivery system more residency time in or around to deliver any loaded therapeutic, possibly extending antimicrobial activity. There are numerous potential clinical implications beyond infection prevention and treatment for acyl-modified local delivery

systems. Expanded potential clinical applications for these include delivering hydrophobic drugs, i.e., chemotherapeutics and tissue and bone regeneration methods.

# CHAPTER 6

## Recommendations for Future Work

Additional research evaluations on acylated chitosan-based biomaterials should seek to understand better their properties and functionality for local antimicrobial therapeutic delivery and infection prevention. These properties include determining the degree of substitution and utilizing nuclear magnetic resonance to gain more knowledge of molecular structure changes if they exist. Functionality investigations should evaluate the acyl-modified chitosan-based biomaterials' antimicrobial efficacy without any additionally loaded antimicrobials. Further *in vitro* elution evaluations and activity research with other hydrophobic antimicrobials, such as ciprofloxacin or rifampin, may increase potential clinical applications of acylated chitosan-based biomaterials. Auxiliary *in vitro* elution evaluations should incorporate certain well-known antibiotics, e.g., vancomycin or amikacin, to determine functionality with standard clinical treatment options. Therapeutic loading capacities require testing to maximize the infection prevention time-frame and elution properties. Additionally, if the therapeutics include local anesthetics, future studies should maximize the loading levels to benefit pain relief and antimicrobial efficacy. Ongoing studies should evaluate local anesthetics in various combinations against a broad spectrum of microorganisms. Antimicrobial efficacy for the tested local anesthetics varied depending on strain and phenotype, i.e., planktonic versus biofilm. Combining local anesthetics could provide inhibition against polymicrobial infections.

The degradation properties of acylated chitosan-based biomaterials require further assessment. Hydrophilic chitosan-based biomaterials have demonstrated promising *in vitro* and

*in vivo* degradability; however, acylated chitosan-based biomaterials are hydrophobic. The degradation evaluation should correlate with expected residency time within the body, e.g., 30 – 180 days, or at the wound site, which varies depending on the application, i.e., wound dressing or treatment component, and wound severity. Future *in vivo* models of infection prevention should provide a more definitive biofilm and infection inhibition assessment. Finally, upcoming studies should evaluate acylated chitosan-based biomaterials in a large *in vivo* animal model with clinically representative traumatic musculoskeletal wounds.

**References**


1. Logeart-Avramoglou D, Anagnostou F, Bizios R, Petite H. Engineering bone: challenges and obstacles. Journal of cellular and molecular medicine. 2005;9(1):72-84.
2. Patel A, Calfee R, Plante M, Fischer S, Arcand N, Born C. Methicillin-resistant Staphylococcus aureus in orthopaedic surgery. The Journal of bone and joint surgery British volume. 2008;90(11):1401-6.
3. Kumar G, Narayan B. Prevention of infection in the treatment of one thousand and twenty-five open fractures of long bones. Retrospective and prospective analyses. Classic Papers in Orthopaedics: Springer; 2014. p. 527-30.
4. Patzakis MJ, HARVEY JR JP, Ivler D. The role of antibiotics in the management of open fractures. JBJS. 1974;56(3):532-41.
5. Patzakis MJ, Wilkins J. Factors influencing infection rate in open fracture wounds. Clinical orthopaedics and related research. 1989(243):36-40.
6. Church D, Elsayed S, Reid O, Winston B, Lindsay R. Burn wound infections. Clinical microbiology reviews. 2006;19(2):403-34.
7. Arciola CR, Campoccia D, Montanaro L. Implant infections: adhesion, biofilm formation and immune evasion. Nature Reviews Microbiology. 2018;16(7):397-409.
8. Moucha C, Evans R, Clyburn T, Huddleston P, Prokuski L, Joseph J, et al. Orhtopaedic Infection Prevention and Control: An Emerging New Paradigm. in American Academy of Orthopaedic Surgeons, 76th Annual Meeting. Las Vegas, Nevada: American Academy of Orthopaedic Surgeons. 2009.
9. Bozic KJ, Kurtz SM, Lau E, Ong K, Vail TP, Berry DJ. The epidemiology of revision total hip arthroplasty in the United States. JBJS. 2009;91(1):128-33.
10. Murray CK. Epidemiology of infections associated with combat-related injuries in Iraq and Afghanistan. Journal of Trauma and Acute Care Surgery. 2008;64(3):S232-S8.
11. Calhoun JH, Murray CK, Manring M. Multidrug-resistant organisms in military wounds from Iraq and Afghanistan. Clinical orthopaedics and related research. 2008;466(6):1356-62.
12. Sudhan SS, Sharma P, Sharma K, Sharma M, Sambyal SS. Time Related Emergence of Bacterial Pathogens and their Antibiograms in Burn Wound Infections in a Tertiary Care Hospital. Int J Curr Microbiol App Sci. 2017;6(4):416-22.
13. Davis SC, Ricotti C, Cazzaniga A, Welsh E, Eaglstein WH, Mertz PM. Microscopic and physiologic evidence for biofilm-associated wound colonization in vivo. Wound repair and Regeneration. 2008;16(1):23-9.
14. Trampuz A, Widmer AF. Infections associated with orthopedic implants. Current opinion in infectious diseases. 2006;19(4):349-56.
15. Eming SA, Brachvogel B, Odorisio T, Koch M. Regulation of angiogenesis: wound healing as a model. Progress in histochemistry and cytochemistry. 2007;42(3):115-70.
16. Bartkova J, Grøn B, Dabelsteen E, Bartek J. Cell-cycle regulatory proteins in human wound healing. Archives of Oral Biology. 2003;48(2):125-32.
17. Simpson DM, Ross R. The neutrophilic leukocyte in wound repair: a study with antineutrophil serum. The Journal of clinical investigation. 1972;51(8):2009-23.
18. Sherratt JA, Dallon JC. Theoretical models of wound healing: past successes and future challenges. Comptes rendus biologies. 2002;325(5):557-64.
19. Diegelmann RF, Cohen IK, Kaplan AM. The role of macrophages in wound repair: a review. Plastic and reconstructive surgery. 1981;68(1):107-13.

20. Eisinger M, Sadan S, Silver I, Flick R. Growth regulation of skin cells by epidermal cell-derived factors: implications for wound healing. Proceedings of the National Academy of Sciences. 1988;85(6):1937-41.
21. Menke MN, Menke NB, Boardman CH, Diegelmann RF. Biologic therapeutics and molecular profiling to optimize wound healing. Gynecologic oncology. 2008;111(2):S87-S91.
22. Hunt T, Knighton D, Thakral K, Andrews W. Studies on inflammation and wound healing: angiogenesis and collagen synthesis stimulated in vivo by resident and activated wound macrophages. Surgery. 1984;96(1):48-54.
23. Beitz JM. Wound debridement: therapeutic options and care considerations. Critical Care Nursing Clinics. 2012;24(2):239-53.
24. Nelson CL, McLaren SG, Skinner RA, Smeltzer MS, Thomas JR, Olsen KM. The treatment of experimental osteomyelitis by surgical debridement and the implantation of calcium sulfate tobramycin pellets. Journal of Orthopaedic Research. 2002;20(4):643-7.
25. Sieggreen MY, Maklebust J. Debridement: choices and challenges. Advances in wound care: the journal for prevention and healing. 1997;10(2):32-7.
26. Lord J, Rossi G, Daliana M. Intraoperative antibiotic wound lavage: an attempt to eliminate postoperative infection in arterial and clean general surgical procedures. Annals of surgery. 1977;185(6):634.
27. Schwarz EM, Parvizi J, Gehrke T, Aiyer A, Battenberg A, Brown SA, et al. 2018 international consensus meeting on musculoskeletal infection: research priorities from the general assembly questions. Journal of Orthopaedic Research®. 2019;37(5):997-1006.
28. Falanga V. Wound bed preparation and the role of enzymes: a case for multiple actions of therapeutic agents. Wounds. 2002;14:47-57.
29. Steed DL, Donohoe D, Webster MW, Lindsley L. Effect of extensive debridement and treatment on the healing of diabetic foot ulcers. Diabetic Ulcer Study Group. Journal of the American College of Surgeons. 1996;183(1):61-4.
30. Berríos-Torres SI, Umscheid CA, Bratzler DW, Leas B, Stone EC, Kelz RR, et al. Centers for disease control and prevention guideline for the prevention of surgical site infection, 2017. JAMA surgery. 2017;152(8):784-91.
31. Palumbo VD. 2016 WHO Global Guidelines for the Prevention of Surgical Site Infection: A New Step to Improve Patient's Safety Before, During and After Surgery. 2017.
32. Allegranzi B, Zayed B, Bischoff P, Kubilay NZ, de Jonge S, de Vries F, et al. New WHO recommendations on intraoperative and postoperative measures for surgical site infection prevention: an evidence-based global perspective. The Lancet Infectious Diseases. 2016;16(12):e288-e303.
33. Schmidt K, Estes C, McLaren A, Spangehl MJ. Chlorhexidine antiseptic irrigation eradicates Staphylococcus epidermidis from biofilm: an in vitro study. Clinical orthopaedics and related research. 2018;476(3):648.
34. Fan C-y, Chiang C-C, Chuang T-Y, Chiu F-Y, Chen T-H. Interlocking nails for displaced metaphyseal fractures of the distal tibia. Injury. 2005;36(5):669-74.
35. Kellam JF. Interlocking nail fixation for humeral shaft fractures. Operative techniques in orthopaedics. 1991;1(4):336-46.
36. Perren SM. Evolution of the internal fixation of long bone fractures: the scientific basis of biological internal fixation: choosing a new balance between stability and biology. The Journal of bone and joint surgery British volume. 2002;84(8):1093-110.

37. Schmidt K, Estes C, McLaren A, Spangehl MJ. Chlorhexidine Antiseptic Irrigation Eradicates Staphylococcus epidermidis From Biofilm: An In Vitro Study. Clinical orthopaedics and related research. 2018;476(3):648-53.
38. Crowley D, Kanakaris N, Giannoudis P. Debridement and wound closure of open fractures: the impact of the time factor on infection rates. Injury. 2007;38(8):879-89.
39. Stiffler KS. Internal fracture fixation. Clinical Techniques in Small Animal Practice. 2004;19(3):105-13.
40. Manley MT, Dumbleton JH, Sutton K, editors. Fixation choices for primary hip and knee applications. Seminars in Arthroplasty; 2006: Elsevier.
41. Esterhai J, Gristina A, Poss R, editors. Musculoskeletal Infection. American Academy of Orthopaedic Surgeons; 1992; Park Ridge, IL.
42. Campoccia D, Montanaro L, Arciola CR. The significance of infection related to orthopedic devices and issues of antibiotic resistance. Biomaterials. 2006;27(11):2331-9.
43. Jog S, Cunningham R, Cooper S, Wallis M, Marchbank A, Vasco-Knight P, et al. Impact of preoperative screening for meticillin-resistant Staphylococcus aureus by real-time polymerase chain reaction in patients undergoing cardiac surgery. Journal of Hospital Infection. 2008;69(2):124-30.
44. Klevens RM, Morrison MA, Nadle J, Petit S, Gershman K, Ray S, et al. Invasive methicillin-resistant Staphylococcus aureus infections in the United States. Jama. 2007;298(15):1763-71.
45. Kuehnert MJ, Hill HA, Kupronis BA, Tokars JI, Solomon SL, Jernigan DB. Methicillin-resistant–Staphylococcus aureus hospitalizations, United States. Emerging infectious diseases. 2005;11(6):468.
46. Engemann JJ, Carmeli Y, Cosgrove SE, Fowler VG, Bronstein MZ, Trivette SL, et al. Adverse clinical and economic outcomes attributable to methicillin resistance among patients with Staphylococcus aureus surgical site infection. Clinical infectious diseases. 2003;36(5):592-8.
47. Anstead GM, Owens AD. Recent advances in the treatment of infections due to resistant Staphylococcus aureus. Current opinion in infectious diseases. 2004;17(6):549-55.
48. Rybak L, Ramkumar V. Ototoxicity. Kidney international. 2007;72(8):931-5.
49. Naughton CA. Drug-induced nephrotoxicity. American family physician. 2008;78(6):743-50.
50. Saeed K, McLaren AC, Schwarz EM, Antoci V, Arnold WV, Chen AF, et al. 2018 international consensus meeting on musculoskeletal infection: Summary from the biofilm workgroup and consensus on biofilm related musculoskeletal infections. Journal of Orthopaedic Research. 2019;37(5):1007-17.
51. Scott RD. The direct medical costs of healthcare-associated infections in US hospitals and the benefits of prevention. 2009.
52. Anderson DJ, Kirkland KB, Kaye KS, Thacker PA, Kanafani ZA, Auten G, et al. Underresourced hospital infection control and prevention programs: penny wise, pound foolish? Infection Control & Hospital Epidemiology. 2007;28(7):767-73.
53. Stone PW, Braccia D, Larson E. Systematic review of economic analyses of health care-associated infections. American journal of infection control. 2005;33(9):501-9.
54. Sullivan E, Gupta A, Cook CH. Cost and consequences of surgical site infections: a call to arms. Surgical infections. 2017;18(4):451-4.

55. Miller LG, Kaplan SL. Staphylococcus aureus: a community pathogen. Infectious disease clinics of North America. 2009;23(1):35-52.
56. Klevens RM, Edwards JR, Tenover FC, McDonald LC, Horan T, Gaynes R, et al. Changes in the epidemiology of methicillin-resistant Staphylococcus aureus in intensive care units in US hospitals, 1992–2003. Clinical infectious diseases. 2006;42(3):389-91.
57. Al-Nammari SS, Lucas JD, Lam KS. Hematogenous methicillin-resistant Staphylococcus aureus spondylodiscitis. Spine. 2007;32(22):2480-6.
58. Panlilio AL, Culver DH, Gaynes RP, Banerjee S, Henderson TS, Tolson JS, et al. Methicillin-resistant Staphylococcus aureus in US hospitals, 1975–1991. Infection Control & Hospital Epidemiology. 1992;13(10):582-6.
59. Zalavras CG, Patzakis MJ, Holtom PD, Sherman R. Management of open fractures. Infectious Disease Clinics. 2005;19(4):915-29.
60. Sakoulas G, Moise-Broder PA, Schentag J, Forrest A, Moellering RC, Eliopoulos GM. Relationship of MIC and bactericidal activity to efficacy of vancomycin for treatment of methicillin-resistant Staphylococcus aureus bacteremia. Journal of clinical microbiology. 2004;42(6):2398-402.
61. Steinkraus G, White R, Friedrich L. Vancomycin MIC creep in non-vancomycin-intermediate Staphylococcus aureus (VISA), vancomycin-susceptible clinical methicillin-resistant S. aureus (MRSA) blood isolates from 2001–05. Journal of Antimicrobial Chemotherapy. 2007;60(4):788-94.
62. Jennings JA, Courtney HS, Haggard WO. Cis-2-decenoic acid inhibits S. aureus growth and biofilm in vitro: a pilot study. Clinical orthopaedics and related research. 2012;470(10):2663-70.
63. Stewart PS. Mechanisms of antibiotic resistance in bacterial biofilms. International journal of medical microbiology. 2002;292(2):107-13.
64. Singh R, Ray P, Das A, Sharma M. Penetration of antibiotics through Staphylococcus aureus and Staphylococcus epidermidis biofilms. Journal of antimicrobial chemotherapy. 2010;65(9):1955-8.
65. Thurlow LR, Hanke ML, Fritz T, Angle A, Aldrich A, Williams SH, et al. Staphylococcus aureus biofilms prevent macrophage phagocytosis and attenuate inflammation in vivo. The Journal of Immunology. 2011;186(11):6585-96.
66. Coia J, Duckworth G, Edwards D, Farrington M, Fry C, Humphreys H, et al. Guidelines for the control and prevention of meticillin-resistant Staphylococcus aureus (MRSA) in healthcare facilities. Journal of hospital infection. 2006;63:S1-S44.
67. Zimmerli W. Clinical presentation and treatment of orthopaedic implant-associated infection. Journal of internal medicine. 2014;276(2):111-9.
68. Saginur R, StDenis M, Ferris W, Aaron SD, Chan F, Lee C, et al. Multiple combination bactericidal testing of staphylococcal biofilms from implant-associated infections. Antimicrobial agents and chemotherapy. 2006;50(1):55-61.
69. Whitehouse JD, Friedman ND, Kirkland KB, Richardson WJ, Sexton DJ. The impact of surgical-site infections following orthopedic surgery at a community hospital and a university hospital adverse quality of life, excess length of stay, and extra cost. Infection Control & Hospital Epidemiology. 2002;23(4):183-9.
70. Lewis K. Persister cells and the riddle of biofilm survival. Biochemistry (Moscow). 2005;70(2):267-74.

71. Berlanga M, Gomez-Perez L, Guerrero R. Biofilm formation and antibiotic susceptibility in dispersed cells versus planktonic cells from clinical, industry and environmental origins. Antonie Van Leeuwenhoek. 2017;110(12):1691-704.
72. Stewart PS, Costerton JW. Antibiotic resistance of bacteria in biofilms. The lancet. 2001;358(9276):135-8.
73. Mader JT, Wang J, Calhoun JH. Antibiotic therapy for musculoskeletal infections. JBJS. 2001;83(12):1878-90.
74. Zuelzer DA, Hayes CB, Hautala GS, Akbar A, Mayer RR, Jacobs CA, et al. Early antibiotic administration is associated with a reduced infection risk when combined with primary wound closure in patients with open tibia fractures. Clinical Orthopaedics and Related Research®. 2021;479(3):613-9.
75. Weinstein RA, Darouiche RO. Device-associated infections: a macroproblem that starts with microadherence. Clinical Infectious Diseases. 2001;33(9):1567-72.
76. Davies DG, Marques CN. A fatty acid messenger is responsible for inducing dispersion in microbial biofilms. Journal of bacteriology. 2009;191(5):1393-403.
77. Desbois AP, Smith VJ. Antibacterial free fatty acids: activities, mechanisms of action and biotechnological potential. Applied microbiology and biotechnology. 2010;85(6):1629-42.
78. Kenny JG, Ward D, Josefsson E, Jonsson M, Hinds J, Rees HH, et al. The Staphylococcus aureus response to unsaturated long chain free fatty acids: survival mechanisms and virulence implications. PLoS One. 2009;4(2):e4344.
79. Johnson SM, Saint John BE, Dine AP. Local anesthetics as antimicrobial agents: a review. Surgical infections. 2008;9(2):205-13.
80. Sams VG, Lawson CM, Coan P, Bemis D, Newkirk K, Karlstad M, et al. Effect of local anesthetic on microorganisms in a murine model of surgical site infection. Journal of Trauma and Acute Care Surgery. 2012;73(2):441-5.
81. Orive G, Gascon AR, Hernández RM, Domínguez-Gil A, Pedraz JL. Techniques: new approaches to the delivery of biopharmaceuticals. Trends in Pharmacological Sciences. 2004;25(7):382-7.
82. Hanssen AD. Local antibiotic delivery vehicles in the treatment of musculoskeletal infection. Clinical Orthopaedics and Related Research®. 2005;437:91-6.
83. McLaren AC. Alternative materials to acrylic bone cement for delivery of depot antibiotics in orthopaedic infections. Clinical Orthopaedics and Related Research®. 2004;427:101-6.
84. Schwarz EM, McLaren AC, Sculco TP, Brause B, Bostrom M, Kates SL, et al. Adjuvant antibiotic-loaded bone cement: concerns with current use and research to make it work. Journal of Orthopaedic Research®. 2020.
85. Bronzino JD. Biomedical engineering handbook: CRC press; 1999.
86. Cárdenas G, Anaya P, von Plessing C, Rojas C, Sepúlveda J. Chitosan composite films. Biomedical applications. Journal of Materials Science: Materials in Medicine. 2008;19(6):2397-405.
87. Xu J, McCarthy SP, Gross RA, Kaplan DL. Chitosan film acylation and effects on biodegradability. Macromolecules. 1996;29(10):3436-40.
88. Caner C, Vergano P, Wiles J. Chitosan film mechanical and permeation properties as affected by acid, plasticizer, and storage. Journal of food science. 1998;63(6):1049-53.
89. Prashanth KH, Kittur F, Tharanathan R. Solid state structure of chitosan prepared under different N-deacetylating conditions. Carbohydrate Polymers. 2002;50(1):27-33.

90. Mi F-L, Tan Y-C, Liang H-F, Sung H-W. In vivo biocompatibility and degradability of a novel injectable-chitosan-based implant. Biomaterials. 2002;23(1):181-91.
91. Frank A, Rath SK, Venkatraman SS. Controlled release from bioerodible polymers: effect of drug type and polymer composition. Journal of controlled release. 2005;102(2):333-44.
92. Dhanikula AB, Panchagnula R. Development and characterization of biodegradable chitosan films for local delivery of paclitaxel. The AAPS Journal. 2004;6(3):88-99.
93. Kofuji K, Ito T, Murata Y, KAWASHIMA S. The controlled release of a drug from biodegradable chitosan gel beads. Chemical and Pharmaceutical Bulletin. 2000;48(4):579-81.
94. Fujimoto T, Tsuchiya Y, Terao M, Nakamura K, Yamamoto M. Antibacterial effects of Chitosan solution® against Legionella pneumophila, Escherichia coli, and Staphylococcus aureus. International journal of food microbiology. 2006;112(2):96-101.
95. N Mengatto L, M Helbling I, A Luna J. Recent advances in chitosan films for controlled release of drugs. Recent patents on drug delivery & formulation. 2012;6(2):156-70.
96. Khor E, Lim LY. Implantable applications of chitin and chitosan. Biomaterials. 2003;24(13):2339-49.
97. Lončarević A, Ivanković M, Rogina A. Lysozyme-induced degradation of chitosan: the characterisation of degraded chitosan scaffolds. Journal of Tissue Repair and Regeneration. 2017;1(1):12.
98. Abarrategi A, Civantos A, Ramos V, Sanz Casado JV, López-Lacomba JL. Chitosan film as rhBMP2 carrier: delivery properties for bone tissue application. Biomacromolecules. 2008;9(2):711-8.
99. Aimin C, Chunlin H, Juliang B, Tinyin Z, Zhichao D. Antibiotic loaded chitosan bar: an in vitro, in vivo study of a possible treatment for osteomyelitis. Clinical Orthopaedics and Related Research®. 1999;366:239-47.
100. Aranaz I, Acosta N, Civera C, Elorza B, Mingo J, Castro C, et al. Cosmetics and cosmeceutical applications of chitin, chitosan and their derivatives. Polymers. 2018;10(2):213.
101. Goy RC, Britto Dd, Assis OB. A review of the antimicrobial activity of chitosan. Polímeros. 2009;19(3):241-7.
102. Mohebbi S, Nezhad MN, Zarrintaj P, Jafari SH, Gholizadeh SS, Saeb MR, et al. Chitosan in biomedical engineering: a critical review. Current stem cell research & therapy. 2019;14(2):93-116.
103. Burkatovskaya M, Castano AP, Demidova-Rice TN, Tegos GP, Hamblin MR. Effect of chitosan acetate bandage on wound healing in infected and noninfected wounds in mice. Wound Repair and Regeneration. 2008;16(3):425-31.
104. Pusateri AE, McCarthy SJ, Gregory KW, Harris RA, Cardenas L, McManus AT, et al. Effect of a chitosan-based hemostatic dressing on blood loss and survival in a model of severe venous hemorrhage and hepatic injury in swine. Journal of Trauma and Acute Care Surgery. 2003;54(1):177-82.
105. Greene AH, Bumgardner JD, Yang Y, Moseley J, Haggard WO. Chitosan-coated stainless steel screws for fixation in contaminated fractures. Clinical orthopaedics and related research. 2008;466(7):1699.
106. Suh J-KF, Matthew HW. Application of chitosan-based polysaccharide biomaterials in cartilage tissue engineering: a review. Biomaterials. 2000;21(24):2589-98.
107. Cevher E, Orhan Z, Mülazımoğlu L, Şensoy D, Alper M, Yıldız A, et al. Characterization of biodegradable chitosan microspheres containing vancomycin and treatment of experimental

osteomyelitis caused by methicillin-resistant Staphylococcus aureus with prepared microspheres. International journal of pharmaceutics. 2006;317(2):127-35.
108. Kim I-Y, Seo S-J, Moon H-S, Yoo M-K, Park I-Y, Kim B-C, et al. Chitosan and its derivatives for tissue engineering applications. Biotechnology advances. 2008;26(1):1-21.
109. Leffler CC, Müller BW. Influence of the acid type on the physical and drug liberation properties of chitosan–gelatin sponges. International journal of pharmaceutics. 2000;194(2):229-37.
110. Noel SP, Courtney H, Bumgardner JD, Haggard WO. Chitosan films: a potential local drug delivery system for antibiotics. Clinical orthopaedics and related research. 2008;466(6):1377-82.
111. Ueno H, Yamada H, Tanaka I, Kaba N, Matsuura M, Okumura M, et al. Accelerating effects of chitosan for healing at early phase of experimental open wound in dogs. Biomaterials. 1999;20(15):1407-14.
112. Wells CM, Beenken KE, Smeltzer MS, Courtney HS, Jennings JA, Haggard WO. Ciprofloxacin and rifampin dual antibiotic-loaded biopolymer chitosan sponge for bacterial inhibition. Military medicine. 2018;183(suppl_1):433-44.
113. Wu C, Su H, Karydis A, Anderson KM, Ghadri N, Tang S, et al. Mechanically stable surface-hydrophobilized chitosan nanofibrous barrier membranes for guided bone regeneration. Biomedical Materials. 2017;13(1):015004.
114. Murali VP, Fujiwara T, Gallop C, Wang Y, Wilson JA, Atwill MT, et al. Modified electrospun chitosan membranes for controlled release of simvastatin. International Journal of Pharmaceutics. 2020:119438.
115. Smith JK, Moshref AR, Jennings JA, Courtney HS, Haggard WO. Chitosan sponges for local synergistic infection therapy: a pilot study. Clinical Orthopaedics and Related Research®. 2013;471(10):3158-64.
116. Jennings JA, Beenken KE, Parker AC, Smith JK, Courtney HS, Smeltzer MS, et al. Polymicrobial Biofilm Inhibition Effects of Acetate-Buffered Chitosan Sponge Delivery Device. Macromolecular Bioscience. 2016;16(4):591-8.
117. Parker AC, Jennings JA, Bumgardner JD, Courtney HS, Lindner E, Haggard WO. Preliminary investigation of crosslinked chitosan sponges for tailorable drug delivery and infection control. Journal of Biomedical Materials Research Part B: Applied Biomaterials. 2013;101(1):110-23.
118. Boles LR, Bumgardner JD, Fujiwara T, Haggard WO, Guerra FD, Jennings JA. Characterization of trimethyl chitosan/polyethylene glycol derivatized chitosan blend as an injectable and degradable antimicrobial delivery system. International journal of biological macromolecules. 2019;133:372-81.

# Appendices

## Appendix A.

## Animal Use Protocol Approvals

1. Mississippi State University Institutional Animal Care and Use Committee Protocol Approval Letter

   Protocol 20-153 Approval: Efficacy of Chitosan-Mannitol Paste Loaded with Bupivacaine for Treatment of a Rat *S. Aureus* Infection Model

MISSISSIPPI STATE UNIVERSITY

Office of Research Compliance
Institutional Animal Care and Use Committee

P.O. Box 6223
53 Morgan Avenue
Mississippi State, MS 39762
P. 662.325.3294

www.orc.msstate.edu

June 22, 2020

Lauren Priddy

Ag & Bio Engineering

Re: Protocol # **IACUC-20-153**

Dear Lauren:

The Mississippi State Institutional Animal Care and Use Committee (IACUC) has completed it's review of your protocol titled Biomaterial delivery vehicles for antimicrobial treatment of osteomyelitis. In light of federal policies on the care and use of animals in research and requirements established specifically for the Institute, the committee has chosen to grant approval of this protocol on June 22, 2020. The expiration date for this project will be June 21, 2023 and the approval number is IACUC-20-153.

If you would like to involve additional members in this protocol or change aspects of the protocol in the future, please submit a Protocol Amendment Form for review.

Concurrent with this approval, please be advised the MSU-IACUC holds the principal investigator(s) named in this protocol responsible in ensuring that each procedure described in the protocol will be followed exactly (unless amended and such amendment is approved by the IACUC before implementation).

If the animal care and use aspects of this study change, approval of a new protocol or of an amendment is necessary. The project must be reviewed by the IACUC annually with the number of animals used during the year reported to the IACUC on the annual update form. When the project is complete, please notify the IACUC Administrator, Trina Smith, at 325-0994.

The committee appreciates your cooperation and wish you continued good luck in your research endeavors.

Sincerely,

Brian Rude

Chair, IACUC

brude@ads.msstate.edu